รายงานวิจัยฉบับสมบูรณ์

โครงการ การขึ้นรูปและการวิเคราะห์เส้นใยอิเลคโตรสปันจากพอลิเมอร์เปล่งแสงเมื่อถูกกระตุ้นด้วยไฟฟ้าและ/หรือแสง

โดย รองศาสตราจารย์พิชญ์ ศุภผล

กรกฎาคม 2552

สัญญาเลขที่ RMU4980045

รายงานวิจัยฉบับสมบูรณ์

โครงการ การขึ้นรูปและการวิเคราะห์เส้นใยอิเลคโตรสปันจากพอลิเมอร์เปล่งแสงเมื่อถูกกระตุ้นด้วยไฟฟ้าและ/หรือแสง

รองศาสตราจารย์พิชญ์ ศุภผล
วิทยาลัยปิโตรเลียมและปิโตรเคมี จุฬาลงกรณ์มหาวิทยาลัย

สนับสนุนโดยสำนักงานกองทุนสนับสนุนการวิจัยและสำนักงานคณะกรรมการการอุดมศึกษา
(ความเห็นในรายงานนี้เป็นของผู้วิจัย สกว.ไม่จำเป็นต้องเห็นด้วยเสมอไป)

กิตติกรรมประกาศ

งานวิจัยเรื่อง การขึ้นรูปและการวิเคราะห์เส้นใยอิเลคโตรสปันจากพอลิเมอร์เปล่งแสงเมื่อถูกกระตุ้นด้วยไฟฟ้าและ/หรือแสง นักวิจัย รองศาสตราจารย์พิชญ์ ศุภผล ได้รับทุนเพิ่มชีดความสามารถด้านการวิจัยของอาจารย์รุ่นกลางในสถาบันอุดศึกษา ตามโครงการความร่วมมือระหว่างสำนักงานคณะกรรมการการอุดมศึกษากับสำนักงานกองทุนสนับสนุนการวิจัย สัญญาเลขที่ RMU4980045 จึงใคร่ขอขอบคุณ มา ณ ที่นี้ด้วย

บทคัดย่อ

รหัสโครงการ : RMU4980045

ชื่อโครงการ : การขึ้นรูปและการวิเคราะห์เส้นใยอิเลคโตรสปันจากพอลิเมอร์เปล่งแสงเมื่อถูกกระตุ้นด้วยไฟฟ้าและ/หรือแสง

ชื่อนักวิจัย : รองศาสตราจารย์พิชญ์ ศุภผล
วิทยาลัยปิโตรเลียมและปิโตรเคมี จุฬาลงกรณ์มหาวิทยาลัย
E-mail Address : pitt.s@chula.ac.th

ระยะเวลาโครงการ : 3 ปี

งานวิจัยนี้ ได้ทำการศึกษาคุณสมบัติทางแสงของสารละลายและเส้นใยอิเลคโตรสปันจากพอลิเมอร์นำไฟฟ้าหลายชนิด เช่น พอลิ(2-เมทอกซี-5-(2'-เอทิลเฮกซิลออกซี)-1,4-ฟินิลีน ไวนิลีน) (MEH-PPV) พอลิ(เอทิลเฮกซีลออกซี-ออกทิลออกซี-พารา-ฟินิลีน เอทิลนิลีน) (EHO-OPPE) และ พอลิ(2,7-(9,9-บิส(2-เอทิลเฮกซิล) ฟลูออรีน (BEH-PF)

พบว่า การปรับเปลี่ยนคุณสมบัติทางแสงของพอลิ(2-เมทอกซี-5-(2'-เอทิลเฮกซิลออกซี)-1,4-ฟินิลีน ไวนิลีน)ในตัวทำละลาย 1,2 ไดคลอโรอีเทน สามารถทำได้โดยการเติมเกลืออินทรีย์ไพริดีเนียมฟอร์เมต การปรับความเข้มข้นของเกลืออินทรีย์ไพริดีเนียมฟอเมตในสารละลายควบคุมตำแหน่งของสเปกตรัมการดูดกลืนและการเปล่งแสงโฟโต้ลูมิเนสเซนส์ของพอลิ(2-เมทอกซี-5-(2'-เอทิลเฮกซิลออกซี)-1,4-ฟินิลีน ไวนิลีน) ได้อย่างเป็นระบบ โดยการเปลี่ยนสีของการเปล่งแสงจากสีส้มเป็นสีเหลืองและเขียว ซึ่งสามารถสังเกตได้ด้วยตาเปล่าในในสารละลายพอลิ(2-เมทอกซี-5-(2'-เอทิลเฮกซิลออกซี)-1,4-ฟินิลีน ไวนิลีน) ที่มีเกลืออินทรีย์ไพริดีเนียมฟอร์เมตร้อยละ 0.1 และ 10 โดยปริมาตร ตามลำดับ เกิดจากการปรับเปลี่ยนโครงสร้างทางเคมีของสายโซ่และกิ่งของพอลิ(2-เมทอกซี-5-(2'-เอทิลเฮกซิลออกซี)-1,4-ฟินิลีน ไวนิลีน)

สำหรับการศึกษากระบวนการปั่นเส้นใยด้วยไฟฟ้าสถิตของพอลิ(เอทิลเฮกซีลออกซี-ออกทิลออกซี-พารา-ฟินิลีน เอทิลนิลีน)และพอลิ(2,7-(9,9-บิส(2-เอทิลเฮกซิล)ฟลูออรีน พบว่า สามารถเตรียมเส้นใยที่มีความละเอียดสูง จากสารละลายพอลิเมอร์ผสมของพอลิเมอร์นำไฟฟ้าดังกล่าวกับพอลิเมอร์แม่แบบที่สามารถขึ้นรูปเส้นใยด้วยกระบวนการปั่นเส้นใยด้วยไฟฟ้าสถิตได้นั่นคือ พอลิสไตรรีน โดยได้ทำการตรวจสอบคุณสมบัติทางสัณฐานวิทยาและคุณสมบัติทางเคมีของเส้นใยอิเลกโตรสปันดังกล่าวด้วยกล้องจุลทรรศน์อิเล็กตรอนแบบส่องกราดและเทคนิคฟูเรียร์ทรานสฟอร์มอินฟราเรดสเปกโตรสโคปี และได้ทำการศึกษาคุณสมบัติทางแสง เช่น การดูดกลืนและการเปล่งแสงโฟโต้ลูมิเนสเซนส์ ด้วยเครื่องยูวีวิซิเบิลสเปกโตรสโคปีและโฟโต้ลูมิเนสเซนส์สเปกโตรสโคปี ตามลำดับ โดยได้ทำการศึกษาเปรียบเทียบกับฟิล์มบางของพอลิเมอร์เปล่งแสงดังกล่าว ที่เตรียมได้จากเทคนิคสปินโค้ตติ้งและเทคนิคการขึ้นรูปด้วยสารละลายอีกด้วย

คำหลัก : พอลิเมอร์เปล่งแสง เส้นใยอิเลคโตรสปัน โฟโต้ลูมิเนสเซนส์

Abstract

Project Code : RMU4980045

Project Title : Fabrication and Characterization of Electrospun Polymeric Fibers with Photoluminescence and/or Electroluminescence Properties

Investigator : Assoc. Prof. Pitt Supaphol

The Petroleum and Petrochemical College, Chulalongkorn University

E-mail Address : pitt.s@chula.ac.th

Project Period : 3 years

The studies on optical properties of various conductive polymers (i.e., poly(2-methoxy-5-(2'-ethylhexyloxy)-1,4-phenylene vinylene) (MEH-PPV), poly(ethylhexyloxy-octyloxy-p-phenylene ethynylene) (EHO-OPPE), poly(2,7-(9,9-bis(2-ethylhexyl)fluorene)) (BEH-PF)) either in their solution or electrospun fibrous form were successfully reported here.

First, a versatile method for tuning optical properties of MEH-PPV in its solution with 1,2-dichloroethane was accomplished by reacting with pyridinium formate (PF), a volatile organic salt. Adjusting the concentration of PF in the solution led to a systematic control for the position of the absorption and the photoluminescent (PL) spectra of MEH-PPV. The changes in the emission color from orange to yellow and, finally, to green were observed by naked eyes in the MEH-PPV solution that contained 0.1 and 10 vol.-% of PF, respectively. The changes in the optical properties were due to chemical modifications along the main chain and the side groups of MEH-PPV.

For the studies on the electrospinning of EHO-OPPE and BEH-PF, ultra-fine fibers from their blend solutions with an electrospinnable and inert template polymer, i.e., polystyrene (PS) were successfully prepared. Scanning electron microscopy (SEM) and Fourier-transformed infrared (FT-IR) spectroscopy were respectively used to observe the morphology and chemical integrity of the electrospun fibers. The optical properties (i.e., absorption and PL emission) were investigated by UV-Visible and PL spectroscopy, respectively. Moreover, the corresponding spin-coated and solution-cast films were also studied for comparison.

Keywords : Light-emitting polymer, Electrospun fibers, Photoluminescence

เนื้อหางานวิจัย

1. VERSATILE ROUTE FOR TUNING OPTICAL PROPERTIES OF POLY(2-METHOXY-5-(2'-ETHYLHEXYLOXY)-1,4-PHENYLENEVINYLENE) (MEH-PPV)

1.1 Introduction

Poly(2-methoxy-5-(2′-ethylhexyloxy)-1,4-phenylenevinylene) (MEH-PPV) is one of the well-known conjugated polymers with many interesting physical properties, such as photoconductivity[1,2] and high luminescence efficiency in both photo- and electroluminescence.[3,4] It, therefore, holds great promises in various electronic applications, such as organic light-emitting diodes (OLED),[5-7] sensors[8-10] and solar cells.[11,12] In the past few decades, many researchers have investigated detailed properties of conjugated polymers in order to understand their fundamental behaviors. In general, the intrinsic nature of conjugated polymers derives mainly from their architectures consisting of alternating single and double/triple bonds along the main chain. The appropriate arrangement of π-orbitals in the backbone could provide a convenient pathway for π-electrons to delocalize over the entire molecule. However, this ideal situation is never realized because of the flexibility of the polymer chain. The delocalization of the π-electrons is normally confined within some distances, called conjugation lengths. Various chromophores with different conjugation lengths exist in one conjugated chain.[13,14] Therefore, its electronic properties are dictated by the distribution of chromophores within the system.[15-17]

One of the challenges for developing conjugated polymers is the tuning of their electronic and optical properties, which are necessary for specific applications. This includes, for example, the engineering of colors to obtain a full range of spectrum in OLED and the manipulation of HOMO-LUMO energy levels in solar cells. The methods for tuning the properties of conjugated polymers generally involve the synthesis of new macromolecules[18-21] or the modification of the chemical structure of the existing conjugated polymers.[22-26] MEH-PPV is an example of a modified chemical structure of polyphenylenevinylene-based conjugated polymers. The incorporation of the flexible MEH side groups increases the solubility of this polymer in a common solvent, which, in turn, facilitates its fabrication into thin films. The bulkiness of the MEH side groups also reduces the segmental aggregation of the main chain, an important factor that affects its photoemission color and efficiency.[27-29] Furthermore, the phenyl rings along the MEH-PPV backbone become more difficult to rotate around single bonds, resulting in the extension of conjugation lengths.

It has been shown that the tuning of optical properties of conjugated polymers can also be achieved via polymer-polymer blending approach.[30-34] Although the procedure is quite simple, this

method does not modify the HOMO-LUMO energy levels of each polymer in the blend. The photo- and electroluminescence spectra always constitute of multiple regions, contributed from simultaneous emitting of different luminophores in the system.[30,32,33] The manipulation of the emitting colors can be done by simply adjusting the ratio of the blend and the extent of energy transfer. Furthermore, the polymer-polymer blends tend to exhibit micro- and nano-phase separation due to the immiscibility of the components, which, in turn, leads to inhomogeneity in local properties.[31-34] The issue of phase separation can be overcome by a copolymerization approach.[35-37] The structural change of luminophores in copolymers allows for a direct engineering of HOMO-LUMO energy levels, which yields narrow photo- and electroluminescence spectra. However, the copolymerization is normally a multi-step process, which requires complicated procedures and expensive catalysts/chemicals. Therefore, it is important to seek a simple and cheap method for chemically modifying conjugated polymers that provides an easy control over their optical properties.

In a recent study by some of us, fibers of MEH-PPV were electrospun from its solutions in 1,2-dichloroethane (DCE) with polystyrene being used as the fiber-forming template and pyridinium formate (PF), a volatile organic salt, being used as the conductivity modifier. It was accidentally observed that the solutions changed their color from orange to yellow after being aged at ambient conditions for 1 month.[38] It was postulated, based on the infrared spectroscopic result, that partial decomposition of MEH side groups (~15%) was responsible for this observation. We envisioned that such a side chain decomposition induced by the addition of PF could be a simple approach to modify the chemical configuration of MEH-PPV, resulting in the chemical structure that resembles that of a random copolymer between PPV and MEH-PPV. Despite such an implication, a detailed study on any structural change that affects the change in the color of MEH-PPV in the presence of PF based on a more direct method, such as nuclear magnetic resonance spectroscopy (NMR), is necessary to gain an insight into the color-changing process of this polymer.

In the present study, we performed systematic experiments to investigate the photophysical change of MEH-PPV solutions in DCE in the presence of PF, which could lead to a simple procedure for controlling the electronic properties of this polymer. Effects of concentrations of MEH-PPV and PF were investigated. The changes in the absorption and the photoemission spectra were followed as a function of time. Fourier-transformed infrared spectroscopy (FT-IR) and NMR were used to characterize the structural change of MEH-PPV in the system.

1.2 Experimental

The MEH-PPV used in this study was synthesized according to the procedure described in literature.[26] All solvents purchased from different sources (Carlo Erba and Merck) were analytical grade. Fresh solutions of MEH-PPV (0.001, 0.005 and 0.01% w/v) were prepared by dissolving

measured amounts of the polymer powder in DCE. Different concentrations (0.1 and 10 vol.-%) of PF, prepared by mixing pyridine and formic acid in an equimolar quantity, were then added into the system. The mixed solutions were sealed in vials and left in darkness at ambient conditions. Absorption and photoemission spectra of the solutions were recorded as a function of time until no noticeable change was observed.

The absorption spectra were measured using a Hewlett-Packard 8254A diode array UV-vis spectrophotometer. Quartz cuvettes with thicknesses of 2 mm or 10 mm, depending on the polymer concentration, were used. The emission spectra were measured using a Perkin-Elmer LS50 luminescence spectrometer. An inner filter effect was minimized by using a 2 mm-thick quartz cuvette in all measurements. Any structural change of MEH-PPV was investigated by a Bruker Avance-AC400 proton-nuclear magnetic resonance spectroscopy (^{1}H-NMR), operating at 400 MHz, and a Thermo-Nicolet Nexus 670 Fourier-transform infrared spectrometer (FT-IR). Samples for these measurements were prepared by evaporating the solvent at 130 $^{\circ}$C for 1 h. Only small amount of the solvent remained after this procedure. The samples were subsequently dried at 80 $^{\circ}$C in a vacuum oven for 12 h. Solutions of MEH-PPV in DCE and PF in DCE were also subjected to the same drying procedure. These were used as control samples.

1.3 Results and discussion

In the first section, we investigated the variation in the absorption spectra as a function of the reaction time, which reflects the photophysical changes of MEH-PPV chromophores in ground state. Figure 1.1 illustrates the results obtained from the system of 0.01 % w/v MEH-PPV solution containing 10 vol.% PF. The spectrum of the freshly-prepared solution (0 day) exhibits a broad pattern with the maximum absorption (λ_{max}) at about 500 nm. The broadness of the spectrum arises from an intrinsic nature of the conjugated chain, which consists of various chromophores with different conjugation lengths.[14,17] Therefore, the shape of the whole spectrum envelops all possible electronic transitions, which take place at different wavelengths, depending on HOMO-LUMO energy gaps of each particular chromophore.

The pattern of the absorption spectrum changes significantly upon aging in ambient conditions for 1 day. Its absorbance markedly drops while the λ_{max} shifts to a higher energy region. Increasing the reaction time to 2 days causes a blue-shift of the spectrum by about 30 nm. We also observe the increase in the absorbance at the high-energy region (λ < 450 nm), while the absorbance at the low-energy region simultaneously decreases. The progress of reaction continues up to about 14 days. Increasing the reaction time further to 37 days hardly affects the pattern of the absorption spectrum, suggesting the completion of this process. The solution of the final product exhibits λ_{max} at

about 434 nm, while the absorbance drops by about 55% compared to that of the original solution. In addition, the pattern of the spectrum appears much broader with the high-energy region becoming wider. The blue-shift of the absorption spectra corresponds to the widening of HOMO-LUMO energy gap of the modified MEH-PPV. In other words, long chromophores are converted to shorter ones upon the reaction with PF. In addition, the decrease of the absorbance indicates the lowering of the molar absorption coefficient.

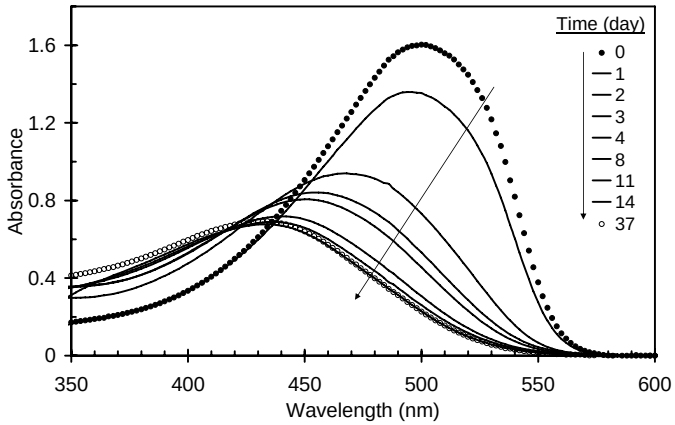

Figure 1.1 Absorption spectra of 0.01% (w/v) MEH-PPV in 1,2-dichloroethane (DCE) with the addition of 10 vol.-% pyridinium formate (PF) measured as a function of reaction time. Arrow indicates the change in the spectra with increasing the reaction time.

We carried out additional experiments to explore other parameters that affected the progress of the reaction. The solutions of MEH-PPV at various concentrations [e.g., 0.001, 0.005 and 0.01% (w/v)] were prepared while the PF content was kept constant at 10 vol.-%. All solutions exhibit the blue-shift in the absorption spectra and the decrease in the absorbance with increasing the reaction time. Plots of λ_{max} and the absorbance as a function of time are shown in Figure 1.2(a) and (b). The rate of the reaction is found to increase with a decrease in the concentration of MEH-PPV (or with an increase in the PF to MEH-PPV ratio). The reactions of 0.001, 0.005 and 0.01% (w/v) solutions are completed after the solutions having been aged for 8, 11 and 14 days, respectively. Despite that, the λ_{max} of the final products is detected at practically the same location (λ_{max} ~ 434 nm). The change in the absorbance shows a consistent trend. These observations indicate that the concentration of the added PF is an important parameter for controlling the HOMO-LUMO energy gap of the modified MEH-PPV.

As mentioned earlier, the broadness of the absorption spectra reflects the distribution of chromophores with various conjugation lengths in the conjugated backbone of MEH-PPV. One can follow the variation in the size distribution of chromophores by plotting the ratios between the

integrated areas under two different energy regions of the absorption spectrum, i.e., [350-490 nm]/[490-600 nm], as illustrated in Figure 1.2(c). This ratio is about 1 for the original solutions of MEH-PPV. It gradually increases with an increase in the reaction time for all solutions. The rate of change is highest for the 0.001% (w/v) solution, which is consistent with the variation of λ_{max} and the absorbance. The ratios of the integrated areas reach the value of about 8 after the completion of the reaction, corresponding to the markedly increase in the high-energy chromophores in the system. We also observe that the final product of each solution exhibits slightly different values of the ratios.

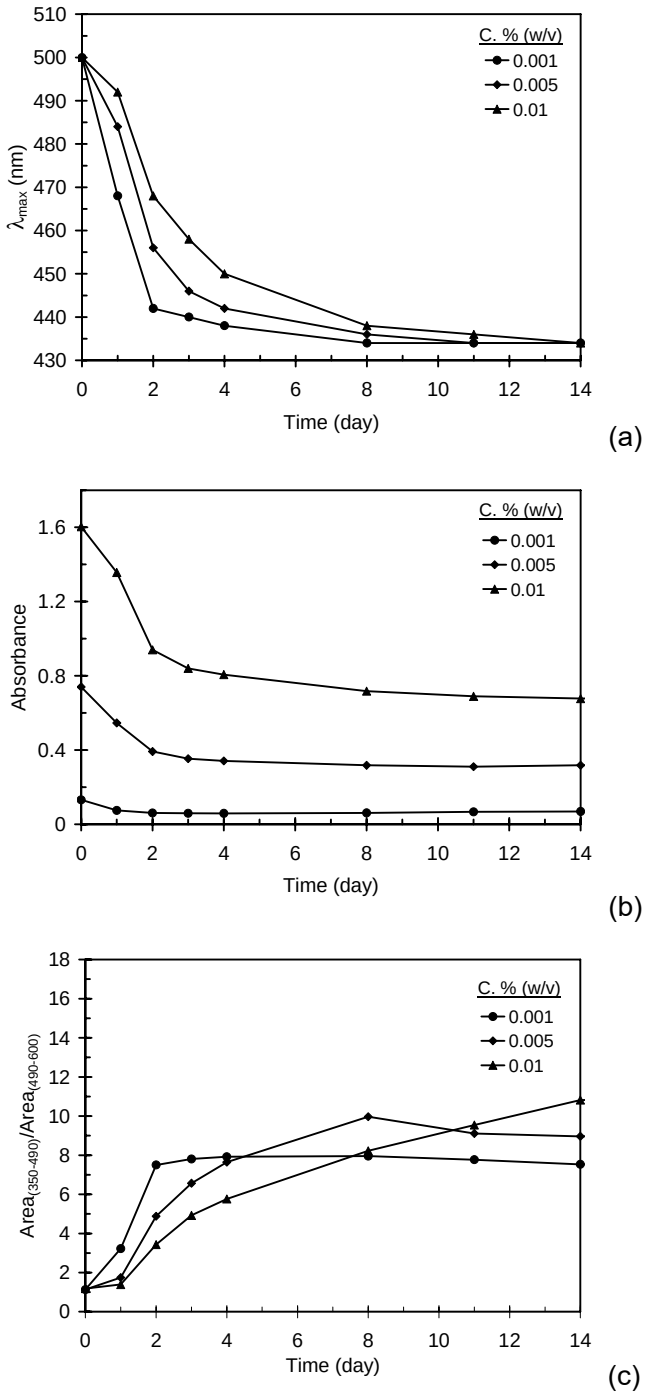

Figure 1.2 Plots of (a) λ_{max}, (b) absorbance and (c) $Area_{(350-490)}/Area_{(490-600)}$ of the absorption spectra of MEH-PPV at various concentrations in DCE with the addition of 10 vol.-% PF measured as a function of reaction time.

In the next section, we performed similar experiments to investigate the effects of PF concentration. The solutions of MEH-PPV with concentrations of 0.001, 0.005 and 0.01% (w/v) were prepared while the quantity of PF was reduced from 10 to 0.1 vol.-%. Figure 1.3 illustrates the results obtained from the 0.01% (w/v) MEH-PPV solution with 0.1 vol.-% PF. It is obvious that the blue-shift and the decrease of the absorbance occur with increasing the reaction time. However, the

rate of change is much slower as compared to the solution of 0.01% (w/v) MEH-PPV in the presence of 10 vol.-% PF. The absorption spectrum changes slightly after 4 days. The reaction yields the final product after 14 days and its absorption spectrum exhibits λ_{max} at ~476 nm. Previously, it was found that the solutions of MEH-PPV with 10 vol.-% PF showed the final products with λ_{max} of the absorption spectra at ~434 nm. These results indicate that the change in the PF concentration leads to the modified MEH-PPV with different optical properties. In other words, PF with different concentrations could be used to tune the peak position of the absorption spectrum or the conjugation length of chromophores of the conjugated polymer.

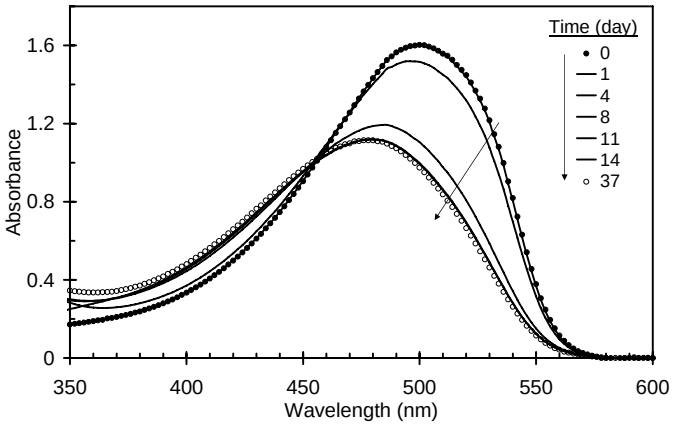

Figure 1.3 Absorption spectra of 0.01% (w/v) MEH-PPV in DCE with the addition of 0.10 vol.-% PF measured as a function of reaction time. Arrow indicates the change in the spectra with increasing the reaction time.

The results obtained from the solutions of 0.001 and 0.005% (w/v) with 0.1 vol.-% PF confirm our finding. The changes in the absorption spectra with increasing the reaction time are summarized in Figure 1.4. The λ_{max} of all the solutions decreases with increasing the reaction time and reaches a constant value at ~476 nm after 14 days. The variation in the absorbance shows similar results. Figure 1.4(c) shows the ratios between the integrated areas under two different energy regions of the absorption spectrum, i.e., [350-490 nm]/[490-600 nm], which shows the increase of the values by about 2 times. It is important to note that the MEH-PPV solutions with 10 vol.-% PF exhibit the change in this value by about 8 times. Therefore, the variation in the PF concentration can be used to tune the average conjugation length (λ_{max}), the molar absorption coefficient and the size distribution of chromophores in the modified MEH-PPV. The concentration of the polymer also affects the rate of the overall process. The experiments performed on both systems show the increase of the reaction rate with decreasing the polymer concentration (or with increasing the PF to MEH-PPV ratio). To summarize all results, we plot the absorption spectra of the final products obtained at two

concentrations of the added PF as shown in Figure 1.5. The absorption spectrum of the original MEH-PPV solution with identical concentration is included for comparison.

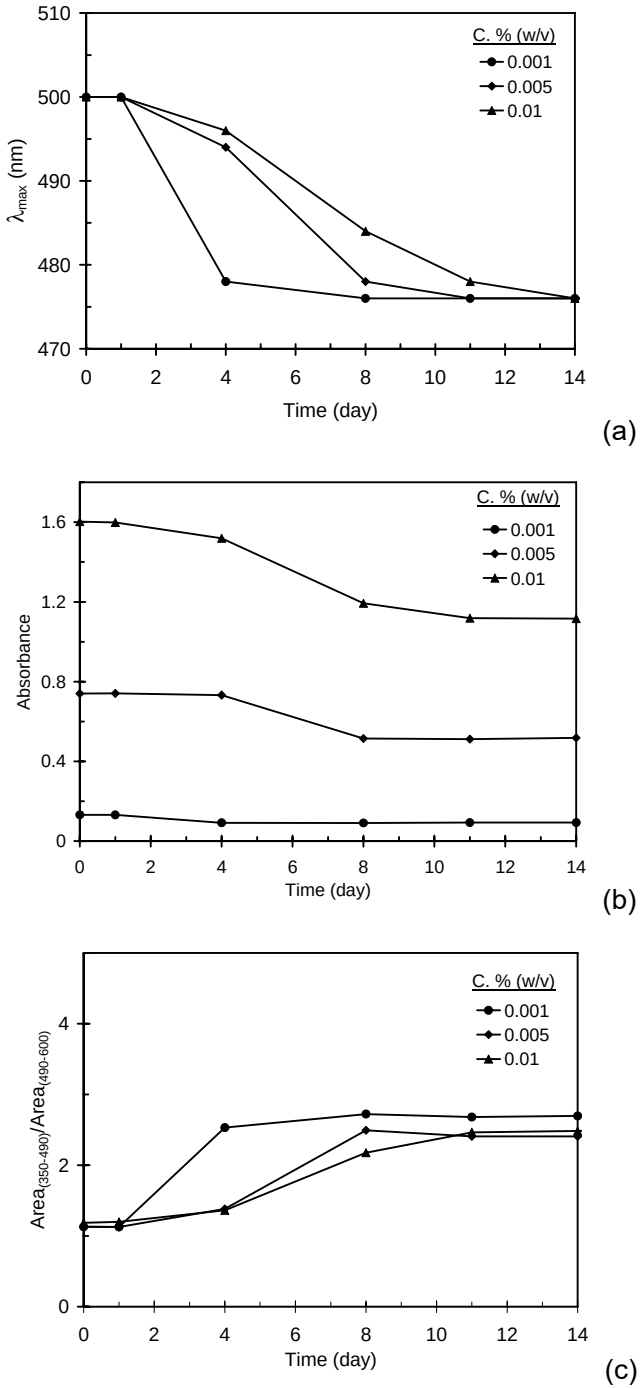

Figure 1.4 Plots of (a) λ_{max}, (b) absorbance and (c) $Area_{(350-490)}/Area_{(490-600)}$ of the absorption spectra of MEH-PPV at various concentrations in DCE with the addition of 0.1 vol.-% PF measured as a function of reaction time.

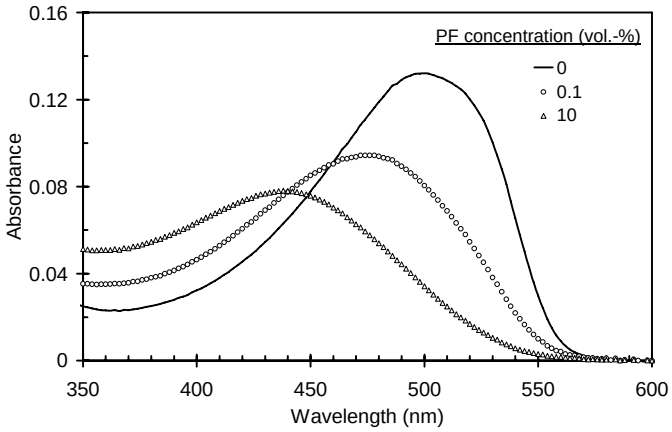

Figure 1.5 Absorption spectra of 0.001% (w/v) MEH-PPV in DCE at various concentrations of PF after having been aged for 37 days.

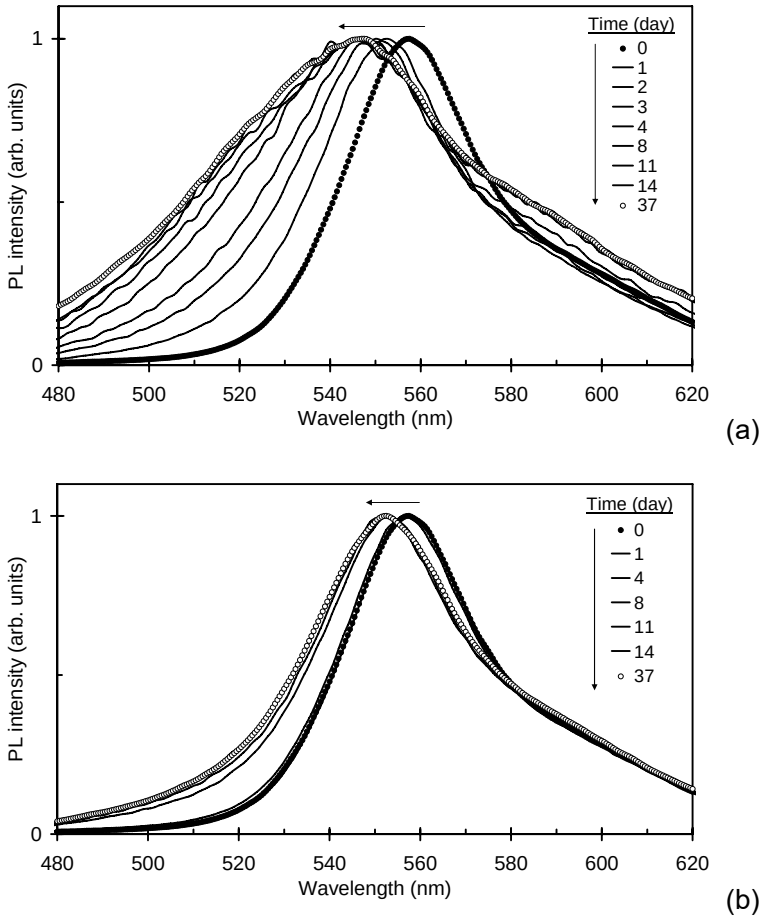

Figure 1.6 Emission spectra of 0.01% (w/v) MEH-PPV in DCE with the addition of (a) 10 or (b) 0.1 vol.-% PF measured as a function of reaction time. Arrow indicates the change in the spectra with increasing the reaction time. All spectra are normalized for clarity.

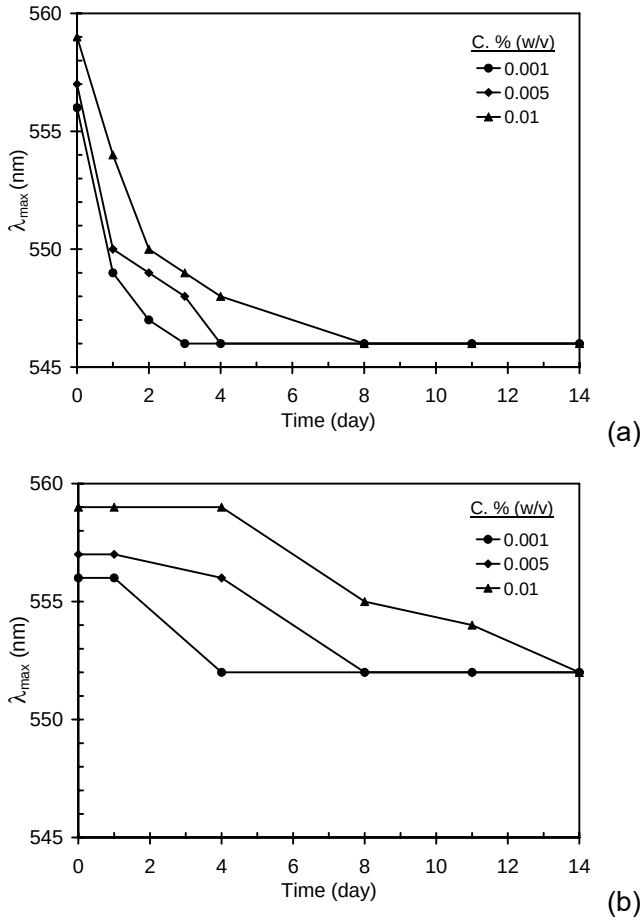

Figure 1.7 Plots of λ_{max} of the emission spectra of MEH-PPV at various concentrations in DCE with the addition of (a) 10 or (b) 0.1 vol.-% PF measured as a function of reaction time.

The results on photoluminescence show a similar behavior to that of the absorption, previously discussed. The results obtained from the systems of 0.01 % (w/v) MEH-PPV solutions with 10 and 0.1 vol.-% PF are respectively shown in Figure 1.6(a) and (b). All of the photoluminescent (PL) spectra were recorded with an excitation wavelength of 450 nm. The PL spectrum of the original MEH-PPV solution exhibits λ_{max} at about 559 nm along with a broad shoulder at about 590 nm. The spectra gradually shift to a high-energy region with an increase in the reaction time and become stable after 14 days. The products of MEH-PPV with 10 or 0.1 vol.-% PF exhibit the PL spectra with λ_{max} of ~546 nm and ~552 nm, respectively. The solutions appear green and yellow, respectively, under the illumination of a black light (λ ~ 385 nm). The experiments carried out on 0.005 and 0.001% (w/v) MEH-PPV solutions produced similar results. Figure 1.7 shows that λ_{max} as measured on all of the solutions investigated decreases with an increase in the reaction time. Similar to the behavior of the absorption spectra, the final values of λ_{max} are dictated by the PF concentration,

while the rate of change increases with a decrease in the polymer concentration. Interestingly, the peak position of the PL spectra of the original MEH-PPV solutions slightly shifts to a low-energy region with increasing the polymer concentration. This corresponds to the inner-filter effect in which the emitted photons with relatively high energy are re-absorbed by neighboring chromophores. Such an effect becomes dominant upon increasing the concentration of chromophores, causing the PL spectra to red-shift and the overall emission intensity to decrease.

The PL spectra of the modified MEH-PPV which has been aged for 14 days exhibit a much broader shape compared to that of the original solution (see Figure 1.6(a)), which corresponds to the increase in the size distribution of chromophores in the systems. The ratios between the integrated areas under two different energy regions of the PL spectrum, i.e., [470-550 nm]/[550-660 nm], of each solution are calculated and plotted in Figure 1.8(a) and (b). The ratio is about 0.4 for the original MEH-PPV solution. The value gradually increases with the reaction time, which corresponds to the conversion of the low-energy chromophores to the higher-energy ones. The ratios reach final values of about 1.1 and 0.6 for the systems containing 10 and 0.1 vol.-% PF, respectively.

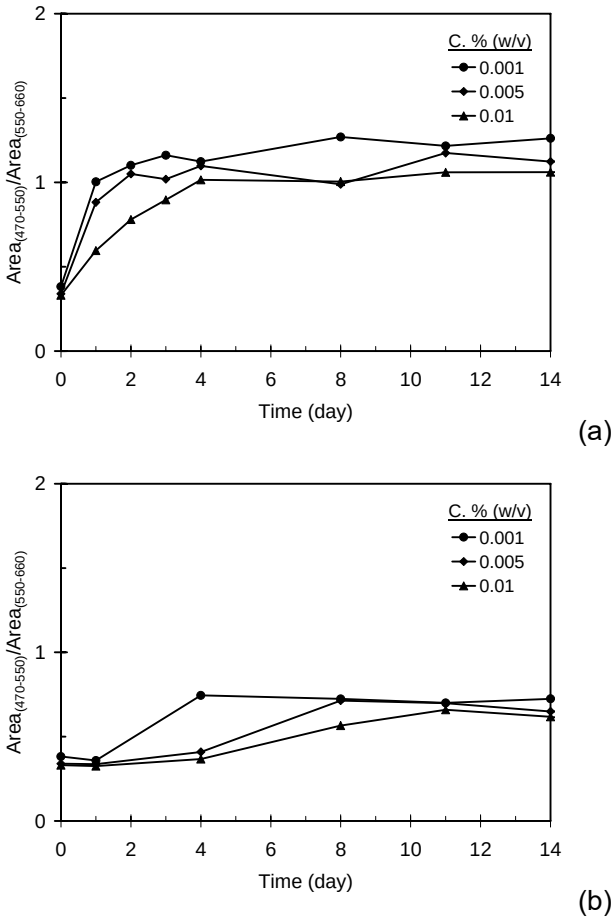

Figure 1.8 $Area_{(470-550)}/Area_{(550-660)}$ of the emission spectra of MEH-PPV at various concentrations in DCE with the addition of (a) 10 or (b) 0.1 vol.-% PF measured as a function of reaction time.

In the next section, NMR and FT-IR spectroscopy were used to investigate any change in the structure of MEH-PPV, upon coming into contact with PF, that might be responsible for the observed optical properties. Figure 1.9 displays ^{1}H-NMR spectra of the original MEH-PPV, PF and the modified MEH-PPV. The comparison between the spectra of PF and the modified MEH-PPV indicates that the organic salt is completely removed from our samples. The spectrum of the original MEH-PPV constitutes the peaks at 7.19 and 7.50 ppm, corresponding to olefinic and aromatic protons along the conjugated backbone.[39] The signals of methoxy and alkoxy protons of the side groups are also detected at about 3.7 to 4.0 ppm. Series of new signals, as illustrated in Figure 1.9c, are detected when the MEH-PPV is reacted with 0.1 vol.-% PF. The intensity of these peaks becomes much more pronounced when the concentration of PF increases to 10 vol.-% (viz. the increase in the extent of the reaction). Some additional peaks are also observed (see Figure 1.9d). The appearance of these new peaks is accompanied by a simultaneous decrease in the intensity of the peaks at 7.19 and 7.50 ppm of the original MEH-PPV. In addition, the peaks of the side groups at ~4 ppm become

much broader. The detection of new peaks near 5.6 and 8 ppm suggests the incorporation of formate ($HCOO^-$) groups, probably by the addition reaction with reactive double bonds in the conjugated backbone. The peaks near 5 ppm suggest the existence of phenolic groups in the modified polymer, which is likely to be due to the breaking of ether groups of the side groups (see below). The peaks near 10 ppm also suggest the existence of aldehyde groups. However, it is not our intention to try to identify the exact origin of each peak, as one needs to carry out further experiments to follow the reaction.

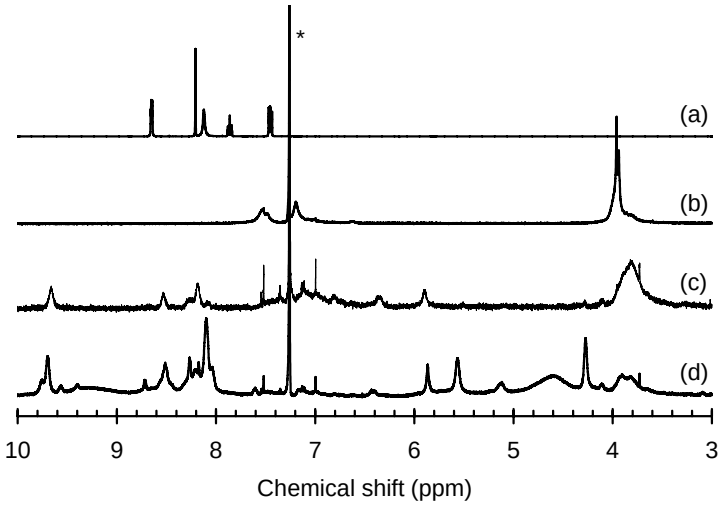

Figure 1.9 ^{1}H-NMR spectra of (a) PF, (b) the original MEH-PPV, (c) MEH-PPV that had been reacted with 0.1 vol.-% PF and (d) MEH-PPV that had been reacted with 10 vol.-% PF in *d*-chloroform. The solutions in (c) and (d) had been aged for 4 days prior to the removal of PF and solvent (see text). Peak marked with asterisk (*) is due to the residual solvent. For clarity of the presentation, peaks belonging to other protons of the alkyl side groups are not included.

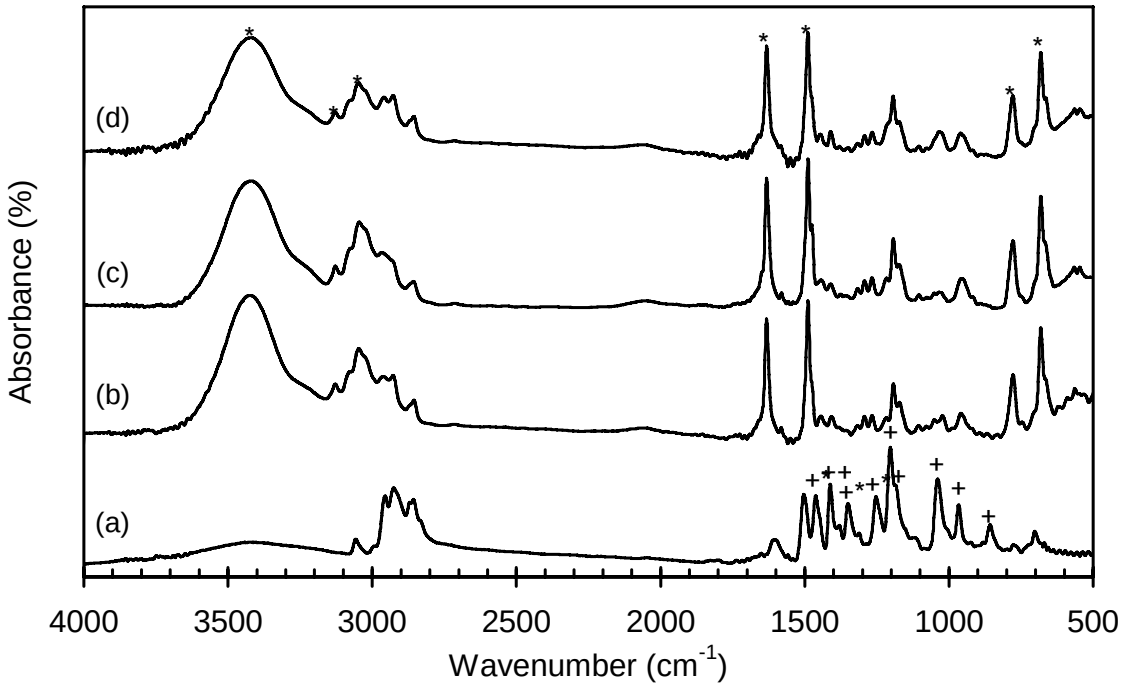

Figure 1.10 FT-IR spectra of (a) the original MEH-PPV and the modified MEH-PPV from (b) 0.001, (c) 0.005 or (d) 0.01% (w/v) MEH-PPV in DCE with the addition of 10 vol.-% PF. The solutions had been aged for 75 days prior to the removal of PF and solvent.

* = The intensity of the peak was greatly increased after PF addition.

+ = The intensity of the peak was greatly decreased after PF addition.

Figure 1.10 illustrates FT-IR spectra of the original MEH-PPV along with that of the modified one. The modified MEH-PPV was obtained by reacting with 10 vol.-% PF for 75 days. We note that the use of 0.01, 0.005 and 0.001% (w/v) of the original MEH-PPV solutions leads to the same FT-IR pattern of the dried samples. This indicates that the solvent and PF are completely removed from the samples, which is confirmed by the absence of the FT-IR spectrum of the pure PF (not shown). Table 1.1 summarizes some absorption peaks corresponding to different vibrational modes of the polymeric segments. It is apparent that the absorbance of the peaks at 1040, 1190 and 1250 cm^{-1} of the original MEH-PPV is greatly reduced in the modified polymer. Since these peaks are specific to the vibrations of aryl–alkyl ether linkage (C-O-C) of the MEH side groups, this indicates the reduction in the number of MEH side groups in the modified MEH-PPV. In addition, the concentration of tetrahedral defects along the polymeric main chain appears to increase significantly. This is indicated by the detection of new intense peak at 1630 cm^{-1} in the modified MEH-PPV, which is specific to the C=C stretching vibration of the non-conjugated chains. In other words, a number of the C=C bonds is converted to single bonds, which interrupt the conjugation along the conjugated backbone. The

detection of a broad peak at 3420 cm^{-1} also indicates the presence of hydroxyl groups in the modified MEH-PPV. These results suggest that the reaction between MEH-PPV and PF results in the reduced number of MEH side groups and the increased number of non-conjugated segments, which are responsible for the observed decrease in the conjugation lengths of the modified polymer.

Table 1.1 Analysis of FT-IR spectra of the original MEH-PPV and modified MEH-PPV. The polymer solutions were mixed with 10 vol.-% PF and left to age for 75 days. Original concentrations of MEH-PPV are shown in the table

MEH-PPV		Assignment
Original	Modified	
-	* 682	CH bending vibrations in CH deformation
-	* 777	CH out-of-plane bending vibrations in -CH=CH-(cis) group
+ 875	-	CH out-of-plane bending vibrations in $-C=CH_2$ group
+ 966	958	CH out-of-plane bending vibrations in -CH=CH-(trans) group
+ 1040	1020	aryl alkyl ether (C-O-C) symmetric stretching vibrations in acetates group
+ 1190	1190	aryl alkyl ether (C-O-C) stretching vibrations in formates group
+ 1200	1200	ring stretching vibrations and CH deformation
+ 1250	1270	aryl alkyl ether (C-O-C) asymmetric stretching vibrations in benzoates group
+ 1350	-	CH bending vibrations in $-CH_3$ deformation
+ 1410	1410	CH bending vibrations in $-CH_2$ deformation
+ 1460	1440	asymmetric CH bending vibrations in $-CH_3$ group
1500	* 1490	C=C stretching vibrations in conjugated
-	* 1630	C=C stretching vibrations in non-conjugated
2860	2860	symmetric CH stretching vibrations in $-CH_2$ group
2930	2930	asymmetric CH stretching vibrations in $-CH_2$ group
2950	2950	asymmetric CH stretching vibrations in $-CH_3$ group
3060	* 3040	CH stretching vibrations in =C-H, $=CH_2$ group and CH group
-	* 3130	NH stretching vibrations in H bonded NH group
-	* 3420	OH stretching vibrations of intramolecular H bonds

* = The intensity of the peak was greatly increased after PF addition.

+ = The intensity of the peak was greatly decreased after PF addition.

1.4 Conclusions

We have demonstrated a versatile method for tuning the optical properties of one of the most investigated conjugated polymers, MEH-PPV. This is accomplished by the reaction of the polymer with pyridinium formate (PF), a volatile organic salt. The absorption and the emission spectra (i.e., colors) of the modified MEH-PPV can be controlled by the variations in the concentration of PF and the reaction time. This method results in the displacement of the λ_{max} of the absorption spectra and the emission spectra by 60 nm and 15 nm, respectively. The size distribution of chromophores in the main chain is also affected significantly. The modified MEH-PPV chains contain a larger number of shorter chromophores. Structural analysis by using NMR and FT-IR spectroscopy indicates that the variation in the optical properties arises from the breaking of some double bonds along the conjugated chains and the removal of MEH side groups. The extent of these structural changes dictates the optical properties of the modified MEH-PPV. The results obtained in this work signify the ability to systematically tuning the optical properties of MEH-PPV, which can be utilized for a wide range of applications such as OLED and solar cells. Our method is a one step process which is much simpler compared to the common copolymerization approach. It also requires relatively cheap chemicals and takes a simple procedure for purification.

1.5 References

[1] Lee, C. H.; Yu, G.; Sariciftci, N. S.; Heeger, A. J.; Zhang, C. Synth Met 1995, 75, 127-131.

[2] Rothberg, L. J.; Yan, M.; Kwock, E. W.; Miller, T. M.; Galvin, M. E.; Son, S.; Papadimitrakopoulos, F. IEEE Trans Electron Dev 1997, 44, 1258-1262.

[3] Gettinger, C. L.; Heeger, A. J.; Drake, J. M.; Pine, D. J. J Chem Phys 1994, 101, 1673-1678.

[4] Kang, H. S.; Kim, K. H.; Kim, M. S.; Park, K. T.; Kim, K. M.; Lee, T. H.; Joo, J.; Kim, K.; Lee, D. W.; Jin, J. I. Curr Appl Phys 2001, 1, 443-446.

[5] Friend, R. H.; Gymer, R. W.; Holmes, A. B.; Burroughes, J. H.; Marks, R. N.; Taliani, C.; Bradley, D. D. C.; Dossantos, D. A.; Brédas, J. L.; Lögdlund, M.; Salaneck, W. R. Nature 1999, 397, 121-128.

[6] Shin, J. H.; Matyba, P.; Robinson, N. D.; Edman, L. Electrochim Acta 2007, 52, 6456-6462.

[7] Kulkarni, A. P.; Tonzola, C. J.; Babel, A.; Jenekhe, S. A. Chem Mater 2004, 16, 4556-4573.

[8] McQuade, D. T.; Pullen, A. E.; Swager, T. M. Chem Rev 2000, 100, 2537-2574.

[9] Pistor, P.; Chu, V.; Prazeres, D. M. F.; Conde, J. P. Sensor Actuator B 2007, 123, 153-157.

[10] Lange, U.; Roznyatovskaya, N. V.; Mirsky, V. M. Anal Chim Acta 2008, 614, 1-26.

[11] Spanggaard, H.; Krebs, F. C. Solar Energy Mater Solar cells 2004, 83, 125-146.

[12] Lee, J. K.; Fujida, K.; Tsutsui, T.; Kim, M. R. Solar Energy Mater Solar cells 2007, 91, 892-896.

[13] Schindler, F.; Lupton, J. M.; Feldmann, J.; Scherf, U. Proc Natl Acad Sci USA 2004, 101, 14695-14700.

[14] Barbara, P. F.; Gesquiere, A. J.; Park, S. J.; Lee, Y. J. Acc Chem Res 2005, 38, 602-610.

[15] Padmanaban, G.; Ramakrishnan, S. J Am Chem Soc 2000, 122, 2244-2251.

[16] Traiphol, R.; Charoenthai, N. Synth Met 2008, 158, 135-142.

[17] Traiphol, R.; Sanguansat, P.; Srikhirin, T.; Kerdcharoen, T.; Osotchan, T. Macromolecules 2006, 39, 1165-1172.

[18] Klaerner, G.; Miller, R. D. Macromolecules 1998, 31, 2007-2009.

[19] Bunz, U. H. F. Chem Rev 2000, 100, 1605-1644.

[20] Ding, L.; Lu, Z.; Egbe, D. A. M.; Karasz, F. E. Macromolecules 2004, 37, 6124-6131.

[21] Huang, C.; Zhen, C. G.; Su, S. P.; Vijila, C.; Balakrisnan, B.; Auch, M. D. J.; Loh, K. P.; Chen, Z. K. Polymer 2006, 47, 1820-1829.

[22] Padmanaban, G.; Ramakrishnan, S. J Phys Chem B 2004, 108, 14933-14941.

[23] Scherf, U.; List, E. J. W. Adv Mater 2002, 14, 477-487.

[24] Vak, D.; Chun, C.; Lee, C. L.; Kim, J. J.; Kim, D. Y. J Mater Chem 2004, 14, 1342-1346.

[25] Assaka, A. M.; Rodrigues, P. C.; de Oliveira, A. R. M.; Ding, L.; Hu, B.; Karasz, F. E.; Akcelrud, L. Polymer 2004, 45, 7071-7081.

[26] Neef, C. J.; Ferraris, J. P. Macromolecules 2000, 33, 2311-2314.

[27] Collison, C. J.; Rothberg, L. J.; Treemaneekarn, V.; Li, Y. Macromolecules 2001, 34, 2346-2352.

[28] Menon, A.; Galvin, M.; Walz, K. A.; Rothberg, L. Synth Met 2004, 141, 197-202.

[29] Traiphol, R.; Charoenthai, N.; Srikhirin, T.; Kerdcharoen, T.; Osotchan, T.; Maturos, T. Polymer 2007, 48, 813-826.

[30] Wu, C.; Peng, H.; Jiang, Y.; Mcneill, J. J Phys.Chem. B 2006, 110, 14148-14154.

[31] Nagesh, K.; Kabra, D.; Narayan, K.S.; Ramakrishnan, S. Synth Met 2005, 155, 295-298.

[32] Ananthakrishnan, N.; Padmanaban, G.; Ramakrish, S.; Reynolds, J. R. Macromolecules 2005, 38, 7660-7669.

[33] Babel, A.; Jenekhe, S. A. Macromolecules 2004, 37, 9835-9840.

[34] Iyengar, N. A.; Harrison, B.; Duran, R. S.; Schanze, K. S.; Reynolds, J. R. Macromolecules 2003, 36, 8978-8985.

[35] Lee, Y.-Z.; Chen, X.; Chen, S.-A.; Wei, P.-K.; Fann, W.-S. J Am Chem Soc 2001, 123, 2296-2307.

[36] Bai, H.; Wu, X.; Shi, G. Polymer 2006, 47, 1533-1537.

[37] Ding, L.; Lu, Z.; Egbe, D. A. M.; Karasz, F. E. Macromolecules 2004, 37, 10031-10035.

[38] Chuangchote, S.; Srikhirin, T.; Supaphol, P. Macromol Rapid Commun 2007, 28, 651-659.

[39] Traiphol, R.; Srikhirin, T.; Kerdcharoen, T.; Osotchan, T.; Scharnagl, N.; Willumeit, R. Eur Polym J 2007, 43, 478-487.

2. MORPHOLOGY AND PHOTOPHYSICAL PROPERTIES OF ELECTROSPUN LIGHT-EMITTING POLYSTYRENE/POLY(P-PHENYLENE ETHYNYLENE) FIBERS

2.1 Introduction

Since the discovery of the electrical conductivity in π-conjugated polymers thirty years ago,[1] (semi)conducting polymers have become the focus of intense research and development activities around the world.[2] Their use as synthetic metals[3] and as organic semiconductors in light-emitting diodes,[4] field-effect transistors,[5] photovoltaic devices,[6] sensors[7] and many other applications, has led to rapid growth of the field. Many different families of conjugated polymers, for example, poly(phenylene vinylene)s (PPVs),[8] poly(fluorene)s (PFs),[9] and poly(phenylene ethynylene)s (PPEs),[10] are being studied, often with the objective of tailoring their properties to meet the needs of these applications. PPE and its derivatives represent an interesting family because of their nonlinear optical characteristics,[11] photo-[12] and electroluminescent properties,[13] charge-carrier mobility,[14] and chemical responsiveness,[15] which make them attractive for use in applications that include organic light-emitting diodes,[16] light polarizers,[17] liquid crystal displays (LCDs),[18] transistors,[19] solar cells[20] and sensors.[21] Recently, cross-linked PPE networks[22] were demonstrated to be of a microporous nature with specific surface areas that exceed those of activated carbons and offer investigations with regards to the properties of PPEs have been in either solution or thin films, relatively little attention has been paid to the study of the polymers in the form of ultra-fine fibers, which offer high aspect and high surface area to volume or mass ratios.

Recently, Bunz and coworkers reported the investigation of the morphology and photophysical properties of electrospun (e-spun) poly(arylene ethynylene)s (PAEs) with dioctyl or polycaprolactone (PCL) side chains.[24] Interestingly, poly(2,5-dioctyl-p-phenylene ethynylene) with a degree of polymerization (DP) of 60 could only be sprayed into microspheres with average diameters of 1–1.5 μm, but not spun into fibers. On the other hand, grafting PCL chains with a DP of at least 65 to either a poly(p-phenylene ethynylene) or poly(benzothiadiazoleco-alkyne-co-benzene-co-alkyne) core resulted in materials that could, under optimized conditions, be spun into welldefined fibers with diameters ranging from 50 nm to 1 μm. The nature of the solvent, the concentration of the polymer in the spinning solution, and the DPs of the PCL side chains and the PAE core were all found to play a major role in determining the morphology of the electrospun products obtained. Most importantly, the high-molecular-weight PCL side chains employed by Bunz contribute significantly to the viscosity of the solution, allowing electrospinning (e-spinning) of high-quality fibers.[24] On the other hand, e-spinning of a more common PPE derivative (i.e., one in which the electrospinnability is not imparted through high molecular weight side chains) into fiber form has not yet been reported. This appears directly related to rheological limitations.[25–32] PAEs are often produced as materials of rather low-

molecular weight, sometimes deliberately to maintain good solubility,[12a] so that even at their solubility limit they form solutions of low viscosity.[24]

We here report an approach that is orthogonal to the high-DP side chain route, namely the e-spinning of blends of a common poly(2,5-dialkoxy-p-phenylene ethynylene) derivative featuring an alternate substitution of ethylhexyloxy and octyloxy in the 2 and 5 positions of the phenylene rings (EHO-OPPE;[12a] see Figure 2.1) and polystyrene (PS) as an 'inert' carrier polymer. We demonstrate that this approach allows one to produce ultra-fine fibers with diameters that range from hundreds of nanometers to one micrometer.

2.2 Experimental

2.2.1 Materials and Preparation of Solutions for Spinning and Casting Films

EHO-OPPE ($M_n \approx$ 14,000 Da; Figure 2.1) was synthesized following a procedure previously described.[12a] PS ($M_w \approx 3.0 \times 10^5$ Da; pellet form) was a general purpose grade from Dow Chemicals (USA). The solvents used were 1,2-dichloroethane [DCE; Lab-Scan (Asia), Thailand] and chloroform (CF; Carlo Erba, Italy). Pyridinium formate (PF), a volatile organic salt, was prepared by reacting pyridine [Lab-Scan (Asia), Thailand] and formic acid (Merck, England) in an equimolar quantity. Solutions of 8.5% (w/v) PS/EHO-OPPE in DCE or CF (the compositional weight ratio between PS and EHO-OPPE being 7.5:1) with or without the addition of 8 vol.-% PF were prepared by combining all compounds and stirring at room temperature for 5 min. A solution of 8.5% (w/v) PS in DCE was prepared in similar fashion and was used as a reference.

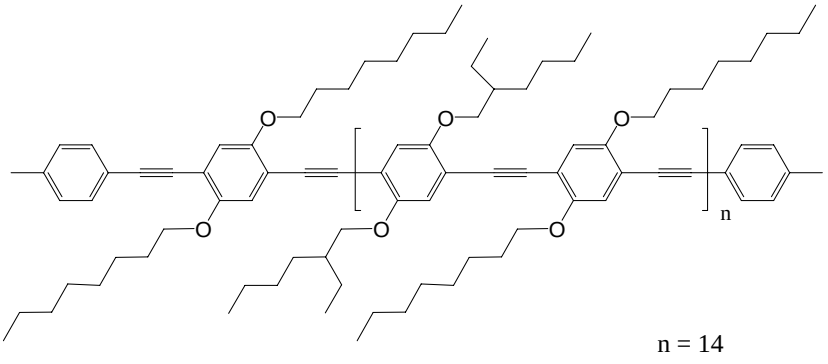

Figure 5.1 Chemical structure of EHO-OPPE, the PPE derivative used.

2.2.2 Electrospining

E-spinning of the as-prepared solutions was carried out under an electrical potential of between 7.5 and 20 kV. Unless otherwise indicated, products (i.e., fibers and/or beads) were spun at an applied electrical potential of 15 kV. The collection distance and the collection time were fixed at

10 cm and 1 min, respectively. Each of the freshly-prepared spinning solutions was placed in a 5 mL plastic syringe, the open end of which was connected to a blunt 20 gauge stainless steel hypodermic needle (outer diameter = 0.91 mm), which was used as the nozzle. An aluminum foil wrapped around a rigid plastic sheet was used as the collector plate. The emitting electrode of positive polarity from a Gamma High-Voltage Research ES30P DC power supply (Florida, USA) was connected to the needle, while the grounding electrode was connected to the collector plate. The feed rate of the solution was controlled by means of a Kd Scientific syringe pump at 1 $mL \cdot h^{-1}$. Where applicable, the e-spun fibers were annealed for between 5 min and 1 h at 110 °C, which is above the glass transition temperature (Tg) of PS (95 °C[33]).

2.2.3 Spin-Coating and Solution-Casting

Films of the PS/EHO-OPPE blends were produced by either spin coating or solution casting from solutions comprising 8–10 $mg \cdot mL^{-1}$ of the polymer blend. Spin coating was done on a Specialty Coating Systems model P6700 with spinning speeds of 1,500–2,000 rpm to achieve a final thickness of 0.5–1 μm. Solution casting was done on glass slides and resulted films of a final thickness of 1–3 μm.

2.2.4 Characterizations

The morphological appearance of the e-spun fibers was examined by a JEOL JSM-5410LV scanning electron microscope (SEM). The average bead diameters and the number of beads per unit area (i.e., the bead density) of the electrosprayed beads or the e-spun beaded fibers were calculated from measurements of SEM images at ×500 magnification. Diameters of the e-spun fibers, where applicable, were determined from SEM images at ×1,000 magnification, with the average value being calculated from at least 50 measurements (for each spinning condition). For beaded fibers, only the diameters of the fiber segments between beads were measured. A Thermo-Nicolet Nexus 670 Fourier-transform infrared (FT-IR) spectroscope was used to characterize the as-received PS pellets, the as-synthesized EHO-OPPE, and some of the e-spun PS/EHO-OPPE products. Optical absorption and photoluminescence emission spectra of the PS/EHO-OPPE solutions in DCE and CF with or without PF addition, the corresponding pristine and annealed e-spun fibers, spin-coated films, and solution-cast films were measured by a Hewlett Packard-8254A diode array UV-vis spectrophotometer (UV-vis) and a Perkin-Elmer LS50 luminescence spectrometer (PL). For the solution measurements, a 1mmthick quartz cuvette was used in order to reduce the self-absorption effect, allowing the detection of photon emission from front surface. For PL experiments, samples were excited at 400 nm.

2.3 Results and discussion

Polystyrene (PS), a non-luminescent glassy-amorphous polymer, was chosen as an 'inert' carrier polymer for the present study. Neat PS was e-spun for reference purposes from 1,2-dichloroethane (DCE) to determine the morphology of the neat polymer template when processed under the conditions selected for this study. Figure 2.2 shows representative SEM images of the products obtained from a 8.5% (w/v) solution of PS in DCE under various electrical potentials between 7.5 and 20 kV. The e-spinning of a 8.5% (w/v) PS solution in DCE only resulted in the formation of beads, with average size in the range of 22.6–29.0 μm (see Figure 2.2 and Table 2.1). The density of the beads on the collection plate was between 0.17×10^5 and 0.56×10^5 beads·cm^{-2}. This tendency to form beads rather than ultra-fine fibers was previously observed and reported for PS that was e-spun from DCE or chloroform (CF), the second solvent employed here, if the concentration of the PS solutions was less than 10 wt.-%.[34]

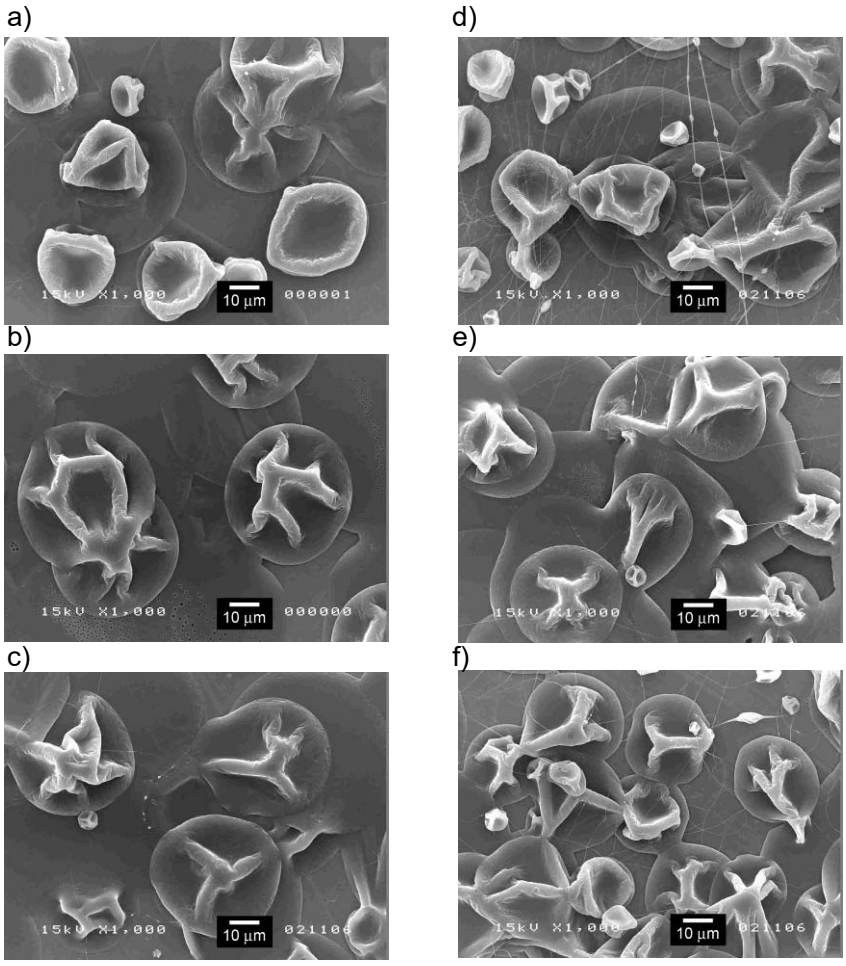

Figure 2.2 SEM images of the electrosprayed PS beads from 8.5% (w/v) solutions of PS in DCE (×1000, scale bar = 10 μm). The applied electrical potential for the electrospinning was: a) 7.5, b) 10, c) 12.5, d) 15, e) 17.5, and f) 20 kV.

Table 2.1 Average fiber diameter, bead size and bead density of the electrospun products from 8.5% (w/v) solutions of PS in DCE and 8.5% (w/v) solutions of PS/EHO-OPPE (PS:EHO-OPPE = 7.5:1) in DCE and CF without and with the addition of 8 vol.-% PF. The table lists parameters for materials e-spun at different applied electrical potentials (HV). The collection distance was 10 cm, the collection time was 1 min and the solution flow rate was 1 mL·h^{-1}

Solution	HV (kV)	Fiber Diameters (μm)	Bead Size (μm)	Bead Density (beads·cm^{-2})
PS/EHO-OPPE /CF	7.5	0.51 ± 0.12	13.65 ± 0.65	4.13×10^5
	10.0	0.56 ± 0.12	14.05 ± 0.80	4.23×10^5
	12.5	0.63 ± 0.14	15.14 ± 0.82	5.25×10^5
	15.0	0.66 ± 0.15	16.11 ± 1.19	2.76×10^5
	17.5	0.68 ± 0.20	17.80 ± 1.31	2.82×10^5
	20.0	0.68 ± 0.15	18.05 ± 1.23	2.46×10^5
PS/EHO-OPPE /CF + PF	7.5	1.04 ± 0.33	1.06 ± 0.55	0.66×10^5
	10.0	1.04 ± 0.39	4.24 ± 1.84	2.26×10^5
	12.5	1.05 ± 0.37	4.41 ± 2.21	1.71×10^5
	15.0	1.12 ± 0.53	5.00 ± 2.64	1.51×10^5
	17.5	1.16 ± 0.38	5.23 ± 2.24	1.47×10^5
	20.0	1.20 ± 0.37	5.76 ± 3.74	1.36×10^5

Interestingly, the electro-spinnability of the PS solution in DCE was significantly improved in the presence of a comparably small amount of EHO-OPPE [i.e., PS:EHO-OPPE = 7.5:1 (w/w)]. Representative SEM images of the e-spun products (see Figure 2.3a) clearly show the appearance of ultra-fine fibers with a limited density of elongated beads. The average fiber diameters, bead size, and bead density of the beaded fibers obtained are in the range of 0.43–0.83 μm, 2.77–3.65 μm and 1.43×10^5–3.77×10^5 beads·cm^{-2}, respectively (see Table 2.1). To further improve the electro-spinnability of the PS/EHO-OPPE solution, the volatile organic salt pyridinium formate (PF) was added.[32] Figure 2.3b shows representative SEM images of the e-spun products. Either smooth or beaded fibers with fewer beads were observed. The average fiber diameter range increased to 0.55–0.87 μm, while the bead size range remained about the same at 2.12–4.89 μm. However, the bead density range decreased to 0.04×10^5–1.32×10^5 beads·cm^{-2}. This substantial decrease in the bead density shows that the addition of PF helps to promote uniform fiber formation.

Table 2.1 (Cont.) Average fiber diameter, bead size and bead density of the electrospun products from 8.5% (w/v) solutions of PS in DCE and 8.5% (w/v) solutions of PS/EHO-OPPE (PS:EHO-OPPE = 7.5:1) in DCE and CF without and with the addition of 8 vol.-% PF. The table lists parameters for materials e-spun at different applied electrical potentials (HV). The collection distance was 10 cm, the collection time was 1 min and the solution flow rate was 1 $mL \cdot h^{-1}$

Solution	HV (kV)	Fiber Diameters (μm)	Bead Size (μm)	Bead Density (beads·cm^{-2})
PS/EHO-OPPE /CF	7.5	0.51 ± 0.12	13.65 ± 0.65	4.13×10^5
	10.0	0.56 ± 0.12	14.05 ± 0.80	4.23×10^5
	12.5	0.63 ± 0.14	15.14 ± 0.82	5.25×10^5
	15.0	0.66 ± 0.15	16.11 ± 1.19	2.76×10^5
	17.5	0.68 ± 0.20	17.80 ± 1.31	2.82×10^5
	20.0	0.68 ± 0.15	18.05 ± 1.23	2.46×10^5
PS/EHO-OPPE /CF + PF	7.5	1.04 ± 0.33	1.06 ± 0.55	0.66×10^5
	10.0	1.04 ± 0.39	4.24 ± 1.84	2.26×10^5
	12.5	1.05 ± 0.37	4.41 ± 2.21	1.71×10^5
	15.0	1.12 ± 0.53	5.00 ± 2.64	1.51×10^5
	17.5	1.16 ± 0.38	5.23 ± 2.24	1.47×10^5
	20.0	1.20 ± 0.37	5.76 ± 3.74	1.36×10^5

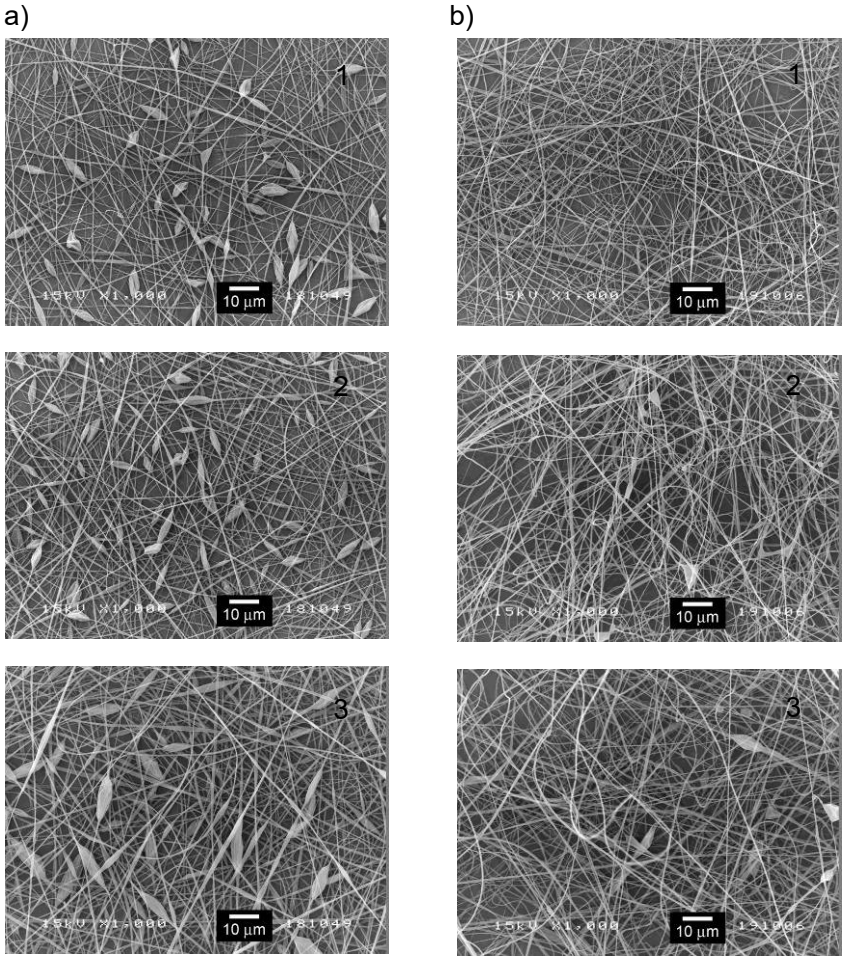

Figure 2.3 SEM images of the electrospun products from 8.5% (w/v) solutions of PS/EHO-OPPE (PS:EHO-OPPE = 7.5:1) in DCE without (a) and with (b) the addition of 8 vol.-% PF (×1,000, scale bar = 10 μm). The applied electrical potential for the electrospinning was (1) 7.5, (2) 10, (3) 12.5, (4) 15, (5) 17.5 and (6) 20 kV.

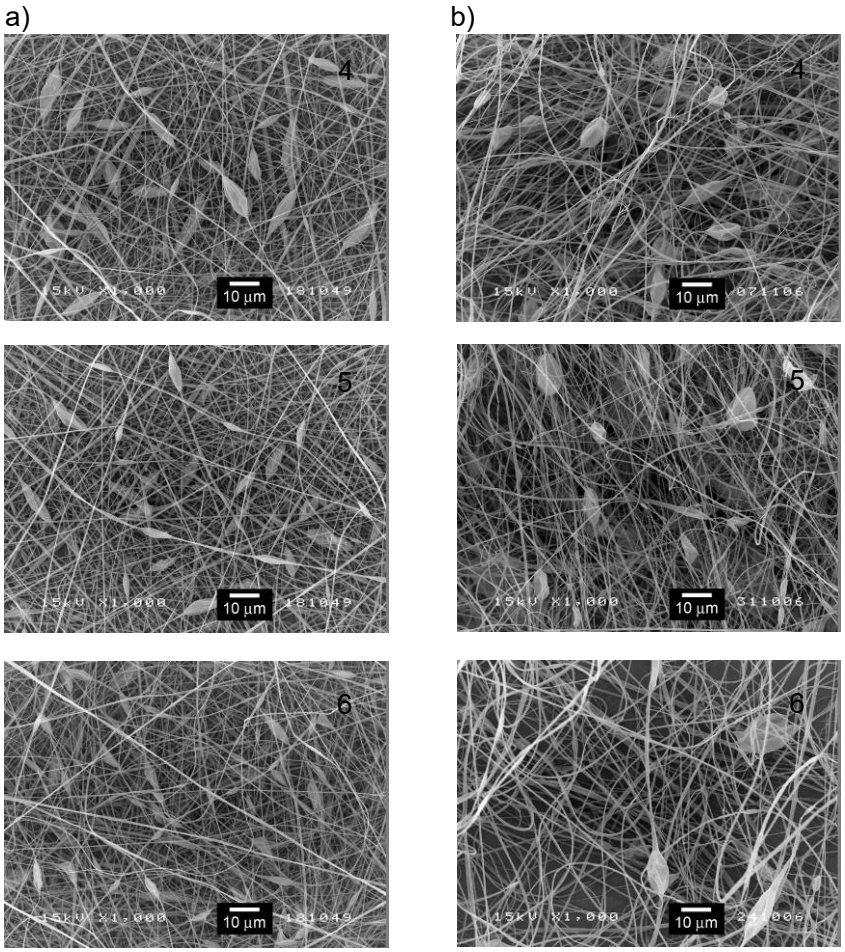

Figure 2.3 (cont.) SEM images of the electrospun products from 8.5% (w/v) solutions of PS/EHO-OPPE (PS:EHO-OPPE = 7.5:1) in DCE without (a) and with (b) the addition of 8 vol.-% PF (×1,000, scale bar = 10 μm). The applied electrical potential for the electrospinning was (1) 7.5, (2) 10, (3) 12.5, (4) 15, (5) 17.5 and (6) 20 kV.

The same trends were observed when CF was used as the solvent (see Figure 2.4a and b). In this case, the average fiber diameters, bead sizes, and bead densities of the e-spun PS/EHO-OPPE fibers from the blend solution without the addition of PF are in the range of 0.51–0.68 μm, 13.65–18.05 μm and 2.46 × 10^5–5.25 × 10^5 beads·cm^{-2}, respectively (see Table 2.1). Here, the addition of PF in the blend solution also resulted in an observed increase of the average fiber diameters in the range of 1.04–1.20 μm and an observed decrease of the bead density in the range of 0.66 × 105–1.71 × 10^5 beads·cm^{-2}. On the other hand, the bead size was found to decrease in the range of 1.06–5.76 μm (see Table 2.1).

Based on these results, it appears that DCE is a better solvent than CF for the e-spinning of the blend solution of PS and EHO-OPPE, because the average fiber diameters, bead sizes, and bead densities of the products obtained from the blend solutions – with and without PF – in DCE are lower than those of the products obtained from the corresponding blend solutions in CF. Based on the quantitative results summarized in Table 2.1, it is evident that the average diameter of the e-spun fibers increases with increasing applied electrical potential. This is a direct result of the increase in the total number of charged species within the jet segment, which, in turn, causes an increase in the electrostatic forces. The increase in such forces leads to an increase in the speed of the jet and a hypothetic decrease in the total path trajectory of the jet, which results in an increase in the feed flow rate and ultimately the diameters of the obtained fibers.[35,36] Clearly, the addition of PF to the spinning solution also improves significantly the electro-spinnability of the spinning solution, as shown from the substantial decrease in the bead density (see Table 2.1). In view of previous studies, which based the results on an increase in the number of charge carriers within the jet due to the addition of PF, this result does not come as a surprise.[35,37,38]

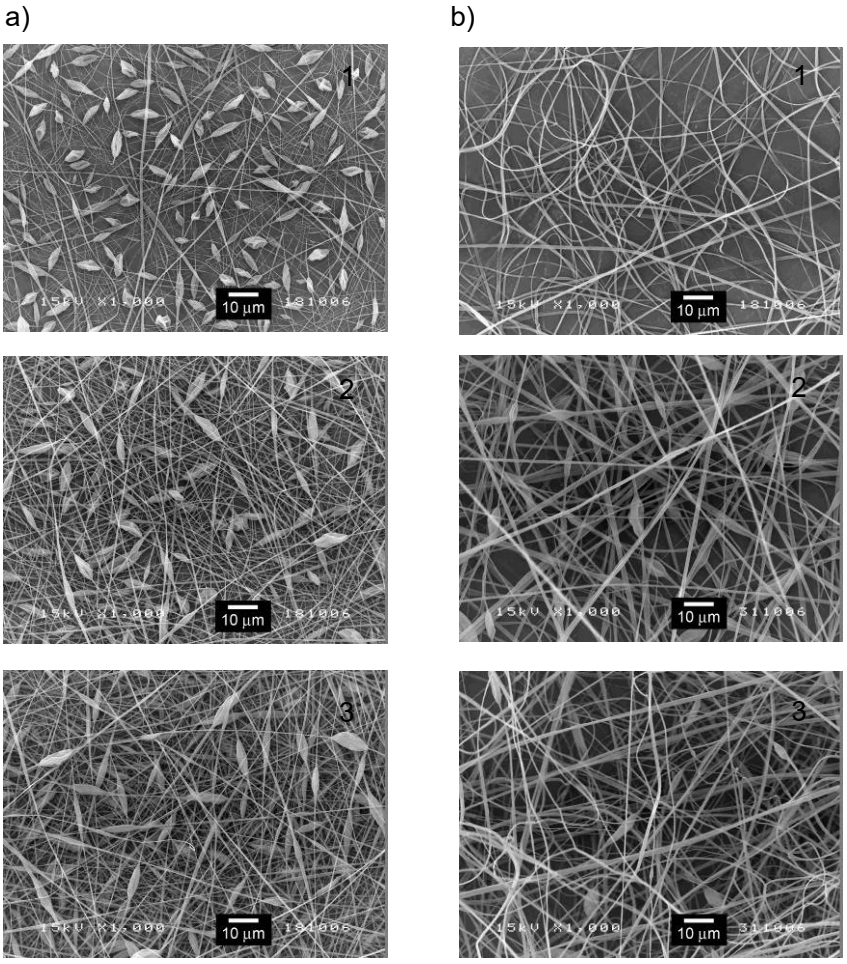

Figure 2.4 SEM images of the electrospun products from 8.5% (w/v) solutions of PS/EHO-OPPE (PS:EHO-OPPE = 7.5:1) in CF without (a) and with (b) the addition of 8 vol.-% PF (×1,000, scale bar = 10 μm). The applied electrical potential for the electrospinning was (1) 7.5, (2) 10, (3) 12.5, (4) 15, (5) 17.5 and (6) 20 kV.

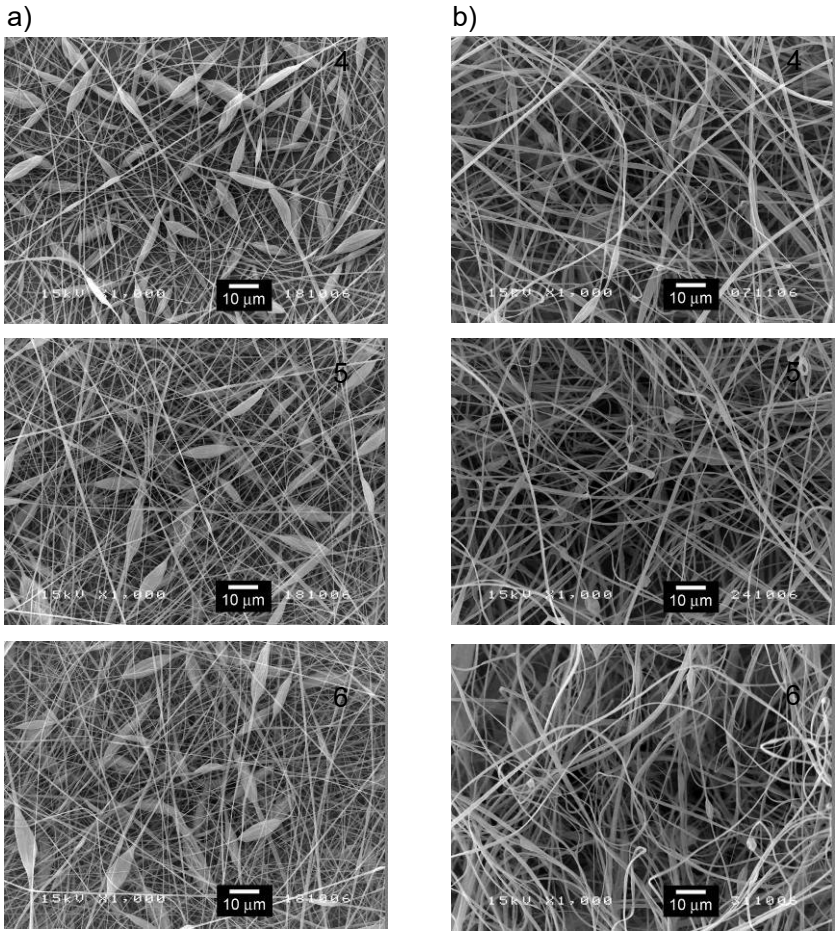

Figure 2.4 (cont.) SEM images of the electrospun products from 8.5% (w/v) solutions of PS/EHO-OPPE (PS:EHO-OPPE = 7.5:1) in CF without (a) and with (b) the addition of 8 vol.-% PF (×1,000, scale bar = 10 μm). The applied electrical potential for the electrospinning was (1) 7.5, (2) 10, (3) 12.5, (4) 15, (5) 17.5 and (6) 20 kV.

FT-IR spectroscopy was conducted to confirm the existence of both PS and EHO-OPPE constituents in the e-spun blend fibers (see Figure 2.5). Individual spectra are shown of the as-received PS, the as-synthesized EHO-OPPE, and the selected fiber mats which had been e-spun from 8.5% (w/v) solution of PS in DCE and 8.5% (w/v) solutions of PS/EHO-OPPE in DCE or CF with and without the addition of PF at an electrical potential of 15 kV. Table 2.2 summarizes some absorption peaks specific to chemical functionalities of the PS and the EHO-OPPE components in the e-spun fibers. Clearly, the peaks characteristic to the PS component are observed in all of the FT-IR spectra of the e-spun fibers (i.e., at 697–698, 754–756, 906, 1 490, 2,920, 3,030 and 3,060 cm^{-1}). Moreover, some peaks characteristic to the EHO-OPPE component (e.g., at 1,210 and 1,270

cm^{-1}) are also observed in the FT-IR spectra of the e-spun fibers. The peak at 1,210 cm^{-1} corresponds to ring stretching vibrations and C–H deformation, while the peak at 1,270 cm^{-1} is specific to aryl alkyl ether (C–O–C) asymmetric stretching vibrations. These results confirm the existence and the chemical integrity of both the PS and the EHO-OPPE components in the e-spun fibers.

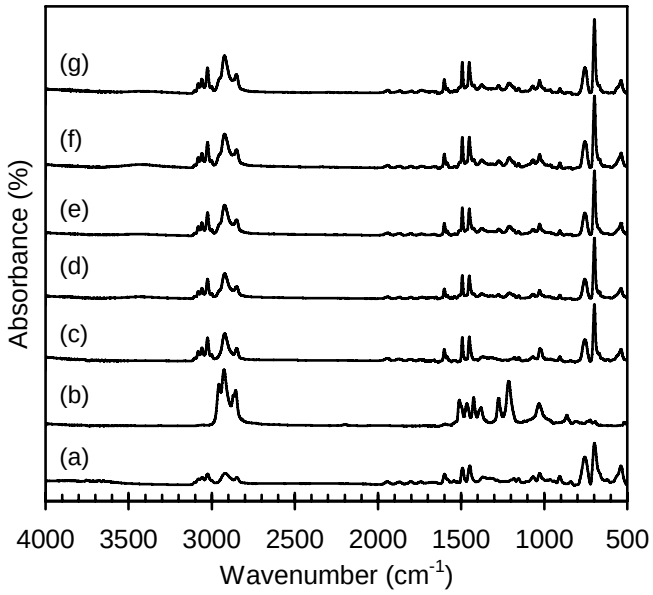

Figure 2.5 FT-IR spectra of a) as-received neat PS, b) EHO-OPPE powder, and the electrospun fibers from, c) 8.5% (w/v) solution of PS in DCE, 8.5% (w/v) solutions of PS/EHO-OPPE (PS:EHO-OPPE = 7.5:1) in DCE without d) and with e) the addition of 8 vol.-% PF, and 8.5% (w/v) solutions of PS/EHO-OPPE (PS:EHO-OPPE = 7.5:1) in CF without f) and with g) the addition of 8 vol.-% PF.

The optical properties of the spinning solutions, pristine and annealed e-spun fibers, and spin-coated and solution-cast reference films were investigated by UV-Vis absorption and PL spectroscopy and the results are summarized in Table 2.3. Figure 2.6a and b summarize the optical properties of the 8.5% (w/v) spinning solutions of PS/EHO-OPPE (7.5:1 w/w) in DCE and CF with and without 8 vol.-% PF. All spectra were normalized to allow for easy comparison. The emission spectra of 8.5% (w/v) solutions of PS/EHO-OPPE in DCE exhibit sharp peaks at 487 and 508 nm (see Figure 2.6b). The emission spectra of 8.5% (w/v) solutions of PS/EHO-OPPE in CF are almost identical, displaying maxima at 485 and 507 nm, respectively (see Figure 2.6b). While the solvent has a slight solvatochromic effect on the absorption and the emission maxima of EHO-OPPE in DCE and CF, the addition of PS and PF does not exert any appreciable influence on the optical characteristics of the conjugated polymer. The features – splitting of the emission spectra into two

well-resolved bands and the lack of mirror image similarity between absorption and emission – are related to vibronic coupling and are characteristic of alkyloxy-PPE emission.[12a]

Table 2.2 Analysis of FT-IR spectra of as-received PS, EHO-OPPE and the electrospun products from 8.5% (w/v) solutions of PS in DCE and 8.5% (w/v) solutions of PS/EHO-OPPE (PS:EHO-OPPE = 7.5:1) in DCE and CF without and with the addition of 8 vol.-% PF

Absorption Band (cm^{-1})							Assignment
As-received Materials		Electrospun Products					
PS	EHO-OPPE	PS/ DCE	PS/ EHO-OPPE/ DCE	PS/ EHO-OPPE/ DCE + PF	PS/ EHO-OPPE/ CF	PS/ EHO-OPPE/ CF + PF	
698	-	698	697	697	697	697	CH bending vibrations in CH deformation
754	-	756	755	756	755	756	CH out-of-plane bending vibrations in -CH=CH-(cis) group
-	863	-	-	-	-	-	CH out-of-plane bending vibrations in $C=CH_2$ group
906	-	906	906	906	905	905	CH out-of-plane bending vibrations in $-CH=CH_2$ group
-	1,030	1,030	1,030	1,030	1,030	1,030	Aryl alkyl ether (C-O-C) symmetric stretching vibrations
-	1,210	-	1,210	1,210	1,210	1,210	Ring-stretching vibrations and CH deformation
-	1,270	-	1,270	1,270	1,270	1,270	Aryl alkyl ether (C-O-C) asymmetric stretching vibrations
-	1,380	-	-	-	-	-	CH bending vibrations in $-CH_3$ deformation
-	1420	-	-	-	-	-	CH bending vibrations in $-CH_2$ and $-CH_3$ deformation
1,450	1,470	1,450	1,450	1,450	1,450	1,450	Asymmetric CH bending vibrations in $-CH_3$ group
1,490	-	1,490	1,490	1,490	1,490	1,490	CH bending vibrations in $-CH_2$ Scissoring group
1,600	1,510	1,600	1,600	1,600	1,600	1,600	C=C stretching vibrations in Conjugated
2,850	2,860	2,850	2,850	2,850	2,850	2,850	Symmetric CH stretching vibrations in $-CH_2$ group
2,920	-	2,920	2,920	2,920	2,920	2,920	Asymmetric CH stretching vibrations in $-CH_2$ group
-	2,930	-	-	-	-	-	Asymmetric CH stretching vibrations in $-CH_3$ group
-	2,960	-	-	-	-	-	Asymmetric CH stretching vibrations in $-CH_3$ group
3,030	-	3,020	3,020	3,020	3,020	3,020	CH stretching vibrations in =C-H, $=CH_2$ and CH groups
3,060	-	3,060	3,060	3,060	3,060	3,060	CH stretching vibrations in =C-H, $=CH_2$ and CH groups

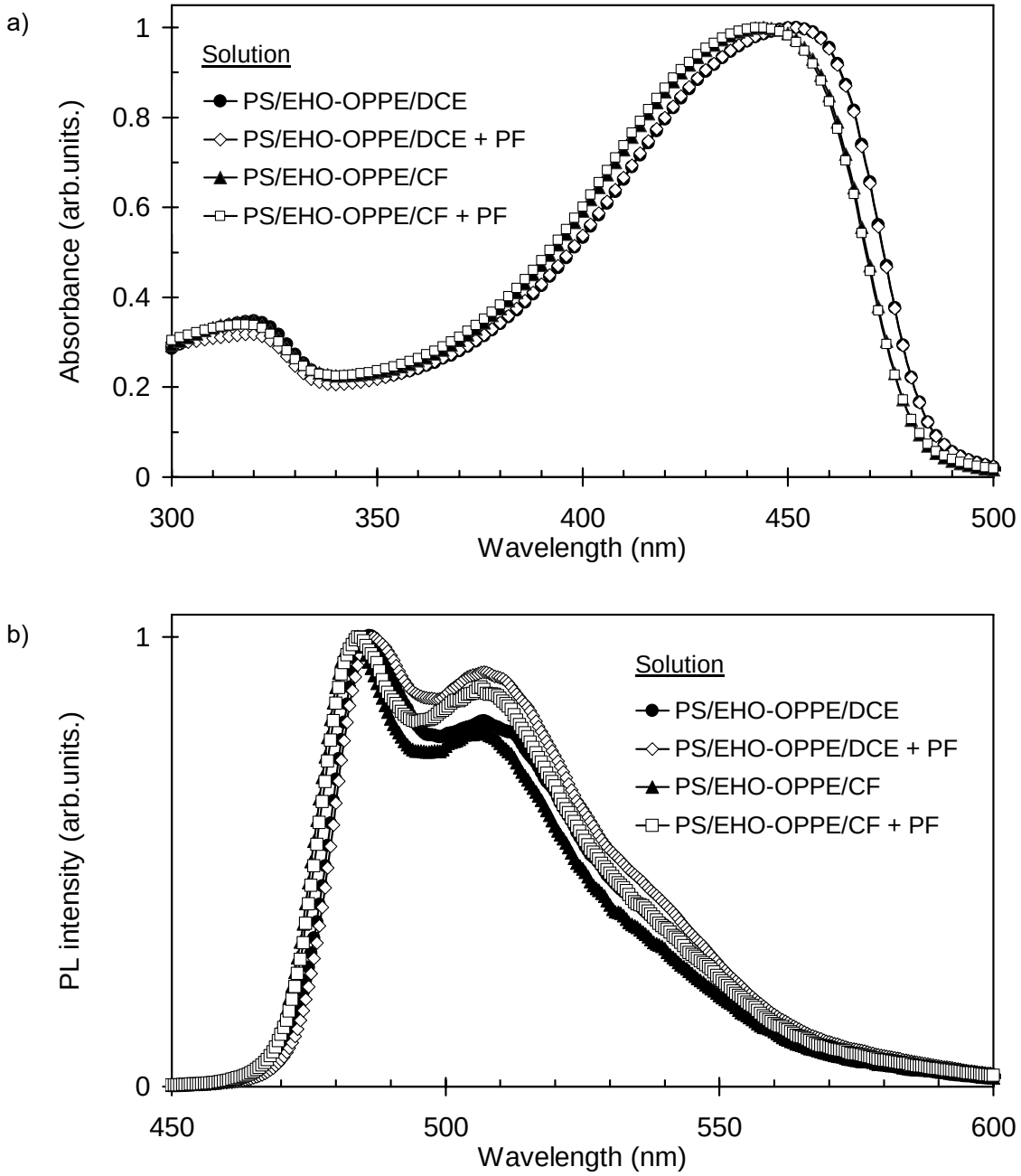

Figure 2.6 a) Absorption and b) PL emission spectra of 8.5% (w/v) solutions of PS/EHO-OPPE (PS:EHO-OPPE = 7.5:1) in DCE and 8.5% (w/v) solutions of PS/EHO-OPPE (PS:EHO-OPPE = 7.5:1) in CF without and with the addition of 8 vol.-% PF.

Figure 2.7a and b show the emission spectra of fibers spun from 8.5% (w/v) solutions of PS/EHO-OPPE with 8 vol.-% PF in DCE and CF, respectively, as a function of the applied electrical potential. All emission spectra exhibit a broad peak centered around 508–519 nm and weak shoulders around 457–461 and 590–599 nm. Compared to the emission spectra of the spinning

solutions, the emission spectra of the e-spun fibers show less-well-resolved features and appear somewhat broadened, indicative of aggregation of the conjugated polymer guest in the PS matrix. While the PL spectra of the fibers that had been e-spun at different electrical potential exhibit minor differences (see Table 2.4), there is no specific correlation between the emission peak positions and the applied electrical potential. It is postulated that the slight variation in the emission peak positions occurs from the fluctuation in the forces acting on jet segments, and hence the EHO-OPPE molecules, during the e-spinning.

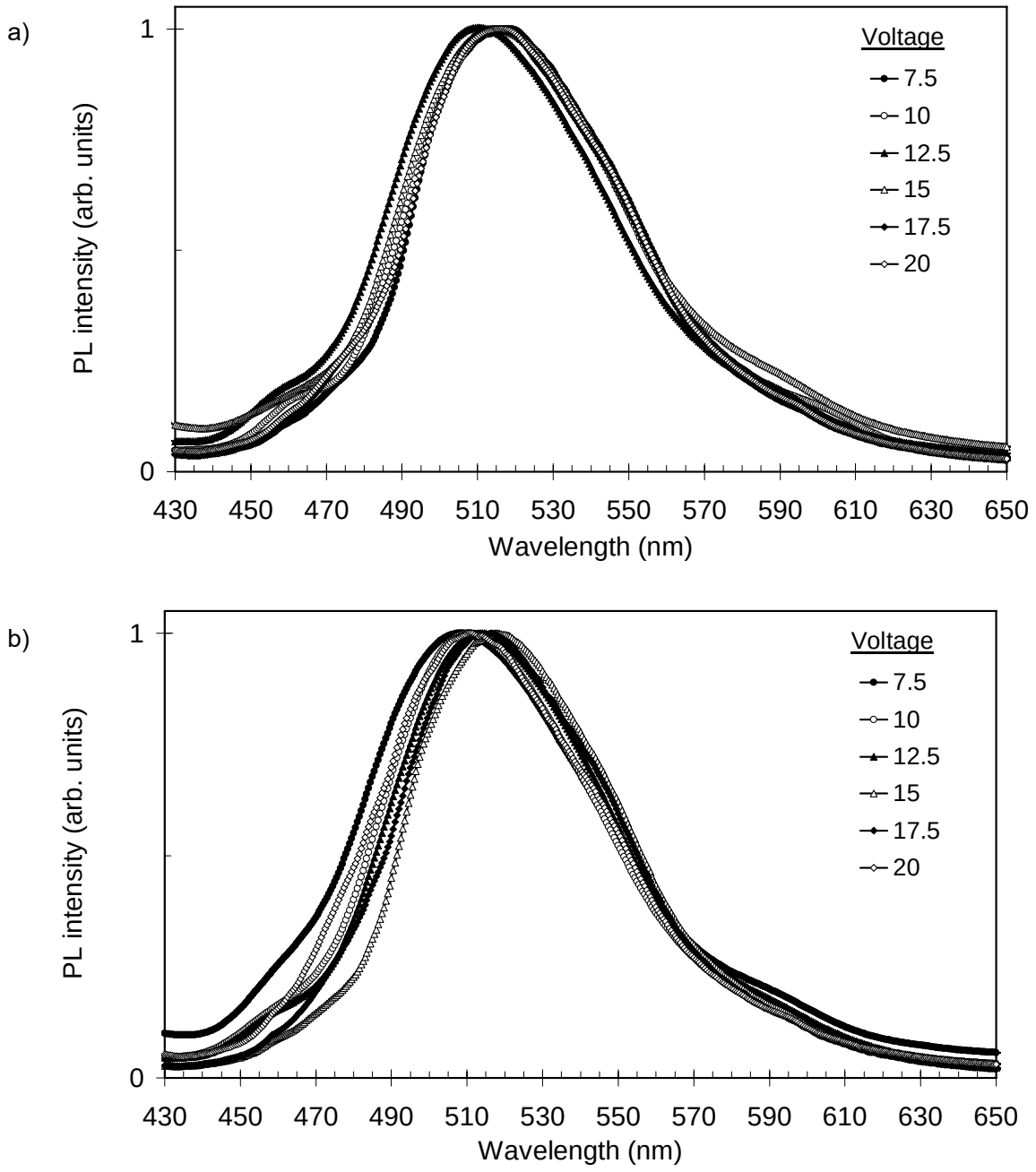

Figure 2.7 PL emission spectra of the electrospun fibers from 8.5% (w/v) solutions of PS/EHO-OPPE (PS:EHO-OPPE = 7.5:1) with the addition of 8 vol.-% PF in a) DCE, and b) CF at various applied electrical potentials.

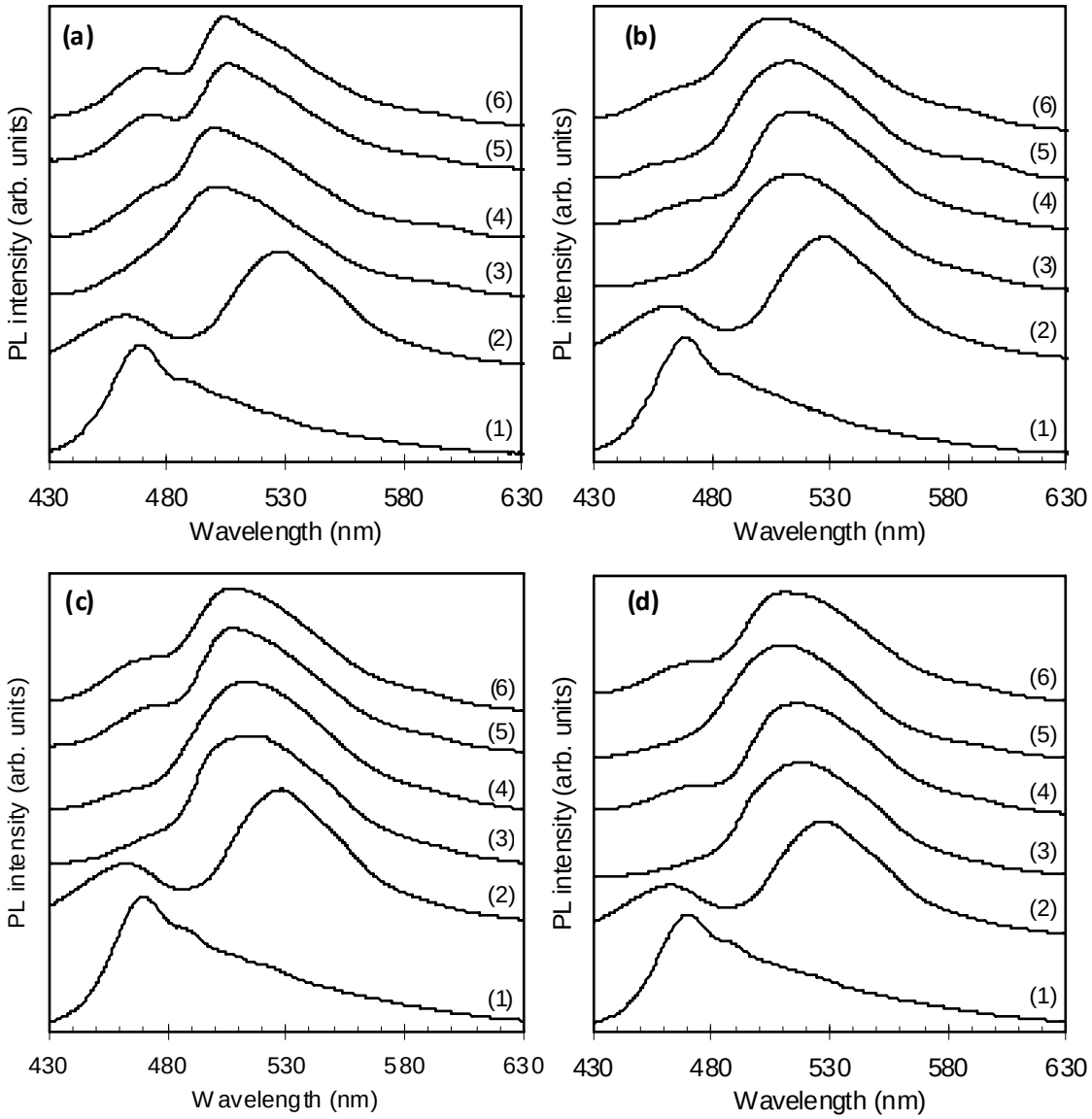

Figure 2.8 Emission spectra of samples produced from solutions of 8.5% (w/v) PS/EHO-OPPE (PS:EHO-OPPE = 7.5:1) in a) DCE, b) DCE with the addition of 8 vol.-% PF, c) CF and d) CF with the addition of 8 vol.-% PF. Samples were (1) spin-coated films, (2) solution-cast films, (3) pristine e-spun fibers, and e-spun fibers annealed at 110 °C for (4) 5 min, (5) 30 min, and (6) 1 h.

For the purpose of comparison, the emission characteristics of films prepared by spin-coating and solution-casting of 8.5% (w/v) solutions of PS/EHO-OPPE in DCE and CF with and without 8 vol.-% PF were also investigated. All spin-coated films [Figure 2.8a–d, Series (1)] show virtually identical spectra with well-resolved features and maxima at ≈ 470 and ≈ 508 nm. The spectral shape is indicative of emission from well dispersed – as opposed to aggregated – PPE molecules, [12a] suggesting that rapid solvent evaporation during spin-coating produces kinetically-trapped,

molecularly-mixed PS/EHO-OPPE blends. Presumably due to the less polar nature of PS as the solid solvent, the emission spectra are slightly blue-shifted compared to those recorded in DCE and CF solution (Figure 2.7). The emission spectra of the solution-cast films [Figure 2.8a–d, Series (2)] paint a slightly different picture. Here, two major bands centered at ≈ 465–473 and 529 nm are observed. While the former coincides with the high-energy band observed in the spin-coated films and appears to be associated with emission from well-dispersed PPE molecules, the latter suggests emission from a neat (but disordered) PPE phase.[12a,13c] This finding reflects that slow solvent evaporation results in phase-separated PS/EHO-OPPE blends, indicative of thermodynamic immiscibility of the two polymers.

Table 2.3 Summary of the positions of peaks and shoulders of the PL emission spectra of 8.5% (w/v) solutions of PS/EHO-OPPE (PS:EHO-OPPE = 7.5:1) in DCE and CF without and with the addition of 8 vol.-% PF, the corresponding spin-coated and solution-cast films, and the as-annealed (i.e., at 110 °C) PS/EHO-OPPE fibers

Samples	System	Annealing Time (min)	Peaks (nm)		Shoulders (nm)	
			High Intensity	Low Intensity	High Energy	Low Energy
Solutions	DCE	-	487	509	-	-
	DCE + PF	-	487	508	-	-
	CF	-	485	506	-	-
	CF + PF	-	485	508	-	-
Spin-coated films	DCE	-	470	-	490	-
	DCE + PF	-	470	-	490	-
	CF	-	470	-	489	-
	CF + PF	-	470	-	489	-
Solution-cast films	DCE	-	463	529	-	-
	DCE + PF	-	462	529	-	-
	CF	-	463	528	-	-
	CF + PF	-	462	528	-	-

A comparison of the PL emission spectra of pristine e-spun fibers [Figure 2.8a–d, Series (3)] with those of the spin-coated and the solution-cast films shows that the fiber emission is virtually exclusively due to emission from a phase-separated PPE phase. Assuming that annealing above the

T_gs of the polymers (95 °C for PS; 90 °C for EHO-OPPE[12b]) could change the morphology (and therewith the optical properties) of the blends, the e-spun nanofibers were annealed for up to 1 h at 110 °C. The effect of thermal annealing on the emission spectra is reflected by the spectra shown in Figure 2.8a–d, Series 4–6. Interestingly, annealing leads to the appearance of an emission band around ≈ 465–470 nm, the intensity of which increases with the annealing time. This finding is consistent with an increased miscibility of the two polymers at higher temperature, causing at least a minor portion of the conjugated polymer molecules to disperse in the PS host upon annealing. Obviously, that morphology is maintained when the samples are cooled to room temperature.

Table 2.3 (Cont.) Summary of the positions of peaks and shoulders of the PL emission spectra of 8.5% (w/v) solutions of PS/EHO-OPPE (PS:EHO-OPPE = 7.5:1) in DCE and CF without and with the addition of 8 vol.-% PF, the corresponding spin-coated and solution-cast films, and the as-annealed (i.e., at 110 °C) PS/EHO-OPPE fibers

Samples	System	Annealing Time (min)	Peaks (nm)		Shoulders (nm)	
			High Intensity	Low Intensity	High Energy	Low Energy
E-spun fibers	DCE	0	503	-	468	594
		5	503	-	473	595
		30	505	-	473	594
		60	505	-	473	595
	DCE + PF	0	516	-	465	594
		5	515	-	469	595
		30	513	-	465	594
		60	507	-	465	596
	CF	0	516	-	464	595
		5	514	-	464	594
		30	509	-	469	594
		60	507	-	470	593
	CF + PF	0	519	-	466	595
		5	517	-	470	594
		30	511	-	469	595
		60	510	-	470	594

Table 2.4 Summary of the positions of peaks and shoulders of the PL emission spectra of the electrospun fibers from 8.5% (w/v) solutions of PS/EHO-OPPE (PS:EHO-OPPE = 7.5:1) in DCE and CF with 8 vol.-% PF at various applied electrical potentials (HV)

Solution	HV (kV)	Peak (nm)	Shoulders (nm)	
			High Energy	Low Energy
PS/EHO-OPPE /DCE + PF	7.5	517	460	595
	10.0	515	461	599
	12.5	510	457	591
	15.0	516	458	594
	17.5	515	459	595
	20.0	516	460	596
PS/EHO-OPPE /CF+ PF	7.5	508	460	590
	10.0	511	460	593
	12.5	514	457	591
	15.0	519	459	595
	17.5	515	458	594
	20.0	511	459	596

Figure 2.9 shows representative SEM images of the e-spun PS/EHO-OPPE fibers that had been annealed for 1 h. Minor morphological changes are evident. Many fused sections can be observed and some parts of the annealed fibers flattened into ribbons. Moreover, the size of the annealed fibers is slightly larger when compared with that of the pristine fibers (see Table 2.5), a result that is consistent with the expansion of the fused sections.

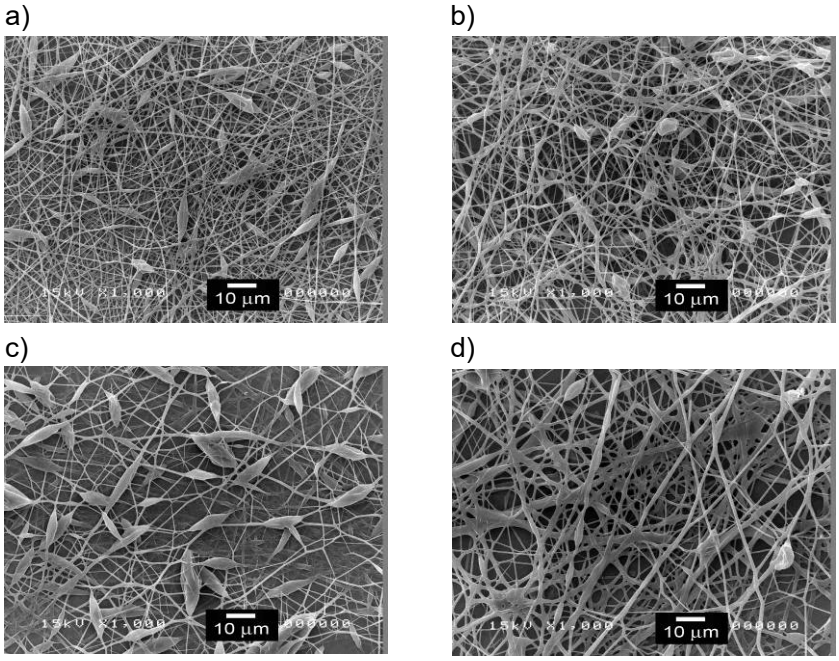

Figure 2.9 SEM images of the as-annealed fibers (1 h at 110 °C) electrospun from 8.5% (w/v) solutions of PS/EHO-OPPE (PS:EHO-OPPE = 7.5:1) in a) DCE, b) DCE with the addition of 8 vol.-% PF, c) CF and d) CF with the addition of 8 vol.-% PF (×1,000, scale bar = 10 μm).

Table 2.5 Average fiber diameter, bead size and bead density of the electrospun fibers from 8.5% (w/v) solutions of PS/EHO-OPPE (PS:EHO-OPPE = 7.5:1) in a) DCE, b) DCE with 8 vol.-% PF, c) CF, and d) CF with 8 vol.-% PF. The fibers were electrospun at an applied electrical potential of 15 kV and then annealed for 1 h at 110 °C

Annealed Fibers	Fiber Diameters (μm)	Bead Size (μm)	Bead Density (beads·cm^{-2})
PS/EHO-OPPE /DCE	0.82 ± 0.25	2.79 ± 1.22	3.26×10^5
PS/EHO-OPPE /DCE + PF	0.76 ± 0.31	3.53 ± 1.52	1.76×10^5
PS/EHO-OPPE /CF	0.68 ± 0.28	6.45 ± 1.11	3.74×10^5
PS/EHO-OPPE /CF + PF	1.15 ± 0.45	3.71 ± 1.34	1.21×10^5

2.4 Conclusions

In this work, ultra-fine PS/EHO-OPPE fibers with average diameters ranging from 430 to 1,200 nm were successfully prepared by electrospinning the solutions of 8.5 wt.-% PS/EHO-OPPE (PS/EHO-OPPE = 7.5:1 w/w) in 1,2-dichloroethane (DCE) and chloroform (CF) with and without the addition of pyridinium formate (PF). While the increase in the electrical potential resulted in the observed increase in the diameters of the e-spun fibers, the addition of PF significantly improved the electro-spinnability of the resulting PS/EHO-OPPE solutions, as shown by the decrease in the bead density of the obtained fibers. FT-IR spectroscopy showed that the chemical structure of PS and EHO-OPPE did not change and still existed in the e-spun fibers. The optical properties (e.g., absorption and emission) of the as-prepared solution, the e-spun fibers, the annealed fibers, and both the spin-coated and the solution-cast reference films were studied by UV-vis and PL spectroscopy. A red-shift was observed in emission spectra of the e-spun fibers and the solution-cast films when compared with those of the corresponding solutions. This shift could be attributed to the phase separation of the EHO-OPPE molecules, which resulted in a higher degree of molecular interaction. The shift in the e-spun fibers was less pronounced when they were annealed. Presumably, this was due to increased PPE mobility to disperse much more evenly in the PS matrix, resulting in even lesser aggregation or the destruction of the precedent aggregation.

2.5 References

[1] E. Shirakawa, E. J. Louis, A. G. MacDiarmid, C. K. Chiang, A. J. Heeger, *J. Chem. Soc. Chem. Comm*. **1977**, 579.

[2] [2a] A. J. Heeger, *Rev. Mod. Phys*. 2001, *73*, 681; [2b] A. G. MacDiarmid, *Rev. Mod. Phys*. **2001**, 73, 701; [2c] H. Shirakawa, *Rev. Mod. Phys*. 2001, *73*, 713.

[3] [3a]‘‘*Handbook of Organic Conductive Molecules and Polymers*’’, H. S. Nalva, Ed., Wiley, New York **1997**; [3b] T. A. Skoetheim, R. L. Elsenbaumer, J. R. Reynolds, Eds., ‘‘*Handbook of Conducting Polymers*’’, Dekker, New York **1998**.

[4] [4a] J. H. Burroughes, D. D. C. Bradley, A. R. Brown, R. N. Marks, K. Mackay, R. H. Friend, P. L. Burns, A. B. Holmes, Nature **1990**, 347, 539; [4b] A. Kraft, A. C. Grimsdale, A. B. Holmes, *Angew. Chem. Int. Ed.* **1998**, 37, 402; [4c] U. Mitschke, P. Bäuerle, *J. Mater. Chem.* **2000**, *10*, 1471; [4d] A. Greiner, C. Weder, in: ‘‘*Encyclopedia of Polymer Science and Technology*’’, J. I. Kroschwitz, Ed., Wiley-Interscience, New York 2003, p. 87.

[5] G. Horowitz, *Adv. Mater.* **1998**, *10*, 365.

[6] C. J. Brabec, N. S. Sariciftci, J. C. Hummelen, *Adv. Funct. Mater*. **2001**, *11*, 15.

[7] D. T. McQuade, A. E. Pullen, T. M. Swager, *Chem. Rev*. **2000**, *100*, 2537.

[8] F. R. Denton, III, P. M. Lahti, ‘‘*Photonic Polymer Systems - Fundamentals, Methods, and Applications*’’, D. L. Wise, G. E. Wnek, D. J. Trantolo, T. M. Cooper, J. D. Gresser, Eds., CRC Press, New York 1998.

[9] U. Scherf, E. J. W. List, *Adv. Mater*. **2002**, *14*, 477.

[10] ‘‘*Poly(Arylene Ethynylene)s – From Synthesis to Applications*’’, C. Weder, Ed., Adv. Polym. Sci. Series, Vol. 177, 2005.

[11] [11a] C. Weder, M. S. Wrighton, R. Spreiter, C. Bosshard, P. Gunter, *J. Phys. Chem.* **1996**, *100*, 18931; [11b] G. S. He, C. Weder, P. Smith, P. N. Prasad, *IEEE J. Quantum Electron.* **1998**, *34*, 2279.

[12] [12a] C. Weder, M. S. Wrighton, *Macromolecules* **1996**, *29*, 5157; [12b] D. Steiger, P. Smith, C. Weder, *Macromol. Rapid Commun.* **1997**, *18*, 643; [12c] S. Dellsperger, F. Dotz, P. Smith, C. Weder, Macromol. *Chem. Phys.* **2000**, *201*, 192; [12d] D. Knapton, P. K. Iyer, S. J. Rowan, C. Weder, *Macromolecules* **2006**, *39*, 4069.

[13] [13a] A. Montali, P. Smith, C. Weder, *Synth. Met.* **1998**, *97*, 123; [13b] C. Schmitz, P. Pösch, M. Thelakkat, H. W. Schmidt, A. Montali, K. Feldman, P. Smith, C. Weder, *Adv. Func. Mater.* **2001**, *11*, 41; [13c] M. Burnworth, J. D. Mendez, M. Schroeter, S. J. Rowan, C. Weder, *Macromolecules* **2008**, *41*, 2157.

[14] [14a] A. Kokil, I. Shiyanovskaya, K. D. Singer, C. Weder, *J. Am. Chem. Soc.* **2002**, *124*, 9978; [14b] A. Kokil, I. Shiyanovskaya, K. D. Singer, C. Weder, *Synth. Met.* **2003**, *138*, 513.

[15] [15a] A. Kokil, P. Yao, C. Weder, *Macromolecules* **2005**, *38*, 3800; [15b] P. K. Iyer, J. B. B. Beck, C. Weder, S. J. Rowan, *Chem. Comm*. **2005**, 319.

[16] G. Voskerician, C. Weder, *Adv. Polym.* Sci. **2005**, *177*, 209.

[17] [17a] C. Weder, C. Sarwa, C. Bastiaansen, P. Smith, *Adv. Mater.* **1997**, *9*, 1035; [17b] A. Montali, G. Bastiaansen, P. Smith, C. Weder, *Nature* **1998**, *392*, 261; [17c] A. R. A. Palmans, M. Eglin, A. Montali, C. Weder, P. Smith, *Chem. Mater.* **2000**, *12*, 472.

[18] C. Weder, C. Sarwa, A. Montali, C. Bastiaansen, P. Smith, *Science* **1998**, *279*, 835.

[19] Y. Xu, P. R. Berger, J. N. Wilson, U. H. F. Bunz, *Appl. Phys. Lett.* **2004**, *85*, 4219.

[20] H. Hoppe, N. S. Sariciftci, D. A. M. Egbe, D. Mühlbacher, M. Koppe, Mol. Cryst. *Liq. Cryst.* **2005**, *426*, 255.

[21] D. Knapton, M. Burnworth, S. J. Rowan, C. Weder, Angew. *Chem. Int. Ed.* **2006**, *45*, 5825.

[22] [22a] E. Hittinger, A. Kokil, C. Weder, Angew. *Chem. Int. Ed.* **2004**, *43*, 1808; [22b] E. Hittinger, A. Kokil, C. Weder, *Macromol. Rapid Commun.* **2004**, *25*, 710.

[23] [23a] J. X. Jiang, F. Su, A. Trewin, C. D. Wood, N. L. Campbell, H. Niu, C. Dickinson, A. Y. Ganin, M. J. Rosseinsky, Y. Z. Khimyak, A. I. Cooper, *Angew. Chem. Int. Ed.* **2007**, *46*, 8574; [23b] C. Weder, Angew. *Chem. Int. Ed.* **2008**, *47*, 448.

[24] Y. Wang, J. S. Park, J. P. Leech, S. Miao, U. H. F. Bunz, *Macromolecules* **2007**, *40*, 1843.

[25] P. Wutticharoenmongkol, P. Supaphol, T. Srikhirin, T. Kerdcharoen, T. Osotchan, *J. Polym. Sci., Part B: Polym. Phys.* **2005**, *43*, 1881.

[26] H. Wang, X. Lu, Y. Zhao, C. Wang, *Mater. Lett.* **2006**, *60*, 2480.

[27] N. Dharmaraj, C. H. Kim, K. W. Kim, H. Y. Kim, E. K. Suh, *Spectrochim. Acta A* **2006**, *64*, 136.

[28] R. Luoh, H. T. Hahn, Compos. *Sci. Technol.* **2006**, *66*, 2436.

[29] S. Tungprapa, I. Jangchud, P. Ngamdee, M. Rutnakornpituk, P. Supaphol, *Mater. Lett.* **2006**, *60*, 2920.

[30] X. Li, X. Hao, D. Xu, G. Zhang, S. Zhong, H. Na, D. Wang, *J. Membrane Sci.* **2006**, *281*, 1.

[31] Y. C. Ahn, S. K. Park, G. T. Kim, Y. J. Hwang, C. J. Lee, H. S. Shin, J. K. Lee, *Curr. Appl. Phys.* **2006**, *6*, 1030.

[32] J. S. Jeong, J. S. Moon, S. Y. Jeon, J. H. Park, P. S. Alegaonkar, J. B. Yoo, *Thin Solid Films* **2007**, *515*, 5136.

[33] D. Kawaguchi, K. Tanaka, A. Takahara, T. Kajiyama, *Macromolecules* **2001**, *34*, 6164.

[34] T. Jarusuwannapoom, W. Hongrojjanawiwat, S. Jitjaicham, L. Wannatong, M. Nithitanakul, C. Pattamaprom, P. Koombhongse, R. Rangkupan, P. Supaphol, *Eur. Polym. J.* **2005**, *41*, 409.

[35] C. Mit-Uppatham, M. Nithitanakul, P. Supaphol, *Macromol. Chem. Phys.* **2004**, *205*, 2327.

[36] S. Chuangchote, T. Srikhirin, P. Supaphol, *Macromol. Rapid Commun.* **2007**, *28*, 651.

[37] H. Fong, I. Chun, D. H. Reneker, *Polymer* **1999**, *40*, 4585.

[38] Z. M. Huang, Y. Z. Zhang, M. Kotaki, S. Ramakrishna, *Compos. Sci. Technol.* **2003**, *63*, 2223.

3. MORPHOLOGY AND PHOTOPHYSICAL PROPERTIES OF ELECTROSPUN LIGHT-EMITTING POLYSTYRENE/POLYFLUORENE DERIVATIVE FIBERS

3.1 Introduction

The electrospinning (e-spinning) process is a very potential method for fabricating ultra-fine fibers with diameters in the nanometer to sub-micrometer range.[1, 2] In the e-spinning process, a high electrical potential is used to create an electrically charged jet of polymer solution which dries or solidifies to deposit a polymer fiber on the collector. One electrode is placed into the spinning solution and the other electrode is attached to a collector. The electrical field is subjected to the end of a capillary tube that contains the polymer fluid held by its surface tension. This induces a charge on the surface of the polymer fluid.[3, 4] Then, the charge repulsion also causes a force directly opposite to the surface tension. This force tends to elongate a hemispherical surface of the fluid at the end of capillary tube form a conical shape known as the Taylor cone as the applied electrical potential increases.[3-5] And this is what makes a continuous flow of the polymer jet shot to the collector. Due to the combination of many forces on the polymer jet, the jet will be shot as a straight line where either splitting or bending instability can be also occurred. Finally, during its flight to the collector the charged jet thins down and, at the same time, it dries out or solidifies leaving ultra-fine fibers on the collector where random orientation is usually observed. Because the e-spinning is a very simple, inexpensive and high throughput continuous production method, thus many researchers have studied the e-spinning of various materials such as biopolymers, conductive polymers, block copolymers, polymer blends, ceramics, and composite materials.[3-8]

In the recently decade, conductive polymers have been widely explored both in chemical and physical properties for various applications. Polyfluorene and its derivatives are one of the most interesting conductive polymers. Due to electronic and optical properties such as high electro- and photoluminescence efficiencies with emission wavelengths in the green to blue color region [9, 10] that can be applied in various electronic devices such as an organic light-emitting device (OLED) [11, 12], and solar cell [13].

Since previous studies on this class of materials usually focused on the properties of either the solutions or the films thereof, it is of our interest to investigate the possibility for fabricating these polymers into ultra-fibrous form that exhibits a high surface area to volume or mass ratio that could be applied as a small-scale electronic and optoelectronic device in the future.

Recently, Kuo and coworkers [14] successful prepared light-emitting electrospun (e-spun) nanofibers of the binary blends of poly(methyl methacrylate) (PMMA) and polyfluorene derivatives (e.g. poly(9,9-dioctylfluoreny-2,7-diyl) (PFO), poly[2,7-(9,9-dihexylfluorene)-*alt*-5,8-quinoxaline] (PFQ), poly[2,7-(9,9-dihexylfluorene)-*alt*-4,7-(2,1,3-benzothiadiazole)] (PFBT), and poly[2,7-(9,9-

dihexylfluorene)-*alt*-5,7-(thieno[3,4-b]pyrazine)] (PFTP)). The uncontinuous fiberlike structure was obtained at the low PFO/PMMA blend ratio but became a core-shell structure at a high PFO blend ratio. The full color light-emitting e-spun nanofibers could be fabricated from the binary blends of polyfluorene derivative/PMMA as the uniform e-spun fibers produced from the binary blends of PFO/PMMA, PFQ/PMMA, PFBT/PMMA, and PFTP/PMMA exhibited the color emission of blue, green, yellow, and red, respectively. After that, Chen and some of previous Kuo's coworkers [15] further fabricated the full color e-spun nanofibers based on ternary blends of PFO/poly[2-methoxy-5-(2-ethylhexyloxy)- 1,4-phenylenevinylene] (MEH-PPV)/PMMA. They found that PFO/MEH-PPV ratio directly affects the morphology and photophysical properties according to the energy transfer between these two polymers.

In the present work, the e-spinning was used as the technique for fabricating other type of polyfluorene derivatives which is poly(2,7-(9,9-bis(2-ethylhexyl)fluorene)) (BEH-PF) into ultra-fine fibers. Polystyrene (PS) was used as the matrix material into BEH-PF which BEH-PF was blended. Chloroform was used as the common solvent. Morphological appearance and chemical integrity of the e-spun fibers were evaluated, while photophysical properties such as absorption and emission directly related to its morphology appearances of the PS/BEH-PF solution and its corresponding e-spun fibers were also studied. Moreover the spin-coated and solution-cast films of PS/BEH-PF blend also produced for using as references.

3.2 Experimental

Poly(2,7-(9,9-bis(2-ethylhexyl)fluorene)) (BEH-PF) (M_n = 3.2 × 10^4 Daltons) which its chemical structure is shown in Figure 3.1 was synthesized following the procedure described in reference [16]. Polystyrene (PS) (M_w = 3.0 × 10^5 Daltons, pellets form) was a general purpose grade from Dow Chemicals (USA). The solvent used was chloroform (CF; Carlo Erba, Italy). Pyridinium formate (PF), an volatile organic salt, was prepared by the reacting an equimolar quantity of pyridine (Lab-Scan (Asia), Thailand) and formic acid (Merck, England). Blend solutions of 8.5% (w/v) PS/BEH-PF in CF (the compositional weight ratio between PS and BEH-PF being 7.5:1) with or without the addition of 8% (v/v) PF were prepared.

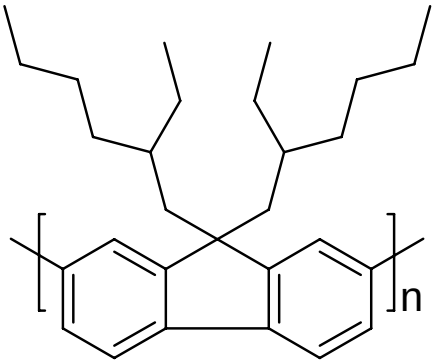

Figure 3.1 Chemical structure of poly(2,7-(9,9-bis(2-ethylhexyl)fluorene)) (BEH-PF).

Blend solutions were carried out for e-spinning under an applied electrical potential, ranging between 7.5 and 20 kV. Both the collection distance and the collection time were fixed at 10 cm and 1 min, respectively. Each of the as-prepared solutions was placed in a 5 ml plastic syringe, the open end of which was connected to a blunt-ended stainless steel gauge 20 needle (the outside diameter = 0.91 mm), used as the nozzle. An aluminum sheet wrapped around a hard plastic sheet used as a backing plate was used as the collector plate. The emitting electrode of positive polarity from a Gamma High-Voltage Research ES30P DC power supply (Florida, USA) was connected to the needle, while the grounding electrode was connected to the collector plate. The feed rate of the solution was controlled by means of a Kd Scientific syringe pump at 1 $mL \cdot h^{-1}$.

The spin coating and solution casting methods were used to prepare the films of that PS/BEH-PF blend solution in CF. In details, the spin coating was done on a glass slide by Specialty Coating Systems model P6700 with the spinning speed of 1,000 rpm to get a final thickness of 0.5-1 μm. Solution casting was also done on a glass slide and the resulted thickness is about 1-2 μm.

Morphological appearance of the as-spun products was examined by a JEOL JSM-5410LV scanning electron microscope (SEM). Diameters of the e-spun fibers were measured directly from SEM images of 1,000× magnification, with the average value being calculated from at least 50 measurements (for each spinning condition). The average bead diameters and the number of beads per unit area (i.e., the bead density) on the e-spun beaded fibers were calculated from measurements on SEM images of 500× magnification. A Thermo-Nicolet Nexus 670 Fourier-transformed infrared spectroscope (FT-IR) was used to characterize the as-received PS pellets, the as-synthesized BEH-PF, and some of the e-spun products. Lastly, absorption spectra and photoluminescence emission spectra of the PS/BEH-PF solutions in CF with or without PF addition,

the corresponding e-spun products, spin-coated and solution- cast films were measured by a Hewlett Packard-8254A diode array UV-VIS spectrophotometer (UV-Vis) and Perkin- Elmer LS50 luminescence spectrometer (PL), respectively. Each sample was excited at 350 nm prior to measurement for PL measurement.

3.3 Results and discussion

Figure 3.2 shows selected SEM images of e-spun products at various applied electrical potential (e.g., 7.5, 10, 12.5, 15, 17.5 and 20 kV) from 8.5% (w/v) solutions of PS/BEH-PF (PS:BEH-PF = 7.5:1) in chloroform (CF) without and with 8% (v/v) pyridinium formate (PF). It is obvious that the discrete beads were observed for the neat PS/BEH-PF solution as shown in series (a) of Figure 3.2 with the average diameter and bead density ranging from 14.65 to 23.05 μm and 0.34×10^5 to 2.10×10^5 beads·cm^{-2} respectively. (see in Table 3.1 which shows average fiber diameters, bead size and bead density of e-spun products from 8.5% (w/v) solutions of PS/BEH-PF in CF without and with 8% (v/v) PF at various applied electrical potential)

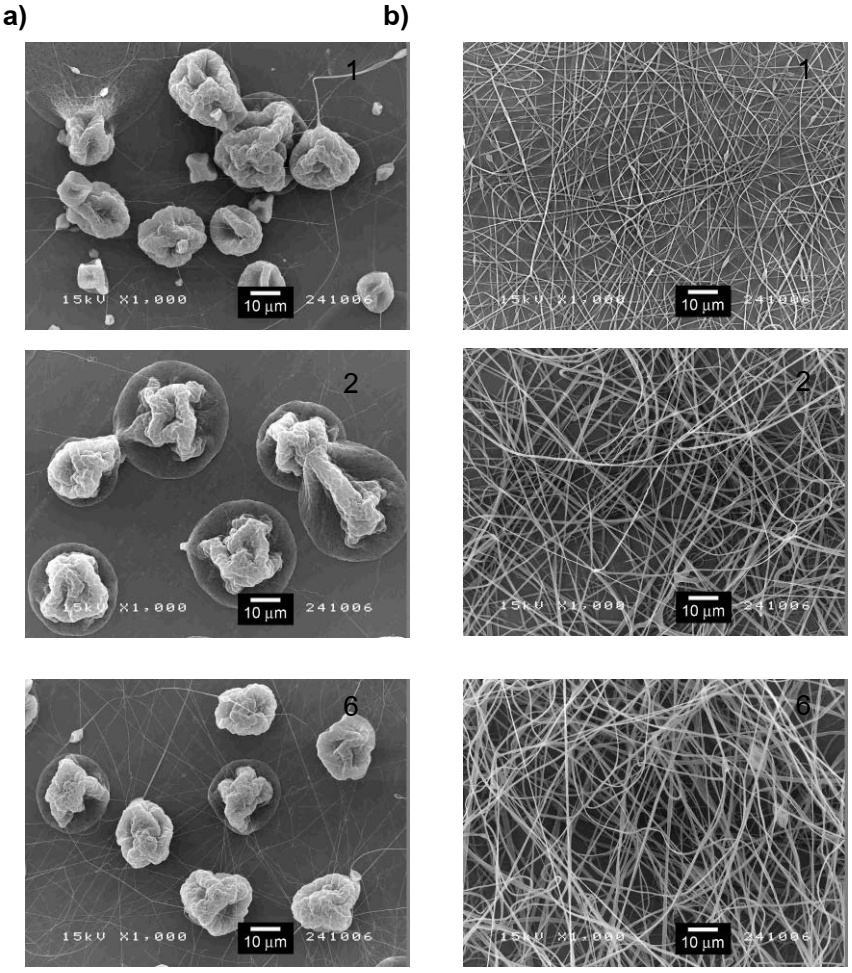

Figure 3.2 Selected SEM images (1000×; scale bar = 10 µm) of the electrospun products from 8.5% (w/v) solutions of PS/BEH-PF (PS:BEH-PF = 7.5:1) in chloroform (CF) without a) and with b) 8% (v/v) pyridinium formate (PF), at applied electrical potential (1) 7.5, (2) 10, (3) 12.5, (4) 15, (6) 17.5 and (6) 20 kV. The collection distance, collection time and solution flow rate were fixed at 10 cm, 1 min, and 1 $mL \cdot h^{-1}$, respectively.

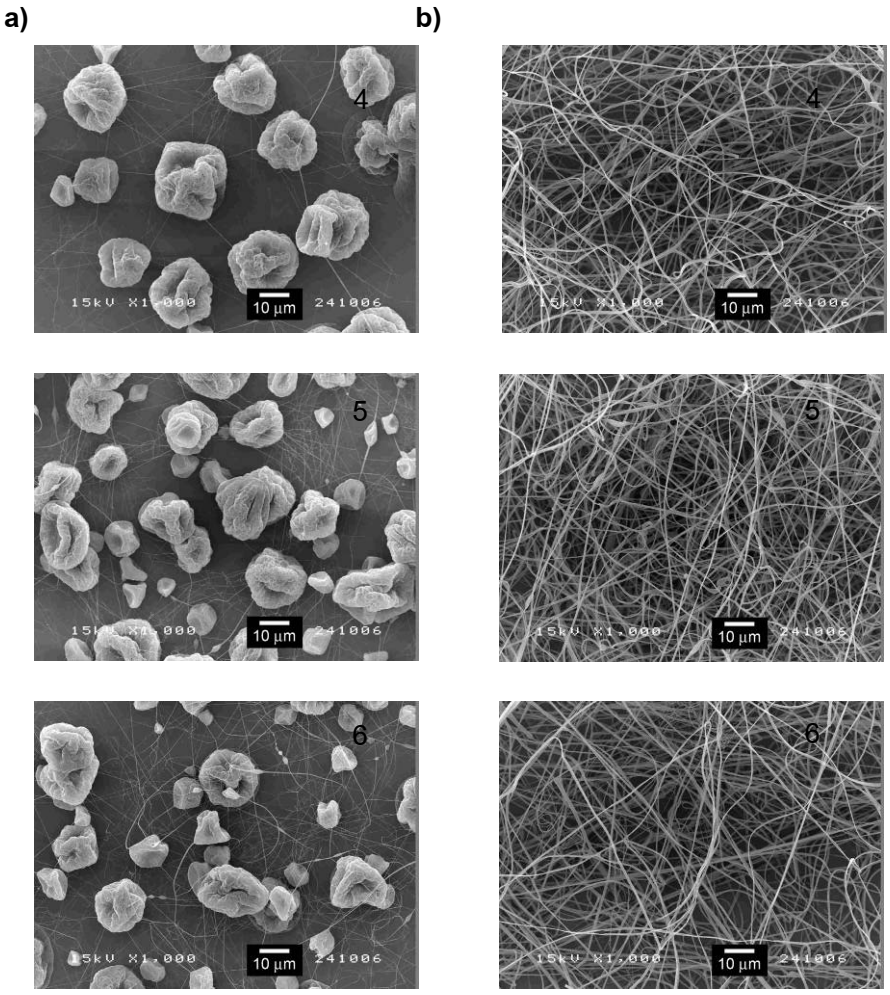

Figure 3.2 (Cont.) Selected SEM images (1000×; scale bar = 10 µm) of the electrospun products from 8.5% (w/v) solutions of PS/BEH-PF (PS:BEH-PF = 7.5:1) in chloroform (CF) without a) and with b) 8% (v/v) pyridinium formate (PF), at applied electrical potential (1) 7.5, (2) 10, (3) 12.5, (4) 15, (6) 17.5 and (6) 20 kV. The collection distance, collection time and solution flow rate were fixed at 10 cm, 1 min, and 1 $mL \cdot h^{-1}$, respectively.

Upon the addition of PF into the PS/BEH-PF solutions (see series (b) in Figure 3.2), the ultra-fine fibers were obtained with the average diameter ranging from 0.68 to 1.04 µm were obtained (see in Table 3.1). These results consistent with the previous and other publications that the addition of PF into the solutions before e-spinning successfully improves the e-spinnability of the solutions as the disappearance of beads in the e-spun product was found due to the significant increase in the total number of charges carried within the jet [4, 17, 18]. Moreover, the average diameter of the e-spun fibers was found to increase with increasing the applied electrical potential, (see in Table 3.1), a direct result of the increase in the total number of charged species within a jet

segment that causes both the electrostatic forces to increase. These, in turn, could result in an increase in the actual feed rate of the solution as well as a decrease in the total path trajectory of the jet segment, due to an increase in the speed of the jet [18, 19].

Table 3.1 Average fiber diameters, bead size and bead density of the electrospun products from 8.5% (w/v) solutions of PS/BEH-PF (PS:BEH-PF = 7.5:1) in chloroform (CF) without and with 8% (v/v) pyridinium formate (PF) at various applied electrical potential. The collection distance, collection time and solution flow rate were fixed at 10 cm, 1 min, and 1 mL·h^{-1}, respectively

Solution	HV (kV)	Fiber Diameters (μm)	Bead Size (μm)	Bead Density (# bead·cm^{-2})
PS/BEH-PF /CF	7.5	-	14.65 ± 6.19	0.40 × 10^5
	10.0	-	23.05 ± 11.25	0.34 × 10^5
	12.5	-	19.14 ± 5.64	0.78 × 10^5
	15.0	-	16.11 ± 4.09	1.18 × 10^5
	17.5	-	16.80 ± 4.29	2.02 × 10^5
	20.0	-	14.05 ± 5.79	2.10 × 10^5
PS/BEH-PF /CF+ PF	7.5	0.68 ± 0.16	-	-
	10.0	0.79 ± 0.19	-	-
	12.5	0.85 ± 0.23	-	-
	15.0	0.92 ± 0.19	-	-
	17.5	0.98 ± 0.15	-	-
	20.0	1.04 ± 0.17	-	-

To confirm the PS and BEH-PF component in the e-spun products by Figure 3.3, which shows the IR spectra (in the wavenumber range of 500-4000 cm^{-1}) of the of PS pellet, BEH-PF powder and some of the e-spun products from 8.5% (w/v) solutions of PS/BEH-PF in CF without and with the presence of PF at applied electrical potential 15 kV. The chemical functionalities of the e-spun products from 8.5% (w/v) PS/BEH-PF solutions in CF without and with the presence of PF were compared with those obtained from the as-received PS pellets and the as-synthesized BEH-PF. Table 3.2 summarizes some absorbance peaks characteristic of the PS and BEH-PF component in the e-spun products. According to Figure 3.3, the peaks characteristic of PS component were evident in all of the FT-IR spectra of the as-spun fibers (e.g., at 696-698, 1,490, and 3,020-3,030 cm^{-1}). Moreover, the peaks characteristic of BEH-PF are 813 and 1,380 cm^{-1} which belongs to CH out-of-

plane bending vibrations in $C=CH_2$ group and CH bending vibrations in CH_3 deformation, respectively. Additionally, the peak at 2,850 and 2,920 cm^{-1} are specific to symmetric CH stretching vibrations in $-CH_2$ group and asymmetric CH stretching vibrations in $-CH_2$ group, respectively. These results indicate that PS and BEH-PF still exist in the e-spun products and no change in their chemical structure.

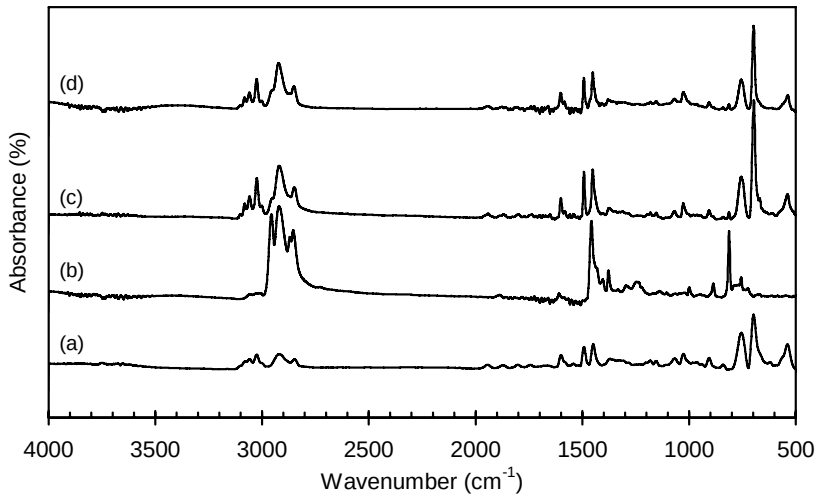

Figure 3.3 IR spectra of a) PS pellet, b) BEH-PF powder and the electrospun products from 8.5% (w/v) solutions of PS/BEH-PF (PS:BEH-PF = 7.5:1) in chloroform (CF) without c) and with d) 8% (v/v) pyridinium formate (PF) at applied electrical potential 15 kV. The collection distance, collection time and solution flow rate were fixed at 10 cm, 1 min, and 1 $mL \cdot h^{-1}$, respectively.

Table 3.2 Analysis of IR spectra of as-received PS pellet, BEH-PF powder and the electrospun products from 8.5% (w/v) solutions of PS/BEH-PF (PS:BEH-PF = 7.5:1) in chloroform (CF) without and with 8% (v/v) pyridinium formate (PF) at applied electrical potential 15 kV. The collection distance, collection time and solution flow rate were fixed at 10 cm, 1 min, and 1 $mL \cdot h^{-1}$, respectively

As-received materials (cm^{-1})		Electrospun products (cm^{-1})		Assignment
PS	BEH-PF	PS/ BEH-PF /CF	PS/ BEH-PF /CF + PF	
698	-	696	698	CH bending vibrations in CH deformation
754	756	756	756	CH out-of-plane bending vibrations in -CH=CH-(cis) group
-	813	813	813	CH out-of-plane bending vibrations in $C=CH_2$ group
906	886	906	906	CH out-of-plane bending vibrations in $-CH=CH_2$ group
-	1380	1380	1380	CH bending vibrations in $-CH_3$ deformation
1450	1460	1450	1450	Asymmetric CH bending vibrations in $-CH_3$ group
1490	-	1490	1490	CH bending vibrations in CH_2 Scissoring group
1600	1610	1600	1600	C=C stretching vibrations in Conjugated
2850	2850	2850	2850	Symmetric CH stretching vibrations in $-CH_2$ group
2920	2920	2920	2920	Asymmetric CH stretching vibrations in $-CH_2$ group
-	2960	-	-	Asymmetric CH stretching vibrations in $-CH_3$ group
3030	-	3020	3020	CH stretching vibrations in =C-H, $=CH_2$ and CH group
3060	-	3060	3060	CH stretching vibrations in =C-H, $=CH_2$ and CH group

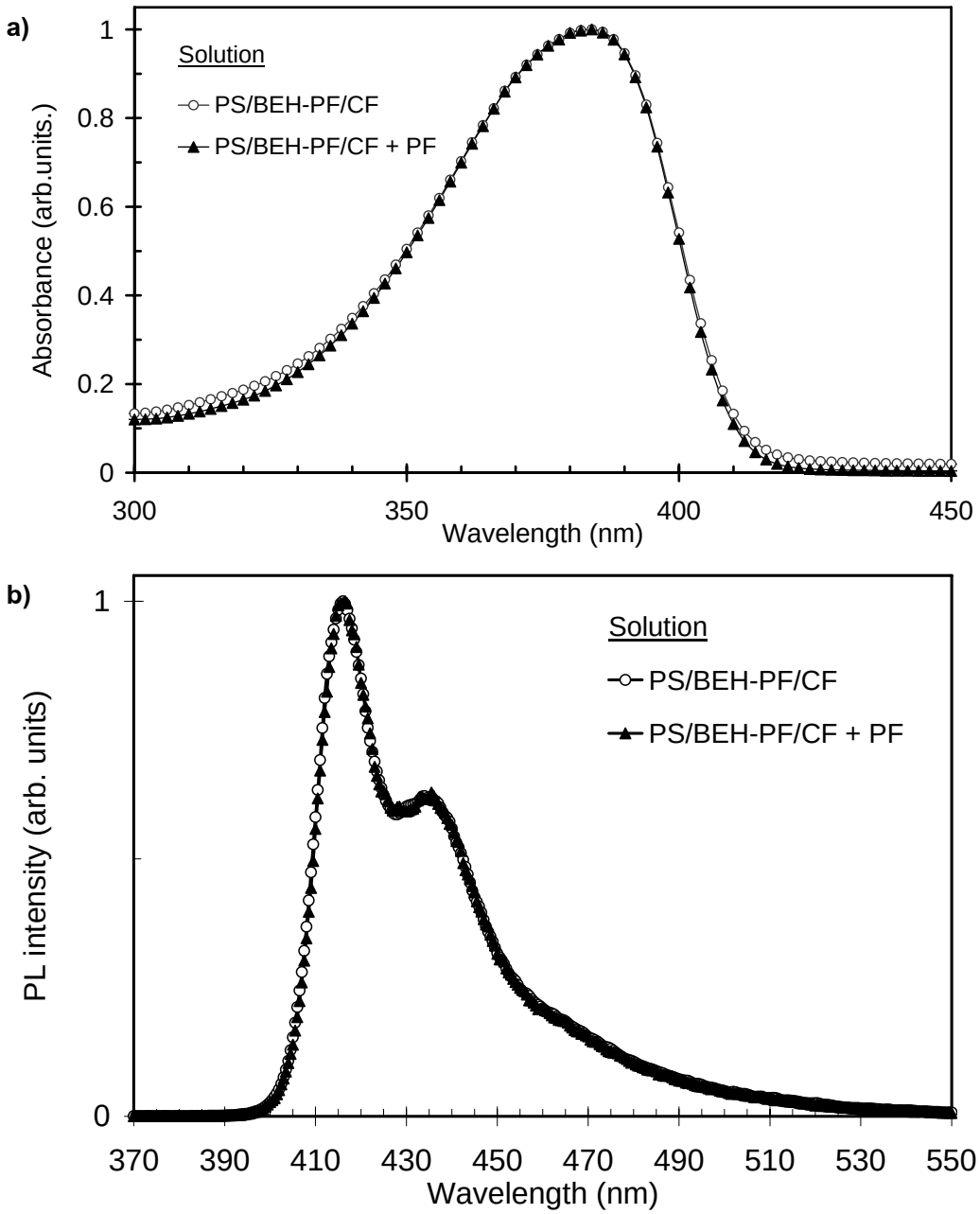

Figure 3.4 a) Absorption and b) PL emission spectra of 8.5% (w/v) solutions of PS/BEH-PF (PS:BEH-PF = 7.5:1) in chloroform (CF) without and with 8% (v/v) pyridinium formate (PF).

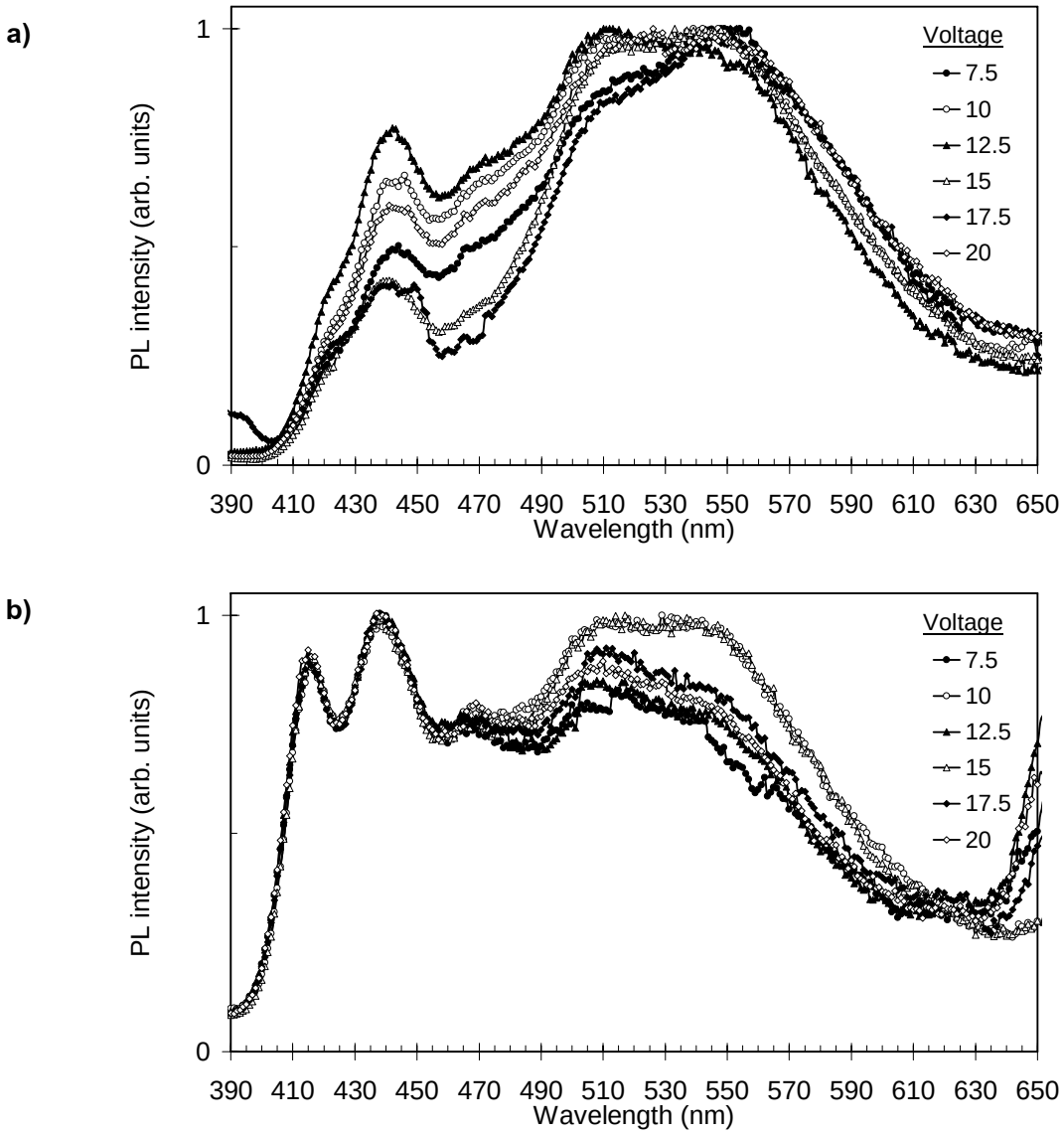

Figure 3.5 PL Emission spectra of the electrospun products spun from 8.5% (w/v) solutions of PS/BEH-PF (PS:BEH-PF = 7.5:1) in chloroform (CF) without a) and with b) 8% (v/v) pyridinium formate (PF) at various applied electrical potential.

To further study the photophysical properties (e.g. absorption and emission) of the as-prepared solution, their e-spun products, spin-coated and solution-cast films, UV-Visible (UV-Vis) and photoluminescence (PL) spectroscopy were used to investigate. All spectra results were normalized for clarity. Figure 3.4(a) shows the absorption spectra of the PS/BEH-PF solutions with or without the presence of PF (all spectra results were normalized for clarity). Apparently, the maxima of both spectra were observed at the same value (i.e., 384 nm). Additionally, Figure 3.4(b) shows the emission patterns of the PS/BEH-PF solutions with or without the presence of PF. For both types of

the solutions, a sharp peak was observed at 416 nm, with a shoulder being observed at 436 nm, corresponding to the violet-blue color emission of BEH-PF. The relaxation of excited π-electrons to different vibrational energy levels of electronic ground state as corresponded to the violet-blue color emission of the solutions. Evidently, the addition of PF into the base PS/BEH-PF solution did not affect both the absorption and the emission spectra of the resulting solution at all. These characteristics of the absorption and emission spectra correspond to the intrinsic nature of conjugated polymers which have chromophores with various conjugation lengths.[20, 21] Because of the random twisting of main chain prevents the delocalization of π-electrons throughout the entire polymeric molecule, according to the specific optical properties of these individual chromophores such as chain conformation, energy levels, HOMO-LUMO energy gap and emission efficiency.[21-26]

With regards to the emission of the e-spun products, it is obvious that the morphology of the e-spun products significantly affected their emission spectra as shown in Figure 5(a) and (b) which show the emission spectra of the e-spun products spun from 8.5% (w/v) solutions of PS/BEH-PF in CF without and with 8 vol.-% PF, respectively, as a function of the applied electrical potential. All emission spectra of the discrete beads exhibit a peak centered around 530 nm and shoulder centered around 442 nm, while the peaks and shoulder of the e-spun fibers are around 439 (1^{st} maximum intensity), 417 (2^{nd} maximum intensity), and 536 nm, respectively. In addition, both of the e-spun products exhibited a red shift in their emission spectra, when compared with those of the solutions, possibly due to the aggregation of BEH-PF in both types of the e-spun products as lower energy emission peaks were observed. The aggregation of BEH-PF chains occurred from the π-π interaction stacking provides the increased number of energy levels of the individual chromophores, resulting in the longer conjugation length arrangement conformations of BEH-PF chains and then the decreasing HOMO-LUMO energy gap of those individual chromophores occurred. [20, 21, 27-30] Moreover, there is no clear relationship between the emission peak positions and the applied electrical potential as both kinds of the e-spun products exhibit minor differences (see Figure 3.5(a) and (b)). It seem to suggest that the fluctuation in the forces (e.g. gravitational force, surface tension, electrostatic force, Coulombic repulsion force, viscoelastic force and drag force) [4, 17, 18, 31] acting on BEH-PF molecules within jet segments during e-spinning.

To further study in more details of PL emission characteristics, the films produced by spin coating and solution casting from solutions of 8.5% (w/v) solutions of PS/BEH-PF (PS:BEH-PF = 7.5:1) in CF were also investigated for comparison with both kinds of the e-spun products (see figure 3.6). The summary of the positions and color emission of peak and shoulders in the PL emission spectra of those samples is shown in Table 3.3. The PL emission pattern of the spin-coated film exhibit a maximum emission centered around 430 nm and shoulders centered around 515 nm. For

the solution-cast film, its emission peak is at about 435 nm and shoulder is at about 522 nm. Both kinds of films also exhibit a red shift in their emission spectra corresponding to the blue-green color emission, when compared with those of the solutions, due to the aggregation of BEH-PF molecules as discussed previously.

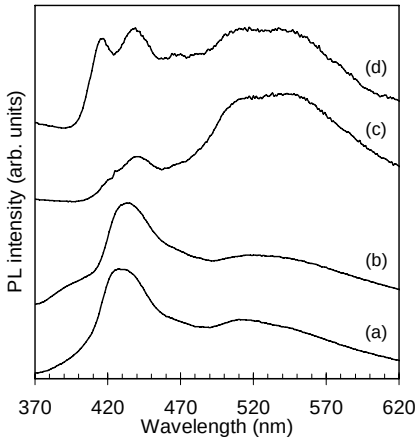

Figure 3.6 PL Emission spectra of samples produced from solutions of 8.5% (w/v) solutions of PS/BEH-PF (PS:BEH-PF = 7.5:1) in chloroform (CF). Samples were a) spin-coated film, b) solution-cast film, the electrospun (e-spun) c) beads, and d) fibers at applied electrical potential 15 kV.

Table 3.3 Summary of the positions and color emission of peak and shoulders in the PL emission spectra of 8.5% (w/v) solutions of PS/BEH-PF (PS:BEH-PF = 7.5:1) in chloroform (CF) without and with 8% (v/v) pyridinium formate (PF), the corresponding spin-coated and solution-cast films, and the electrospun (e-spun) products (beads and fibers) at applied electrical potential 15 kV

Sample	Peak and Shoulders (nm)			Color Emission
	Violet	Blue	Green	
Solutions	*416	+436	-	Violet-Blue
Spin-coated film	-	*430	+515	Blue-Green
Solution-cast film	-	*435	+522	Blue-Green
E-spun beads	-	+442	*530	Green-Blue
E-spun fibers	**417	*439	+536	Blue-Violet-Green

* = peak with the 1st maximum intensity

* * = peak with the 2nd maximum intensity

\+ = shoulder

To consider the peak position of PL emission spectra of all samples (see Table 3.3), the e-spun beads show a much more red shift than e-spun fibers, solution-cast and spin-coated films, respectively. Interestingly, the e-spun fibers only illustrate the emission shoulder at the higher energy region (wavelength around 416 nm) similar to the as-prepared solution. Looking closely at the color emission of the e-spun products, the e-spun beads show the green-blue color emission while the e-spun fibers exhibit the blue-violet-green color emission. It can be concluded that the different morphological appearances significantly affect their color emissions.

3.4 Conclusions

We successful prepared the electrospun (e-spun) fibers with average diameters ranging from 0.68 to 1.04 μm of poly(2,7-(9,9-bis(2-ethylhexyl)fluorene)) (BEH-PF) with polystyrene (PS) from the blend solution of 8.5% (w/v) PS/BEH-PF in chloroform (CF) (the compositional weight ratio between PS and BEH-PF being 7.5:1). Electrospinnability of the PS/BEH-PF solution was improved by the addition of a volatile organic salt, pyridinium formate (PF), to the solution prior to electrospinning as the bead formation disappeared. From FT-IR results of the chemical structure study which indicate that PS and BEH-PF still exist in the e-spun products and no change in their chemical structure. The photophysical properties study shows that the blend solutions exhibit the violet-blue color emission. Additionally, both of the e-spun products (beads and fibers) exhibited a red shift in their emission spectra, when compared with those of the solutions as the green-blue and blue-violet-green color emissions, respectively, observed. This is due to the aggregation of BEH-PF molecules occurring from the π-π interaction stacking. Thus the decrease in HOMO-LUMO energy gap of individual chromophores of BEH-PF was obtained which correspond to their photophysical properties. However, both kinds of films (spin-coated and solution-cast films) also showed the red shift in their emission patterns as we observed the blue-green color emission for both types of film fabrication. It seems to be concluded that the different morphological appearances significantly affect to the color emission. This study leads to application of various morphological materials in a small-scale electronic and optoelectronic devices such as OLED and solar cell which require the full range color and various types of HOMO-LUMO energy gap.

3.5 References

[1] Ahn YC, Park SK, Kim GT, Hwang YJ, Lee CG, Shin HS, Lee JK. Development of high efficiency nanofilters made of nanofibers. Curr Appl Phys 2006;6(6):1030-1035.

[2] Dharmaraj N, Kim CH, Kim KW, Kim HY, Suh EK. Spectral studies of SnO_2 nanofibres prepared by electrospinning method. Spectrochimica Acta Part A 2006;64(1): 136-140.

[3] Huang ZM, Zhang YZ, Kotaki M, Ramakrishna S. A review on polymer nanofibers by electrospinning and their applications in nanocomposites. Compos Sci Technol 2003; 63(15):2223-2253.

[4] Wutticharoenmongkol P, Supaphol P, Srikhirin T, Kerdcharoen T, Osotchan T. Electrospinning of polystyrene/poly(2-methoxy-5-(2'-ethylhexyloxy)-1,4-phenylene vinylene) blends. J Polym Sci Part B Polym Phys 2005;43(14):1881-1891.

[5] Wu Y, Yu JY, He JH, Wan YQ. Controlling stability of the electrospun fiber by magnetic field. Chaos Solitons and Fractals 2007;32(1):5-7.

[6] Li X, Hao X, Xu D, Zhang G, Zhong S, Na H, Wang D. Fabrication of sulfonated poly (ether ether ketone ketone) membranes with high proton conductivity. J Membrane Sci 2006;281(1-2):1-6.

[7] Tungprapa S, Jangchud I, Ngamdee P, Rutnakornpituk M, Supaphol P. Ultrafine electrospun poly(ethylene glycol)–polydimethylsiloxane–poly(ethylene glycol) triblock copolymer/poly(ethylene oxide) blend fibers. Mater Lett 2006;60(24):2920-2924.

[8] Wang H, Lu X, Zhao Y, Wang C. Preparation and characterization of ZnS:Cu/PVA compositenanofibers via electrospinning. Mater Lett 2006;60(20):2480-2484.

[9] Assaka AM, Rodrigues PC, Oliveira ARM, Ding L, Hu B, Karasz FE, Akcelrud L. Novel fluorine containing polyfluorenes with efficient blue electroluminescence. Polymer 2004;45(21):7071-7081.

[10] Liu J, Tu G, Zhou Q, Cheng Y, Geng Y, Wang L, Ma D, Jing X, Wang F. Highly efficient green light emitting polyfluorene incorporated with 4-diphenylamino-1,8-naphthalimide as green dopant. J Mater Chem 2006;16(15):1431-1438.

[11] Bliznyuk VN, Carter SA, Scott JC, Kla1rner G, Miller RD, Miller DC. Electrical and photoinduced degradation of polyfluorene based films and light-emitting devices. Macromolecules 1999;32(2):361-369.

[12] Lee H, Johnson AR, Kanicki J. White LED based on polyfluorene co-polymers blend on plastic substrate. IEEE Transactions Electron Dev 2006;53(3):427-434.

[13] Yohannes T, Zhang F, Svensson M, Hummelen JC, Andersson MR, Inganäs O. Polyfluorene copolymer based bulk heterojunction solar cells. Thin Solid Films 2004;449(1-2):152-157.

[14] Kuo CC, Lin CH, Chen WC. Morphology and photophysical properties of light-emitting electrospun nanofibers prepared from poly(fluorene) derivative/PMMA blends. Macromolecules 2007;40(19):6959-6966.

[15] Chen HC, Wang CT, Liu CL, Liu YC, Chen WC. Full color light-emitting electrospun nanofibers prepared From PFO/MEH-PPV/PMMA ternary blends. J Polym Sci Part B Polym Phys 2009;47(5):463-470.

[16] Scherf U, List E. J. W., Semiconducting polyfluorenes-towards reliable structure-property relationships. Adv. Mater. 2002; 14(7):477-487.

[17] Mit-uppatham C, Nithitanakul M, Supaphol P. Ultrafine electrospun polyamide-6 fibers: effect of solution conditions on morphology and average fiber diameter. Macromol Chem Phys 2004;205:2327-2338.

[18] Chuangchote S, Srikhirin T, Supaphol P. Color change of electrospun polystyrene/MEH-PPV fibers from orange to yellow through partial decomposition of MEH side groups. Macromol Rapid Commun 2007;28(5):651-659.

[19] Fong H, Chun I, Reneker DH. Beaded nanofibers formed during electrospinning. Polymer 1999;40(16):4585-4592.

[20] Kim J, Swager TM. Control of conformational and interpolymer effects in conjugated polymers. Nature 2001;411:1030-1034.

[21] Barbara PF, Gesquiere AJ, Park SJ, Lee Y. Single-molecule spectroscopy of conjugated polymers. J Acc Chem Res 2005;38(7):602-610.

[22] Padmanaban G, Ramakrishnan S. Conjugation length control in soluble poly[2-methoxy-5-((2'-ethylhexyl)oxy)-1,4-phenylenevinylene] (MEH-PPV): synthesis, optical properties, and energy transfer. J Am Chem Soc 2000;122(10):2244-2251.

[23] Brédas JL, Beljonne D, Coropceanu V, Cornil J. Charge-transfer and energy-transfer processes in π-conjugated oligomers and polymers: a molecular picture. Chem Rev 2004;104(11):4971-5003.

[24] Padmanaban G, Ramakrishnan S. Fluorescence spectroscopic studies of solvent- and temperature-induced conformational transition in segmented poly[2-methoxy-5-(2'-ethylhexyl)oxy-1,4-phenylenevinylene] (MEH-PPV). J Phys Chem B 2004;108(39):14933-14941.

[25] Traiphol R, Charoenthai N, Srikhirin T, Kerdcharoen T, Osotchan T, Maturos T. Chain organization and photophysics of conjugated polymer in poor solvents: aggregates, agglomerates and collapsed coils. Polymer 2007;48(3):813-826.

[26] Traiphol R, Srikhirin T, Kerdcharoen T, Osotchan T, Scharnagl N, Willumeit R. Influences of local polymer–solvent π–π-interaction on dynamics of phenyl ring rotation and its role on photophysics of conjugated polymer. Eur Polym J 2007;43(2):478-487.

[27] Nguyen TQ, Martini IB, Liu J, Schwartz BJ. Controlling interchain interactions in conjugated polymers: the effects of chain morphology on exciton-exciton annihilation and aggregation in MEH-PPV Films. J Phys Chem B 2000;104(2):237-255.

[28] Menon A, Galvin M, Walz KA, Rothberg L. Structural basis for the spectroscopy and photophysics of solution-aggregated conjugated polymers. Synthetic Met 2004;141(2):197-202.

[29] Chu Q, Pang Y. Aggregation and self-assembly of oligo(2,5-dialkoxy-1,4-phenyleneethynylene)]s: an improved probe to study inter- and intramolecular interaction. Macromolecules 2005;38(32):517-520.

[30] Amrutha SR, Jayakannan M. Control of π-stacking for highly emissive poly(*p*-phenylenevinylene)s: synthesis and photoluminescence of new tricyclodecane substituted bulky poly(*p*-phenylenevinylene)s and its copolymers. J Phys Chem B 2006;110(9):4083-4091.

[31] Wannatong L, Sirivat A, Supaphol P. Effects of solvents on electrospun polymeric fibers : preliminary study on polystyrene. Polym Int. 2004;53(11):1851-1859.

Output จากโครงการวิจัยที่ได้รับทุนจาก สกว.

1. ผลงานตีพิมพ์ในวารสารวิชาการนานาชาติ (ระบุชื่อผู้แต่ง ชื่อเรื่อง ชื่อวารสาร ปี เล่มที่ เลขที่ และหน้า) พร้อมแจ้งสถานะของการตีพิมพ์ เช่น submitted, accepted, in press, published

1.1 Changsarn, S., Mendez, J. D., Weder, C., and Supaphol, P. Versatile Route for Tuning Optical Properties of Poly(2-methoxy-5-(2'-ethylhexyloxy)-1,4-phenylenevinylene). Journal of Polymer Science: Part B: Polymer Physics, 2009, 47(7), 696-705, Pubblished.

1.2 Changsarn, S., Mendez, J. D., Weder, C., and Supaphol, P. Morphology and Photophysical Properties of Electrospun Light-Emitting Polystyrene/Poly-(*p*-phenylene ethynylene) Fibers. Macromolecular Materials and Engineering, 2008, 293(12), 952-963, Pubblished.

1.3 Changsarn, S., Srikhirin, T., and Supaphol, P. Morphology and Photophysical Properties of Electrospun Light-Emitting Polystyrene/Polyfluorene Derivative Fibers, In preparation.

2. การนำผลงานวิจัยไปใช้ประโยชน์

ได้สร้างเครือข่ายความร่วมมือทั้งในประเทศและต่างประเทศ อีกทั้งได้มีการพัฒนาการเรียนการสอนและนักวิจัยใหม่ เพื่อนำความรู้ที่ได้ไปประยุกต์ใช้กับอุปกร์อิเล็กทรอนิคส์ขนาดเล็กในอนาคตต่อไป

3. อื่นๆ (เช่น ผลงานตีพิมพ์ในวารสารวิชาการในประเทศ การเสนอผลงานในที่ประชุมวิชาการ หนังสือ การจดสิทธิบัตร)

3.1 Changsarn, S., Mendez, J. D., Schroeter, M., Weder, C., and Supaphol, P. (2008, July 28-August 1) Morphology and Photophysical Properties of Electrospun Light-Emitting Polystyrene/Poly(phenylene ethynylene) Nanofibers. Paper presented at International Conference on Electronic Materials 2008 (IUMRS-ICEM 2008), Sydney, Australia.

3.2 Changsarn, S., Srikhirin, T., and Supaphol, P. (2008, April 4-6) Preparation and Characterization of Electrospun PS/BEH-PF Fibers. Paper presented at The Royal Golden Jubilee Ph. D. Congress IX (RGJ-Ph. D. Congress IX), Chonburi, Thailand.

ภาคผนวก

Versatile Route for Tuning Optical Properties of Poly(2-methoxy-5-(2′-ethylhexyloxy)-1,4-phenylenevinylene)

SUTHEERAT CHANGSARN,[1] RAKCHART TRAIPHOL,[2,3] THANUTPON PATTANATORNCHAI,[2] TOEMSAK SRIKHIRIN,[3,4] PITT SUPAPHOL[1]

[1]The Petroleum and Petrochemical College and The Center for Petroleum, Petrochemicals, and Advanced Materials, Chulalongkorn University, Phyathai Road, Pathumwan, Bangkok 10330, Thailand

[2]Laboratory of Advanced Polymers and Nanomaterials, Department of Chemistry and The Center of Excellence for Innovation in Chemistry, Faculty of Science, Naresuan University, Phitsanulok 65000, Thailand

[3]NANOTEC Center of Excellence at Mahidol University, Rama 6 Road, Ratchathewi, Bangkok 10400, Thailand

[4]Department of Physics, Faculty of Science, Mahidol University, Rama 6 Road, Ratchathewi, Bangkok 10400, Thailand

Received 21 October 2008; revised 10 December 2008; accepted 11 January 2009
DOI: 10.1002/polb.21673
Published online in Wiley InterScience (www.interscience.wiley.com).

ABSTRACT: In this contribution, we report a versatile method for tuning optical properties of poly(2-methoxy-5-(2′-ethylhexyloxy)-1,4-phenylenevinylene) (MEH-PPV) in its solution with 1,2-dichloroethane, accomplished by reacting with pyridinium formate (PF), a volatile organic salt. We can systematically control the positions of absorption and photoluminescent (PL) spectra of MEH-PPV by adjusting the concentration of PF in the solution. The addition of 10 vol % PF caused a blue-shift in the absorption spectra by about 65 nm. When the concentration of PF decreased to 0.1 vol %, the blue-shift occurred to a lesser extent, about 25 nm. The measurements of PL spectra showed similar behaviors. The λ_{max} shifted from 558 nm to 546 and 552 nm when 10 and 0.1 vol % of PF were added, respectively. The changes of PL colors from orange to yellow and green, respectively, were observed by naked eyes. Structural investigation by nuclear magnetic resonance and Fourier-transformed infrared spectroscopy indicated that the changes of the optical properties were due to chemical modifications along the main chain and the side groups of MEH-PPV. These results implied a simple route for engineering the HOMO–LUMO energy gap of MEH-PPV, which could be utilized in advanced applications such as organic light-emitting devices and solar cells. © 2009 Wiley Periodicals, Inc. J Polym Sci Part B: Polym Phys 47: 696–705, 2009

Keywords: light-emitting diodes (LED); MEH-PPV; optics; photoluminescence; photophysics; tuning of optical properties

INTRODUCTION

Poly(2-methoxy-5-(2′-ethylhexyloxy)-1,4-phenylenevinylene) (MEH-PPV) is one of the well-known conjugated polymers with many interesting physical properties, such as photoconductivity[1,2] and high luminescence efficiency in both photo-

Correspondence to: R. Traiphol (E-mail: rakchartt@nu.ac.th) or P. Supaphol (E-mail: pitt.s@chula.ac.th)

and electroluminescence.[3,4] It, therefore, holds great promises in various electronic applications, such as organic light-emitting diodes (OLED),[5–7] sensors,[8–10] and solar cells.[11,12] In the past few decades, many researchers have investigated detailed properties of conjugated polymers to understand their fundamental behaviors. In general, the intrinsic nature of conjugated polymers derives mainly from their architectures consisting of alternating single and double/triple bonds along the main chain. The appropriate arrangement of π-orbitals in the backbone could provide a convenient pathway for π-electrons to delocalize over the entire molecule. However, this ideal situation is never realized because of the flexibility of the polymer chain. The delocalization of the π-electrons is normally confined within some distances, called conjugation lengths. Various chromophores with different conjugation lengths exist in one conjugated chain.[13,14] Therefore, its electronic properties are dictated by the distribution of chromophores within the system.[15–17]

One of the challenges for developing conjugated polymers is the tuning of their electronic and optical properties, which are necessary for specific applications. This includes, for example, the engineering of colors to obtain a full range of spectrum in OLED and the manipulation of HOMO–LUMO energy levels in solar cells. The methods for tuning the properties of conjugated polymers generally involve the synthesis of new macromolecules[18–21] or the modification of the chemical structure of the existing conjugated polymers.[22–26] MEH-PPV is an example of a modified chemical structure of polyphenylenevinylene-based conjugated polymers. The incorporation of the flexible MEH side groups increases the solubility of this polymer in a common solvent, which, in turn, facilitates its fabrication into thin films. The bulkiness of the MEH side groups also reduces the segmental aggregation of the main chain, an important factor that affects its photoemission color and efficiency.[27–29] Furthermore, the phenyl rings along the MEH-PPV backbone become more difficult to rotate around single bonds, resulting in the extension of conjugation lengths.

It has been shown that the tuning of optical properties of conjugated polymers can also be achieved via polymer–polymer blending approach.[30–34] Although the procedure is quite simple, this method does not modify the HOMO–LUMO energy levels of each polymer in the blend. The photo- and electroluminescence spectra always constitute of multiple regions, contributed from simultaneous emitting of different luminophores in the system.[30,32,33] The manipulation of the emitting colors can be done by simply adjusting the ratio of the blend and the extent of energy transfer. Furthermore, the polymer–polymer blends tend to exhibit micro- and nanophase separation because of the immiscibility of the components, which, in turn, leads to inhomogeneity in local properties.[31–34] The issue of phase separation can be overcome by a copolymerization approach.[35–37] The structural change of luminophores in copolymers allows for a direct engineering of HOMO–LUMO energy levels, which yields narrow photo- and electroluminescence spectra. However, the copolymerization is normally a multistep process, which requires complicated procedures and expensive catalysts/chemicals. Therefore, it is important to seek a simple and cheap method for chemically modifying conjugated polymers that provides an easy control over their optical properties.

In a recent study by some of us, fibers of MEH-PPV were electrospun from its solutions in 1,2-dichloroethane (DCE) with polystyrene being used as the fiber-forming template and pyridinium formate (PF), a volatile organic salt, being used as the conductivity modifier. It was accidentally observed that the solutions changed their color from orange to yellow after being aged at ambient conditions for 1 month.[38] It was postulated, based on the infrared spectroscopic result, that partial decomposition of MEH side groups (~15%) was responsible for this observation. We envisioned that such a side chain decomposition induced by the addition of PF could be a simple approach to modify the chemical configuration of MEH-PPV, resulting in the chemical structure that resembles that of a random copolymer between PPV and MEH-PPV. Despite such an implication, a detailed study on any structural change that affects the change in the color of MEH-PPV in the presence of PF based on a more direct method, such as nuclear magnetic resonance (NMR) spectroscopy, is necessary to gain an insight into the color-changing process of this polymer.

In this study, we performed systematic experiments to investigate the photophysical change of MEH-PPV solutions in DCE in the presence of PF, which could lead to a simple procedure for controlling the electronic properties of this polymer. Effects of concentrations of MEH-PPV and PF were investigated. The changes in the absorption and the photoemission spectra were followed as a function of time. Fourier-transformed

infrared spectroscopy (FTIR) and NMR were used to characterize the structural change of MEH-PPV in the system.

EXPERIMENTAL

The MEH-PPV used in this study was synthesized according to the procedure described in literature.[26] All solvents purchased from different sources (Carlo Erba and Merck) were analytical grade. Fresh solutions of MEH-PPV (0.001, 0.005, and 0.01% w/v) were prepared by dissolving measured amounts of the polymer powder in DCE. Different concentrations (0.1 and 10 vol %) of PF, prepared by mixing pyridine and formic acid in an equimolar quantity, were then added into the system. The mixed solutions were sealed in vials and left in darkness at ambient conditions. Absorption and photoemission spectra of the solutions were recorded as a function of time until no noticeable change was observed. The absorption spectra were measured using a Hewlett-Packard 8254A diode array UV–vis spectrophotometer. Quartz cuvettes with thicknesses of 2 or 10 mm, depending on the polymer concentration, were used. The emission spectra were measured using a Perkin–Elmer LS50 luminescence spectrometer. An inner filter effect was minimized by using a 2-mm-thick quartz cuvette in all measurements. Any structural change of MEH-PPV was investigated by a Bruker Avance-AC400 proton-nuclear magnetic resonance spectroscopy (^{1}H NMR), operating at 400 MHz, and a Thermo-Nicolet Nexus 670 Fourier-transform infrared spectrometer. Samples for these measurements were prepared by evaporating the solvent at 130 °C for 1 h. Only small amount of the solvent remained after this procedure. The samples were subsequently dried at 80 °C in a vacuum oven for 12 h. Solutions of MEH-PPV in DCE and PF in DCE were also subjected to the same drying procedure. These were used as control samples.

RESULTS AND DISCUSSION

In the first section, we investigated the variation in the absorption spectra as a function of the reaction time, which reflects the photophysical changes of MEH-PPV chromophores in ground state. Figure 1 illustrates the results obtained from the system of 0.01% w/v MEH-PPV solution containing 10 vol % PF. The spectrum of the freshly prepared solution (0 day) exhibits a broad pattern with the maximum absorption (λ_{max}) at about 500 nm. The broadness of the spectrum arises from an intrinsic nature of the conjugated chain, which consists of various chromophores with different conjugation lengths.[14,17] Therefore, the shape of the whole spectrum envelops all possible electronic transitions, which take place at different wavelengths, depending on HOMO–LUMO energy gaps of each particular chromophore.

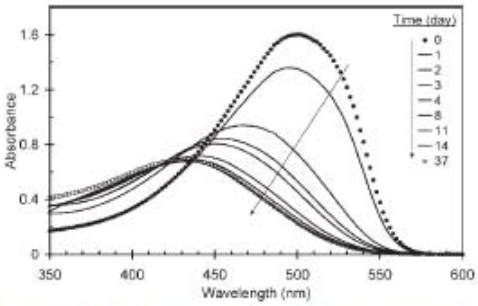

Figure 1. Absorption spectra of 0.01% (w/v) MEH-PPV in 1,2-dichloroethane (DCE) with the addition of 10 vol % pyridinium formate (PF) measured as a function of reaction time. Arrow indicates the change in the spectra with increasing the reaction time.

The pattern of the absorption spectrum changes significantly upon aging in ambient conditions for 1 day. Its absorbance markedly drops while the λ_{max} shifts to a higher energy region. Increasing the reaction time to 2 days causes a blue-shift of the spectrum by about 30 nm. We also observe the increase in the absorbance at the high-energy region (λ < 450 nm), while the absorbance at the low-energy region simultaneously decreases. The progress of reaction continues up to about 14 days. Increasing the reaction time further to 37 days hardly affects the pattern of the absorption spectrum, suggesting the completion of this process. The solution of the final product exhibits λ_{max} at about 434 nm, while the absorbance drops by about 55% compared to that of the original solution. In addition, the pattern of the spectrum appears much broader with the high-energy region becoming wider. The blue-shift of the absorption spectra corresponds to the widening of HOMO–LUMO energy gap of the modified MEH-PPV. In other words, long chromophores are converted to shorter ones upon the reaction with PF. In addition, the decrease of the

absorbance indicates the lowering of the molar absorption coefficient.

We carried out additional experiments to explore other parameters that affected the progress of the reaction. The solutions of MEH-PPV at various concentrations [e.g., 0.001, 0.005, and 0.01% (w/v)] were prepared while the PF content was kept constant at 10 vol %. All solutions exhibit the blue-shift in the absorption spectra and the decrease in the absorbance with increasing the reaction time. Plots of λ_{max} and the absorbance as a function of time are shown in Figure 2(a,b). The rate of the reaction is found to increase with a decrease in the concentration of MEH-PPV (or with an increase in the PF to MEH-PPV ratio). The reactions of 0.001, 0.005, and 0.01% (w/v) solutions are completed after the solutions having been aged for 8, 11, and 14 days, respectively. Despite that, the λ_{max} of the final products is detected at practically the same location ($\lambda_{max} \sim 434$ nm). The change in the absorbance shows a consistent trend. These observations indicate that the concentration of the added PF is an important parameter for controlling the HOMO–LUMO energy gap of the modified MEH-PPV.

As mentioned earlier, the broadness of the absorption spectra reflects the distribution of chromophores with various conjugation lengths in the conjugated backbone of MEH-PPV. One can follow the variation in the size distribution of chromophores by plotting the ratios between the integrated areas under two different energy regions of the absorption spectrum, that is, (350–490 nm)/(490–600 nm), as illustrated in Figure 2(c). This ratio is about 1 for the original solutions of MEH-PPV. It gradually increases with an increase in the reaction time for all solutions. The rate of change is highest for the 0.001% (w/v) solution, which is consistent with the variation of λ_{max} and the absorbance. The ratios of the integrated areas reach the value of about 8 after the completion of the reaction, corresponding to the markedly increase in the high-energy chromophores in the system. We also observe that the final product of each solution exhibits slightly different values of the ratios.

In the next section, we performed similar experiments to investigate the effects of PF concentration. The solutions of MEH-PPV with concentrations of 0.001, 0.005, and 0.01% (w/v) were prepared while the quantity of PF was reduced from 10 to 0.1 vol %. Figure 3 illustrates the results obtained from the 0.01% (w/v) MEH-PPV solution with 0.1 vol % PF. It is obvious that the

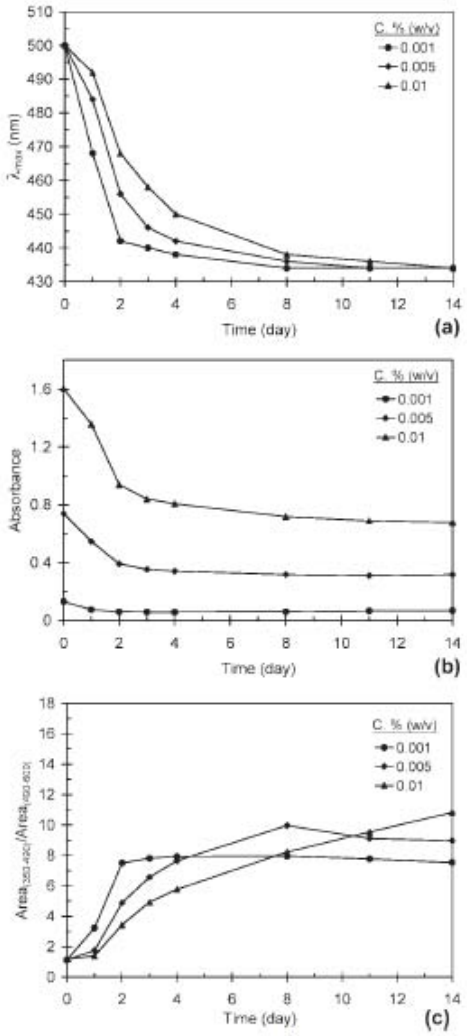

Figure 2. Plots of (a) λ_{max}, (b) absorbance, and (c) $area_{(350-490)}/area_{(490-600)}$ of the absorption spectra of MEH-PPV at various concentrations in DCE with the addition of 10 vol % PF measured as a function of reaction time.

blue-shift and the decrease of the absorbance occur with increasing the reaction time. However, the rate of change is much slower when compared with the solution of 0.01% (w/v) MEH-PPV in the presence of 10 vol % PF. The absorption spectrum changes slightly after 4 days. The reaction yields

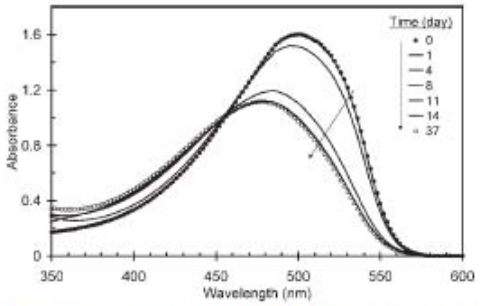

Figure 3. Absorption spectra of 0.01% (w/v) MEH-PPV in DCE with the addition of 0.10 vol % PF measured as a function of reaction time. Arrow indicates the change in the spectra with increasing the reaction time.

the final product after 14 days and its absorption spectrum exhibits λ_{max} at ~476 nm. Previously, it was found that the solutions of MEH-PPV with 10 vol % PF showed the final products with λ_{max} of the absorption spectra at ~434 nm. These results indicate that the change in the PF concentration leads to the modified MEH-PPV with different optical properties. In other words, PF with different concentrations could be used to tune the peak position of the absorption spectrum or the conjugation length of chromophores of the conjugated polymer.

The results obtained from the solutions of 0.001 and 0.005% (w/v) with 0.1 vol % PF confirm our finding. The changes in the absorption spectra with increasing the reaction time are summarized in Figure 4. The λ_{max} of all the solutions decreases with increasing the reaction time and reaches a constant value at ~476 nm after 14 days. The variation in the absorbance shows similar results. Figure 4(c) shows the ratios between the integrated areas under two different energy regions of the absorption spectrum, that is, (350–490 nm)/(490–600 nm), which shows the increase of the values by about two times. It is important to note that the MEH-PPV solutions with 10 vol % PF exhibit the change in this value by about eight times. Therefore, the variation in the PF concentration can be used to tune the average conjugation length (λ_{max}), the molar absorption coefficient, and the size distribution of chromophores in the modified MEH-PPV. The concentration of the polymer also affects the rate of the overall process. The experiments performed on both systems show the increase of the reaction rate with decreasing the polymer concentration (or with increasing the PF to MEH-PPV ratio). To summarize all results, we plot the absorption spectra of the final products obtained at two concentrations of the added PF as shown in Figure 5. The

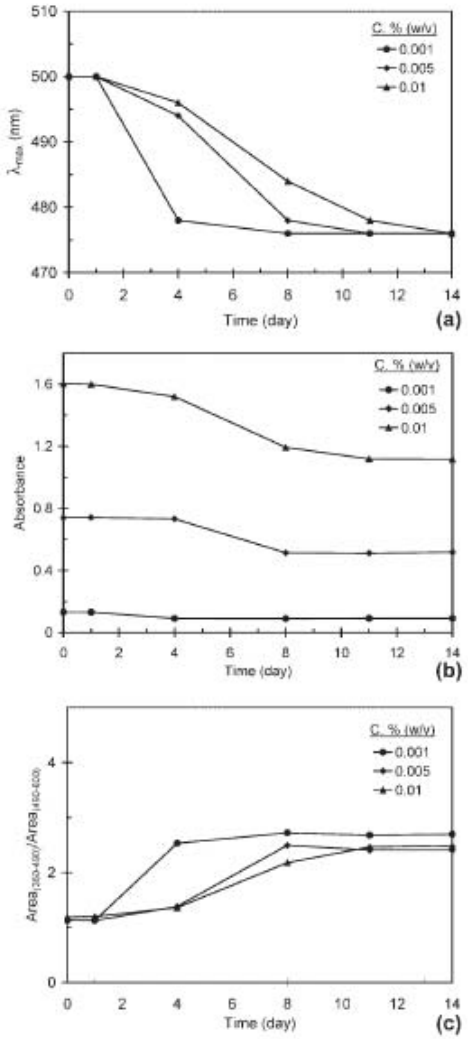

Figure 4. Plots of (a) λ_{max}, (b) absorbance, and (c) $area_{(350-490)}/area_{(490-600)}$ of the absorption spectra of MEH-PPV at various concentrations in DCE with the addition of 0.1 vol % PF measured as a function of reaction time.

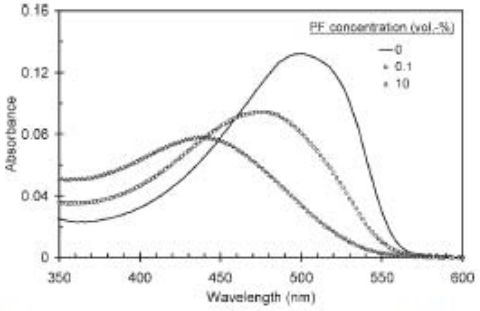

Figure 5. Absorption spectra of 0.001% (w/v) MEH-PPV in DCE at various concentrations of PF after having been aged for 37 days.

absorption spectrum of the original MEH-PPV solution with identical concentration is included for comparison.

The results on photoluminescence show a similar behavior to that of the absorption, previously discussed. The results obtained from the systems

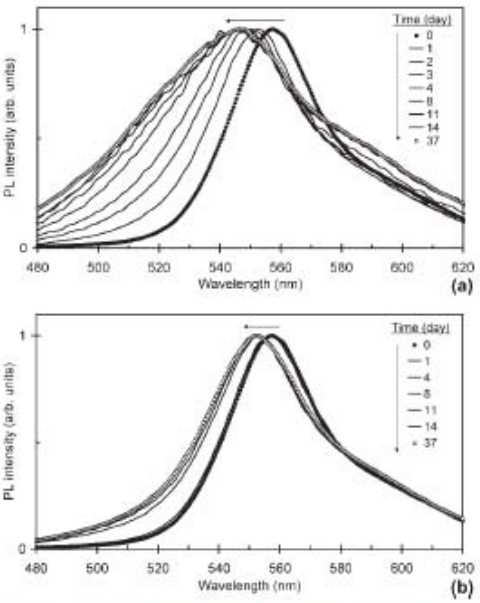

Figure 6. Emission spectra of 0.01% (w/v) MEH-PPV in DCE with the addition of (a) 10 or (b) 0.1 vol % PF measured as a function of reaction time. Arrow indicates the change in the spectra with increasing the reaction time. All spectra are normalized for clarity.

of 0.01% (w/v) MEH-PPV solutions with 10 and 0.1 vol % PF are respectively, shown in Figure 6(a,b). All of the photoluminescent (PL) spectra were recorded with an excitation wavelength of 450 nm. The PL spectrum of the original MEH-PPV solution exhibits λ_{max} at about 559 nm along with a broad shoulder at about 590 nm. The spectra gradually shift to a high-energy region with an increase in the reaction time and become stable after 14 days. The products of MEH-PPV with 10 or 0.1 vol % PF exhibit the PL spectra with λ_{max} of ~546 and ~552 nm, respectively. The solutions appear green and yellow, respectively, under the illumination of a black light ($\lambda \sim 385$ nm). The experiments carried out on 0.005 and 0.001% (w/v) MEH-PPV solutions produced similar results. Figure 7 shows that λ_{max} as measured on all of the solutions investigated decreases with an increase in the reaction time. Similar to the behavior of the absorption spectra, the final

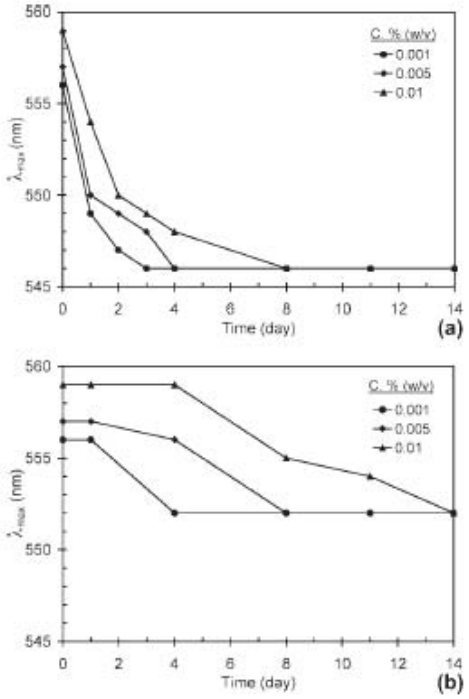

Figure 7. Plots of λ_{max} of the emission spectra of MEH-PPV at various concentrations in DCE with the addition of (a) 10 or (b) 0.1 vol % PF measured as a function of reaction time.

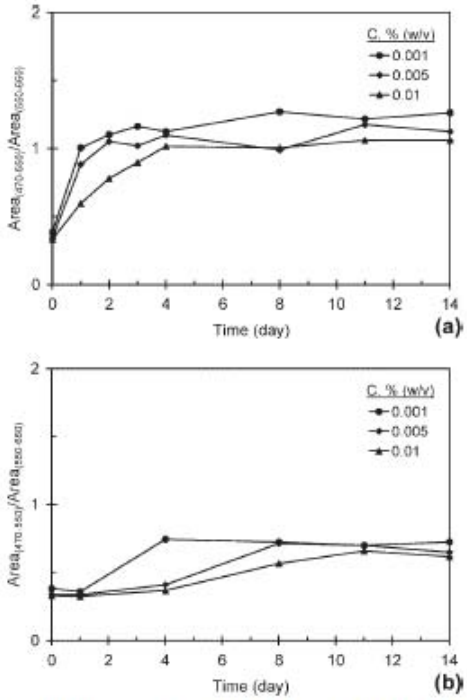

Figure 8. $Area_{(470-550)}/area_{(550-660)}$ of the emission spectra of MEH-PPV at various concentrations in DCE with the addition of (a) 10 or (b) 0.1 vol % PF measured as a function of reaction time.

values of λ_{max} are dictated by the PF concentration, while the rate of change increases with a decrease in the polymer concentration. Interestingly, the peak position of the PL spectra of the original MEH-PPV solutions slightly shifts to a low-energy region with increasing the polymer concentration. This corresponds to the inner-filter effect in which the emitted photons with relatively high energy are reabsorbed by neighboring chromophores. Such an effect becomes dominant upon increasing the concentration of chromophores, causing the PL spectra to red-shift and the overall emission intensity to decrease.

The PL spectra of the modified MEH-PPV, which has been aged for 14 days, exhibit a much broader shape compared to that of the original solution [see Fig. 6(a)], which corresponds to the increase in the size distribution of chromophores in the systems. The ratios between the integrated areas under two different energy regions of the PL spectrum, that is, (470–550 nm)/(550–660 nm), of each solution are calculated and plotted in Figure 8(a,b). The ratio is about 0.4 for the original MEH-PPV solution. The value gradually increases with the reaction time, which corresponds to the conversion of the low-energy chromophores to the higher energy ones. The ratios reach final values of about 1.1 and 0.6 for the systems containing 10 and 0.1 vol % PF, respectively.

In the next section, NMR and FTIR spectroscopy were used to investigate any change in the structure of MEH-PPV, upon coming into contact with PF, that might be responsible for the observed optical properties. Figure 9 displays ^{1}H NMR spectra of the original MEH-PPV, PF, and the modified MEH-PPV. The comparison between the spectra of PF and the modified MEH-PPV indicates that the organic salt is completely removed from our samples. The spectrum of the original MEH-PPV constitutes the peaks at 7.19 and 7.50 ppm, corresponding to olefinic and aromatic protons along the conjugated backbone.[39] The signals of methoxy and alkoxy protons of the side groups are also detected at about 3.7–4.0 ppm. Series of new signals, as illustrated in Figure 9(c), are detected when the MEH-PPV is reacted with 0.1 vol % PF. The intensity of these peaks becomes much more pronounced when the concentration of PF increases to 10 vol % (viz., the

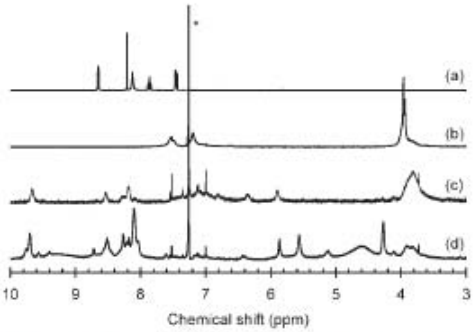

Figure 9. ^{1}H NMR spectra of (a) PF, (b) the original MEH-PPV, (c) MEH-PPV that had been reacted with 0.1 vol % PF, and (d) MEH-PPV that had been reacted with 10 vol % PF in d-chloroform. The solutions in (c) and (d) had been aged for 4 days prior to the removal of PF and solvent (see text). Peak marked with asterisk (*) is due to the residual solvent. For clarity of the presentation, peaks belonging to other protons of the alkyl side groups are not included.

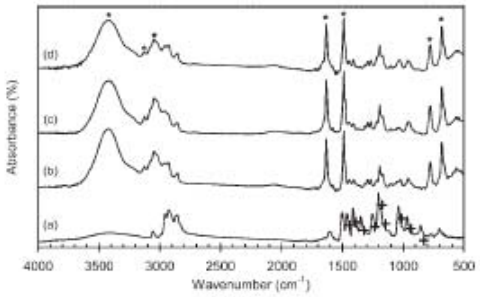

Figure 10. FTIR spectra of (a) the original MEH-PPV and the modified MEH-PPV from (b) 0.001, (c) 0.005, or (d) 0.01% (w/v) MEH-PPV in DCE with the addition of 10 vol % PF. The solutions had been aged for 75 days prior to the removal of PF and solvent. * = The intensity of the peak was greatly increased after PF addition. + = The intensity of the peak was greatly decreased after PF addition.

increase in the extent of the reaction). Some additional peaks are also observed [see Fig. 9(d)]. The appearance of these new peaks is accompanied by a simultaneous decrease in the intensity of the peaks at 7.19 and 7.50 ppm of the original MEH-PPV. In addition, the peaks of the side groups at ~4 ppm become much broader. The detection of new peaks near 5.6 and 8 ppm suggests the incorporation of formate ($HCOO^-$) groups, probably by the addition reaction with reactive double bonds in the conjugated backbone. The peaks near 5 ppm suggest the existence of phenolic groups in the modified polymer, which is likely to be due to the breaking of ether groups of the side groups (see later). The peaks near 10 ppm also suggest the existence of aldehyde groups. However, it is not our intention to try to identify the exact origin of each peak, as one needs to carry out further experiments to follow the reaction.

Figure 10 illustrates the FTIR spectra of the original MEH-PPV along with that of the modified one. The modified MEH-PPV was obtained by reacting with 10 vol % PF for 75 days. We note that the use of 0.01, 0.005, and 0.001% (w/v) of the original MEH-PPV solutions leads to the same FTIR pattern of the dried samples. This indicates that the solvent and PF are completely removed from the samples, which is confirmed by the absence of the FTIR spectrum of the pure PF

Table 1. Analysis of FTIR Spectra of the Original MEH-PPV and Modified MEH-PPV

MEH-PPV		
Original	Modified	Assignment
–	*682	CH bending vibrations in CH deformation
–	*777	CH out-of-plane bending vibrations in —CH=CH—(cis) group
+875	–	CH out-of-plane bending vibrations in —C=CH_2 group
+966	958	CH out-of-plane bending vibrations in —CH=CH—(trans) group
+1040	1020	Aryl alkyl ether (C—O—C) symmetric stretching vibrations in acetates group
+1190	1190	Aryl alkyl ether (C—O—C) stretching vibrations in formates group
+1200	1200	Ring stretching vibrations and CH deformation
+1250	1270	Aryl alkyl ether (C—O—C) asymmetric stretching vibrations in benzoates group
+1350	–	CH bending vibrations in —CH_3 deformation
+1410	1410	CH bending vibrations in —CH_2 deformation
+1460	1440	Asymmetric CH bending vibrations in —CH_3 group
1500	*1490	C=C stretching vibrations in conjugated
–	*1630	C=C stretching vibrations in nonconjugated
2860	2860	Symmetric CH stretching vibrations in —CH_2 group
2930	2930	Asymmetric CH stretching vibrations in —CH_2 group
2950	2950	Asymmetric CH stretching vibrations in —CH_3 group
3060	*3040	CH stretching vibrations in =C—H, =CH_2 group and CH group
–	*3130	NH stretching vibrations in H-bonded NH group
–	*3420	OH stretching vibrations of intramolecular H bonds

The polymer solutions were mixed with 10 vol. % PF and left to age for 75 days. Original concentrations of MEH-PPV are shown in the table.
*, The intensity of the peak was greatly increased after PF addition.
+, The intensity of the peak was greatly decreased after PF addition.

(not shown). Table 1 summarizes some absorption peaks corresponding to different vibrational modes of the polymeric segments. It is apparent that the absorbance of the peaks at 1040, 1190, and 1250 cm^{-1} of the original MEH-PPV is greatly reduced in the modified polymer. Because these peaks are specific to the vibrations of aryl–alkyl ether linkage (C—O—C) of the MEH side groups, this indicates the reduction in the number of MEH side groups in the modified MEH-PPV. In addition, the concentration of tetrahedral defects along the polymeric main chain appears to increase significantly. This is indicated by the detection of new intense peak at 1630 cm^{-1} in the modified MEH-PPV, which is specific to the C=C stretching vibration of the nonconjugated chains. In other words, a number of the C=C bonds is converted to single bonds, which interrupt the conjugation along the conjugated backbone. The detection of a broad peak at 3420 cm^{-1} also indicates the presence of hydroxyl groups in the modified MEH-PPV. These results suggest that the reaction between MEH-PPV and PF results in the reduced number of MEH side groups and the increased number of nonconjugated segments, which are responsible for the observed decrease in the conjugation lengths of the modified polymer.

CONCLUSIONS

We have demonstrated a versatile method for tuning the optical properties of one of the most investigated conjugated polymers, MEH-PPV. This is accomplished by the reaction of the polymer with PF, a volatile organic salt. The absorption and the emission spectra (i.e., colors) of the modified MEH-PPV can be controlled by the variations in the concentration of PF and the reaction time. This method results in the displacement of the λ_{max} of the absorption spectra and the emission spectra by 60 and 15 nm, respectively. The size distribution of chromophores in the main chain is also affected significantly. The modified MEH-PPV chains contain a larger number of shorter chromophores. Structural analysis by using NMR and FTIR spectroscopy indicates that the variation in the optical properties arises from the breaking of some double bonds along the conjugated chains and the removal of MEH side groups. The extent of these structural changes dictates the optical properties of the modified MEH-PPV. The results obtained in this work signify the ability to systematically tuning the optical properties of MEH-PPV, which can be utilized for a wide range of applications such as OLED and solar cells. Our method is a one-step process, which is much simpler compared with the common copolymerization approach. It also requires relatively cheap chemicals and takes a simple procedure for purification.

P. Supaphol acknowledges partial support received from the Thailand Research Fund (TRF) (through a research career development grant: RMU4980045); the Center for Petroleum, Petrochemicals, and Advanced Materials (C-PPAM); and the Petroleum and Petrochemical College (PPC), Chulalongkorn University. S. Changsarn acknowledges a doctoral scholarship received from the Royal Golden Jubilee PhD Program, the Thailand Research Fund (TRF). R. Traiphol thanks the Center of Excellence for Innovation in Chemistry (PERCH-CIC) for supporting some research facilities.

REFERENCES AND NOTES

1. Lee, C. H.; Yu, G.; Sariciftci, N. S.; Heeger, A. J.; Zhang, C. Synth Met 1995, 75, 127–131.
2. Rothberg, L. J.; Yan, M.; Kwock, E. W.; Miller, T. M.; Galvin, M. E.; Son, S.; Papadimitrakopoulos, F. IEEE Trans Electron Dev 1997, 44, 1258–1262.
3. Gettinger, C. L.; Heeger, A. J.; Drake, J. M.; Pine, D. J. J Chem Phys 1994, 101, 1673–1678.
4. Kang, H. S.; Kim, K. H.; Kim, M. S.; Park, K. T.; Kim, K. M.; Lee, T. H.; Joo, J.; Kim, K.; Lee, D. W.; Jin, J. I. Curr Appl Phys 2001, 1, 443–446.
5. Friend, R. H.; Gymer, R. W.; Holmes, A. B.; Burroughes, J. H.; Marks, R. N.; Taliani, C.; Bradley, D. D. C.; Dossantos, D. A.; Brédas, J. L.; Lögdlund, M.; Salaneck, W. R. Nature 1999, 397, 121–128.
6. Shin, J. H.; Matyba, P.; Robinson, N. D.; Edman, L. Electrochim Acta 2007, 52, 6456–6462.
7. Kulkarni, A. P.; Tonzola, C. J.; Babel, A.; Jenekhe, S. A. Chem Mater 2004, 16, 4556–4573.
8. McQuade, D. T.; Pullen, A. E.; Swager, T. M. Chem Rev 2000, 100, 2537–2574.
9. Pistor, P.; Chu, V.; Prazeres, D. M. F.; Conde, J. P. Sens Actuators B 2007, 123, 153–157.
10. Lange, U.; Roznyatovskaya, N. V.; Mirsky, V. M. Anal Chim Acta 2008, 614, 1–26.
11. Spanggaard, H.; Krebs, F. C. Solar Energy Mater Sol Cells 2004, 83, 125–146.
12. Lee, J. K.; Fujida, K.; Tsutsui, T.; Kim, M. R. Solar Energy Mater Sol Cells 2007, 91, 892–896.
13. Schindler, F.; Lupton, J. M.; Feldmann, J.; Scherf, U. Proc Natl Acad Sci USA 2004, 101, 14695–14700.
14. Barbara, P. F.; Gesquiere, A. J.; Park, S. J.; Lee, Y. J. Acc Chem Res 2005, 38, 602–610.

15. Padmanaban, G.; Ramakrishnan, S. J Am Chem Soc 2000, 122, 2244–2251.
16. Traiphol, R.; Charoenthai, N. Synth Met 2008, 158, 135–142.
17. Traiphol, R.; Sanguansat, P.; Srikhirin, T.; Kerdcharoen, T.; Osotchan, T. Macromolecules 2006, 39, 1165–1172.
18. Klaerner, G.; Miller, R. D. Macromolecules 1998, 31, 2007–2009.
19. Bunz, U. H. F. Chem Rev 2000, 100, 1605–1644.
20. Ding, L.; Egbe, D. A. M.; Karasz, F. E. Macromolecules 2004, 37, 6124–6131.
21. Huang, C.; Zhen, C. G.; Su, S. P.; Vijila, C.; Balakrisnan, B.; Auch, M. D. J.; Loh, K. P.; Chen, Z. K. Polymer 2006, 47, 1820–1829.
22. Padmanaban, G.; Ramakrishnan, S. J Phys Chem B 2004, 108, 14933–14941.
23. Scherf, U.; List, E. J. W. Adv Mater 2002, 14, 477–487.
24. Vak, D.; Chun, C.; Lee, C. L.; Kim, J. J.; Kim, D. Y. J Mater Chem 2004, 14, 1342–1346.
25. Assaka, A. M.; Rodrigues, P. C.; de Oliveira, A. R. M.; Ding, L.; Hu, B.; Karasz, F. E.; Akcelrud, L. Polymer 2004, 45, 7071–7081.
26. Neef, C. J.; Ferraris, J. P. Macromolecules 2000, 33, 2311–2314.
27. Collison, C. J.; Rothberg, L. J.; Treemaneekarn, V.; Li, Y. Macromolecules 2001, 34, 2346–2352.
28. Menon, A.; Galvin, M.; Walz, K. A.; Rothberg, L. Synth Met 2004, 141, 197–202.
29. Traiphol, R.; Charoenthai, N.; Srikhirin, T.; Kerdcharoen, T.; Osotchan, T.; Maturos, T. Polymer 2007, 48, 813–826.
30. Wu, C.; Peng, H.; Jiang, Y.; Mcneill, J. J Phys Chem B 2006, 110, 14148–14154.
31. Nagesh, K.; Kabra, D.; Narayan, K. S.; Ramakrishnan, S. Synth Met 2005, 155, 295–298.
32. Ananthakrishnan, N.; Padmanaban, G.; Ramakrish, S.; Reynolds, J. R. Macromolecules 2005, 38, 7660–7669.
33. Babel, A.; Jenekhe, S. A. Macromolecules 2004, 37, 9835–9840.
34. Iyengar, N. A.; Harrison, B.; Duran, R. S.; Schanze, K. S.; Reynolds, J. R. Macromolecules 2003, 36, 8978–8985.
35. Lee, Y.-Z.; Chen, X.; Chen, S.-A.; Wei, P.-K.; Fann, W.-S. J Am Chem Soc 2001, 123, 2296–2307.
36. Bai, H.; Wu, X.; Shi, G. Polymer 2006, 47, 1533–1537.
37. Ding, L.; Lu, Z.; Egbe, D. A. M.; Karasz, F. E. Macromolecules 2004, 37, 10031–10035.
38. Chuangchote, S.; Srikhirin, T.; Supaphol, P. Macromol Rapid Commun 2007, 28, 651–659.
39. Traiphol, R.; Srikhirin, T.; Kerdcharoen, T.; Osotchan, T.; Scharnagl, N.; Willumeit, R. Eur Polym J 2007, 43, 478–487.

Macromolecular
Materials and Engineering

Macromolecular Journals

Full Paper

Morphology and Photophysical Properties of Electrospun Light-Emitting Polystyrene/Poly-(*p*-phenylene ethynylene) Fibers

Sutheerat Changsarn, James D. Mendez, Christoph Weder,* Pitt Supaphol*

Ultra-thin fibers, consisting of blends of a PPE derivative and polystyrene, with average diameters ranging from 430 to 1 200 nm, were produced by electrospinning. The electrospinnability was significantly improved by adding pyridinium formate to the spinning solution. FT-IR spectroscopy was used to confirm the composition of the electrospun fibers and their morphology was probed by SEM. The optical properties of the as-prepared solutions, pristine and annealed fibers, and corresponding spin-coated and solution-cast films were investigated by UV-vis spectroscopy. A comparison of the PL emission spectra revealed aggregation of PPE molecules in the electrospun materials but the extent of aggregation can be reduced if the materials are annealed above the glass transition temperature.

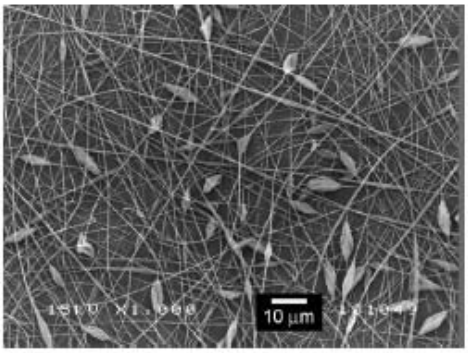

Introduction

Since the discovery of the electrical conductivity in π-conjugated polymers thirty years ago,[1] (semi)conducting polymers have become the focus of intense research and development activities around the world.[2] Their use as synthetic metals[3] and as organic semiconductors in light-emitting diodes,[4] field-effect transistors,[5] photovoltaic devices,[6] sensors[7] and many other applications, has led to rapid growth of the field. Many different families of conjugated polymers, for example, poly(phenylene vinylene)s (PPVs),[8] poly(fluorene)s (PFs),[9] and poly(phenylene ethynylene)s (PPEs),[10] are being studied, often with the objective of tailoring their properties to meet the needs of these applications. PPE and its derivatives represent an interesting family because of their nonlinear optical characteristics,[11] photo-[12] and electroluminescent properties,[13] charge-carrier mobility,[14] and chemical responsiveness,[15] which make them attractive for use in applications that include organic light-emitting diodes,[16] light polarizers,[17] liquid crystal displays (LCDs),[18] transistors,[19] solar cells[20] and sensors.[21] Recently, cross-linked PPE networks[22] were demonstrated to be of a microporous nature with specific surface areas that exceed those of activated carbons and offer significant H_2 storage capacity.[23] While most previous

S. Changsarn, P. Supaphol
Technological Center for Electrospun Fibers and The Petroleum and Petrochemical College, Chulalongkorn University, Soi Chula 12, Phyathai Rd., Pathumwan, Bangkok 10330, Thailand
Fax: +66 2215 4459; E-mail: pitt.s@chula.ac.th
J. D. Mendez, C. Weder
Department of Macromolecular Science and Engineering and Department of Chemistry, Case Western Reserve University, 2100 Adelbert Rd., Cleveland, Ohio 44106-7202, USA
Fax: +1 216 368 4202; E-mail: christoph.weder@case.edu

Macromol. Mater. Eng. **2008**, *293*, 952–963

InterScience®
DOI: 10.1002/mame.200800268

investigations with regards to the properties of PPEs have been in either solution or thin films, relatively little attention has been paid to the study of the polymers in the form of ultra-fine fibers, which offer high aspect and high surface area to volume or mass ratios.

Recently, Bunz and coworkers reported the investigation of the morphology and photophysical properties of electrospun (e-spun) poly(arylene ethynylene)s (PAEs) with dioctyl or polycaprolactone (PCL) side chains.[24] Interestingly, poly(2,5-dioctyl-*p*-phenylene ethynylene) with a degree of polymerization (DP) of 60 could only be sprayed into microspheres with average diameters of 1–1.5 μm, but not spun into fibers. On the other hand, grafting PCL chains with a DP of at least 65 to either a poly(*p*-phenylene ethynylene) or poly(benzothiadiazole-*co*-alkyne-*co*-benzene-*co*-alkyne) core resulted in materials that could, under optimized conditions, be spun into well-defined fibers with diameters ranging from 50 nm to 1 μm. The nature of the solvent, the concentration of the polymer in the spinning solution, and the DPs of the PCL side chains and the PAE core were all found to play a major role in determining the morphology of the electrospun products obtained. Most importantly, the high-molecular-weight PCL side chains employed by Bunz contribute significantly to the viscosity of the solution, allowing electrospinning (e-spinning) of high-quality fibers.[24] On the other hand, e-spinning of a more common PPE derivative (i.e., one in which the electrospinnability is not imparted through high-molecular weight side chains) into fiber form has not yet been reported. This appears directly related to rheological limitations.[25–32] PAEs are often produced as materials of rather low-molecular weight, sometimes deliberately to maintain good solubility,[12a] so that even at their solubility limit they form solutions of low viscosity.[24]

We here report an approach that is orthogonal to the high-DP side chain route, namely the e-spinning of blends of a common poly(2,5-dialkoxy-*p*-phenylene ethynylene) derivative featuring an alternate substitution of ethylhexyloxy and octyloxy in the 2 and 5 positions of the phenylene rings (EHO-OPPE;[12a] see Figure 1) and polystyrene (PS) as an 'inert' carrier polymer. We demonstrate that this approach allows one to produce ultra-fine fibers with diameters that range from hundreds of nanometers to one micrometer.

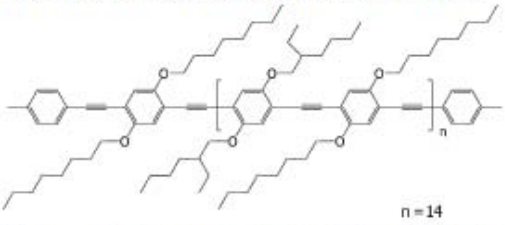

Figure 1. Chemical structure of EHO-OPPE, the PPE derivative used.

Experimental Part

Materials and Preparation of Solutions for Spinning and Casting Films

EHO-OPPE ($\overline{M}_n \approx 14\,000$ Da; Figure 1) was synthesized following a procedure previously described.[12a] PS ($\overline{M}_w \approx 3.0 \times 10^5$ Da; pellet form) was a general purpose grade from Dow Chemicals (USA). The solvents used were 1,2-dichloroethane [DCE; Lab-Scan (Asia), Thailand] and chloroform (CF; Carlo Erba, Italy). Pyridinium formate (PF), a volatile organic salt, was prepared by reacting pyridine [Lab-Scan (Asia), Thailand] and formic acid (Merck, England) in an equimolar quantity. Solutions of 8.5% (w/v) PS/EHO-OPPE in DCE or CF (the compositional weight ratio between PS and EHO-OPPE being 7.5:1) with or without the addition of 8 vol-% PF were prepared by combining all compounds and stirring at room temperature for 5 min. A solution of 8.5% (w/v) PS in DCE was prepared in similar fashion and was used as a reference.

Electrospinning

E-spinning of the as-prepared solutions was carried out under an electrical potential of between 7.5 and 20 kV. Unless otherwise indicated, products (i.e., fibers and/or beads) were spun at an applied electrical potential of 15 kV. The collection distance and the collection time were fixed at 10 cm and 1 min, respectively. Each of the freshly-prepared spinning solutions was placed in a 5 mL plastic syringe, the open end of which was connected to a blunt 20 gauge stainless steel hypodermic needle (outer diameter = 0.91 mm), which was used as the nozzle. An aluminum foil wrapped around a rigid plastic sheet was used as the collector plate. The emitting electrode of positive polarity from a Gamma High-Voltage Research ES30P DC power supply (Florida, USA) was connected to the needle, while the grounding electrode was connected to the collector plate. The feed rate of the solution was controlled by means of a Kd Scientific syringe pump at 1 $mL \cdot h^{-1}$. Where applicable, the e-spun fibers were annealed for between 5 min and 1 h at 110 °C, which is above the glass transition temperature (T_g) of PS (95 °C[33]).

Spin Coating and Solution Casting

Films of the PS/EHO-OPPE blends were produced by either spin coating or solution casting from solutions comprising 8–10 $mg \cdot mL^{-1}$ of the polymer blend. Spin coating was done on a Specialty Coating Systems model P6700 with spinning speeds of 1 500–2 000 rpm to achieve a final thickness of 0.5–1 μm. Solution casting was done on glass slides and resulted films of a final thickness of 1–3 μm.

Characterization

The morphological appearance of the e-spun fibers was examined by a JEOL JSM-5410LV scanning electron microscope (SEM). The average bead diameters and the number of beads per unit area (i.e., the bead density) of the electrosprayed beads or the e-spun

beaded fibers were calculated from measurements of SEM images at ×500 magnification. Diameters of the e-spun fibers, where applicable, were determined from SEM images at ×1 000 magnification, with the average value being calculated from at least 50 measurements (for each spinning condition). For beaded fibers, only the diameters of the fiber segments between beads were measured. A Thermo-Nicolet Nexus 670 Fourier-transform infrared (FT-IR) spectroscope was used to characterize the as-received PS pellets, the as-synthesized EHO-OPPE, and some of the e-spun PS/EHO-OPPE products. Optical absorption and photo-luminescence emission spectra of the PS/EHO-OPPE solutions in DCE and CF with or without PF addition, the corresponding pristine and annealed e-spun fibers, spin-coated films, and solution-cast films were measured by a Hewlett Packard-8254A diode array UV-vis spectrophotometer (UV-vis) and a Perkin-Elmer LS50 luminescence spectrometer (PL). For the solution measurements, a 1 mm thick quartz cuvette was used in order to reduce the self-absorption effect, allowing the detection of photon emission from front surface. For PL experiments, samples were excited at 400 nm.

Results and Discussion

Polystyrene (PS), a non-luminescent glassy-amorphous polymer, was chosen as an 'inert' carrier polymer for the present study. Neat PS was e-spun for reference purposes from 1,2-dichloroethane (DCE) to determine the morphology of the neat polymer template when processed under the conditions selected for this study. Figure 2 shows representative SEM images of the products obtained from a 8.5% (w/v) solution of PS in DCE under various electrical potentials between 7.5 and 20 kV. The e-spinning of a 8.5% (w/v) PS solution in DCE only resulted in the formation of beads, with average size in the range of 22.6–29.0 μm (see Figure 2 and Table 1). The density of the beads on the collection plate was between 0.17×10^5 and 0.56×10^5 beads · cm^{-2}. This tendency to form beads rather than ultra-fine fibers was previously observed and reported for PS that was e-spun from DCE or chloroform (CF), the second solvent employed here, if the concentration of the PS solutions was less than 10 wt.-%.[34]

Interestingly, the electro-spinnability of the PS solution in DCE was significantly improved in the presence of a comparably small amount of EHO-OPPE [i.e., PS:EHO-OPPE = 7.5:1 (w/w)]. Representative SEM images of the e-spun products (see Figure 3a) clearly show the appearance of ultra-fine fibers with a limited density of elongated beads. The average fiber diameters, bead size, and bead density of the beaded fibers obtained are in the range of 0.43–0.83 μm, 2.77–3.65 μm and 1.43×10^5–3.77×10^5 beads · cm^{-2}, respectively (see Table 1). To further improve the electro-spinnability of the PS/EHO-OPPE solution, the volatile organic salt pyridinium formate (PF) was added.[32] Figure 3b shows representative SEM images of the e-spun products. Either smooth or beaded fibers with fewer beads were observed. The average fiber diameter range increased to 0.55–0.87 μm, while the bead size range remained about the same at 2.12–4.89 μm. However, the bead density range decreased to 0.04×10^5–1.32×10^5 beads · cm^{-2}. This substantial decrease in the bead density shows that the addition of PF helps to promote uniform fiber formation.

The same trends were observed when CF was used as the solvent (see Figure 4a and b). In this case, the average

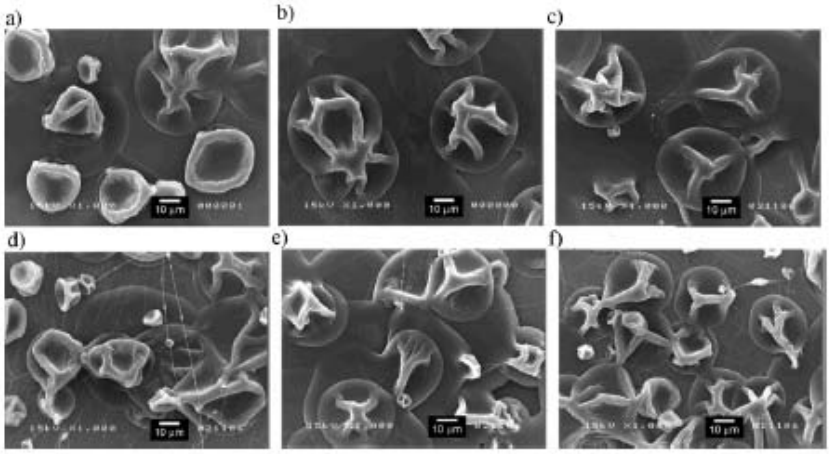

Figure 2. SEM images of the electrosprayed PS beads from 8.5% (w/v) solutions of PS in DCE (×1 000, scale bar = 10 μm). The applied electrical potential for the electrospinning was: a) 7.5, b) 10, c) 12.5, d) 15, e) 17.5, and f) 20 kV.

Macromol. Mater. Eng. **2008**, *293*, 952–963

Macromolecular Journals

DOI: 10.1002/mame.200800268

Table 1. Average fiber diameter, bead size and bead density of the electrospun products from 8.5% (w/v) solutions of PS in DCE and 8.5% (w/v) solutions of PS/EHO-OPPE (PS:EHO-OPPE = 7.5:1) in DCE and CF without and with the addition of 8 vol.-% PF. The table lists parameters for materials e-spun at different applied electrical potentials (HV). The collection distance was 10 cm, the collection time was 1 min and the solution flow rate was 1 mL · h^{-1}.

Solution	HV	Fiber diameter	Bead size	Bead density
	kV	μm	μm	beads · cm^{-2}
PS/DCE	7.5	–	29.05 ± 11.53	0.34 × 10^5
	10.0	–	28.12 ± 12.24	0.17 × 10^5
	12.5	–	27.94 ± 13.94	0.36 × 10^5
	15.0	–	22.57 ± 14.86	0.56 × 10^5
	17.5	–	26.92 ± 11.81	0.29 × 10^5
	20.0	–	24.37 ± 12.08	0.45 × 10^5
PS/EHO-OPPE/DCE	7.5	0.43 ± 0.14	2.88 ± 0.71	3.77 × 10^5
	10.0	0.54 ± 0.21	2.77 ± 0.75	3.52 × 10^5
	12.5	0.61 ± 0.17	3.65 ± 1.02	2.86 × 10^5
	15.0	0.79 ± 0.21	3.18 ± 1.08	2.00 × 10^5
	17.5	0.81 ± 0.18	3.11 ± 1.22	1.59 × 10^5
	20.0	0.83 ± 0.18	2.91 ± 0.85	1.43 × 10^5
PS/EHO-OPPE/DCE + PF	7.5	0.55 ± 0.12	2.12 ± 0.51	0.04 × 10^5
	10.0	0.66 ± 0.19	2.96 ± 0.93	0.57 × 10^5
	12.5	0.70 ± 0.15	3.58 ± 0.96	0.40 × 10^5
	15.0	0.72 ± 0.24	4.89 ± 1.56	1.32 × 10^5
	17.5	0.76 ± 0.28	4.74 ± 2.85	1.25 × 10^5
	20.0	0.87 ± 0.28	4.82 ± 2.08	1.20 × 10^5
PS/EHO-OPPE/CF	7.5	0.51 ± 0.12	13.65 ± 0.65	4.13 × 10^5
	10.0	0.56 ± 0.12	14.05 ± 0.80	4.23 × 10^5
	12.5	0.63 ± 0.14	15.14 ± 0.82	5.25 × 10^5
	15.0	0.66 ± 0.15	16.11 ± 1.19	2.76 × 10^5
	17.5	0.68 ± 0.20	17.80 ± 1.31	2.82 × 10^5
	20.0	0.68 ± 0.15	18.05 ± 1.23	2.46 × 10^5
PS/EHO-OPPE/CF + PF	7.5	1.04 ± 0.33	1.06 ± 0.55	0.66 × 10^5
	10.0	1.04 ± 0.39	4.24 ± 1.84	2.26 × 10^5
	12.5	1.05 ± 0.37	4.41 ± 2.21	1.71 × 10^5
	15.0	1.12 ± 0.53	5.00 ± 2.64	1.51 × 10^5
	17.5	1.16 ± 0.38	5.23 ± 2.24	1.47 × 10^5
	20.0	1.20 ± 0.37	5.76 ± 3.74	1.36 × 10^5

fiber diameters, bead sizes, and bead densities of the e-spun PS/EHO-OPPE fibers from the blend solution without the addition of PF are in the range of 0.51–0.68 μm, 13.65–18.05 μm and 2.46 × 10^5–5.25 × 10^5 beads · cm^{-2}, respectively (see Table 1). Here, the addition of PF in the blend solution also resulted in an observed increase of the average fiber diameters in the range of 1.04–1.20 μm and an observed decrease of the bead density in the range of 0.66 × 10^5–1.71 × 10^5 beads · cm^{-2}. On the other hand, the bead size was found to decrease in the range of 1.06–5.76 μm (see Table 1).

Based on these results, it appears that DCE is a better solvent than CF for the e-spinning of the blend solution of PS and EHO-OPPE, because the average fiber diameters, bead sizes, and bead densities of the products obtained from the blend solutions – with and without PF – in DCE are lower than those of the products obtained from the corresponding blend solutions in CF. Based on the

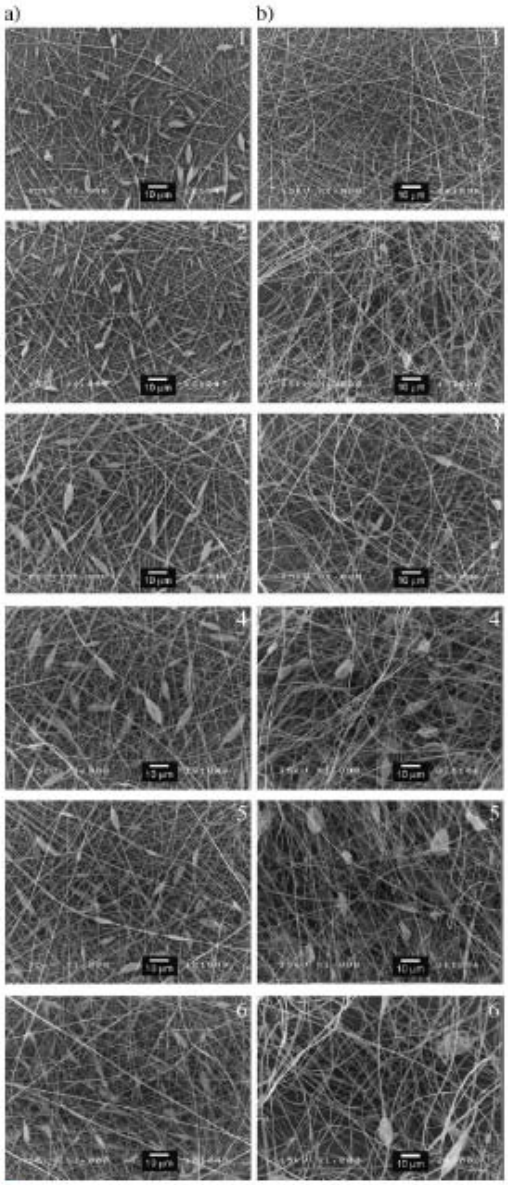

Figure 3. SEM images of the electrospun products from 8.5% (w/v) solutions of PS/EHO-OPPE (PS:EHO-OPPE = 7.5:1) in DCE without (a) and with (b) the addition of 8 vol.-% PF (×1 000, scale bar = 10 μm). The applied electrical potential for the electrospinning was (1) 7.5, (2) 10, (3) 12.5, (4) 15, (5) 17.5 and (6) 20 kV.

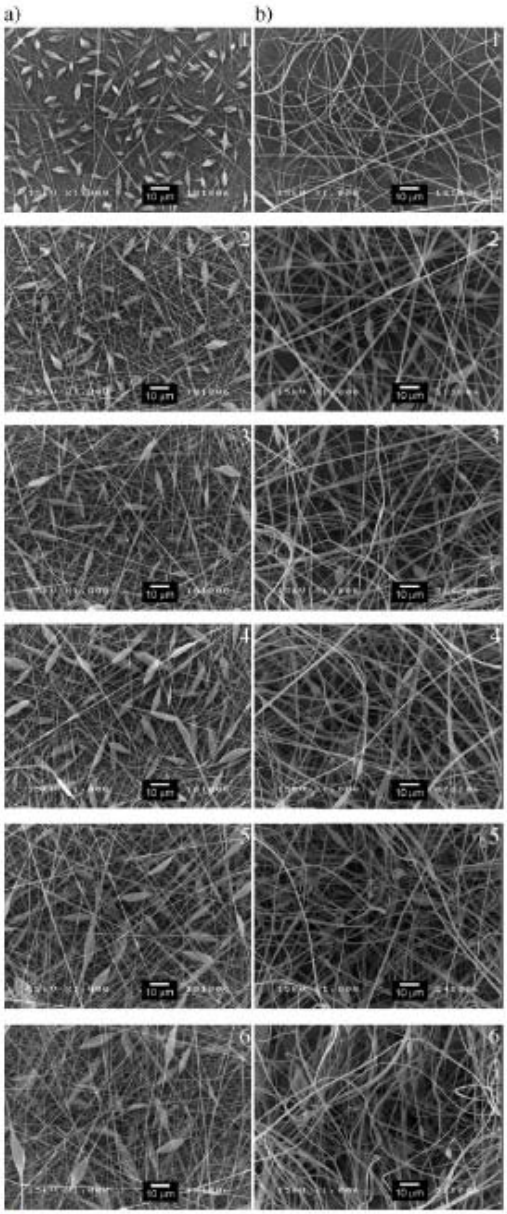

Figure 4. SEM images of the electrospun products from 8.5% (w/v) solutions of PS/EHO-OPPE (PS:EHO-OPPE = 7.5:1) in CF without (a) and with (b) the addition of 8 vol.-% PF (×1000, scale bar = 10 μm). The applied electrical potential for the electrospinning was (1) 7.5, (2) 10, (3) 12.5, (4) 15, (5) 17.5 and (6) 20 kV.

Macromol. Mater. Eng. **2008**, 293, 952–963

Macromolecular Journals

DOI: 10.1002/mame.200800268

quantitative results summarized in Table 1, it is evident that the average diameter of the e-spun fibers increases with increasing applied electrical potential. This is a direct result of the increase in the total number of charged species within the jet segment, which, in turn, causes an increase in the electrostatic forces. The increase in such forces leads to an increase in the speed of the jet and a hypothetic decrease in the total path trajectory of the jet, which results in an increase in the feed flow rate and ultimately the diameters of the obtained fibers.[35,36] Clearly, the addition of PF to the spinning solution also improves significantly the electro-spinnability of the spinning solution, as shown from the substantial decrease in the bead density (see Table 1). In view of previous studies, which based the results on an increase in the number of charge carriers within the jet due to the addition of PF, this result does not come as a surprise.[35,37,38]

FT-IR spectroscopy was conducted to confirm the existence of both PS and EHO-OPPE constituents in the e-spun blend fibers (see Figure 5). Individual spectra are shown of the as-received PS, the as-synthesized EHO-OPPE, and the selected fiber mats which had been e-spun from 8.5% (w/v) solution of PS in DCE and 8.5% (w/v) solutions of PS/EHO-OPPE in DCE or CF with and without the addition of PF at an electrical potential of 15 kV. Table 2 summarizes some absorption peaks specific to chemical functionalities of the PS and the EHO-OPPE components in the e-spun fibers. Clearly, the peaks characteristic to the PS component are observed in all of the FT-IR spectra of the e-spun fibers (i.e., at 697–698, 754–756, 906, 1490, 2920, 3030 and 3060 cm^{-1}). Moreover, some peaks characteristic to the EHO-OPPE component (e.g., at 1210 and 1270 cm^{-1}) are also observed in the FT-IR spectra of the e-spun fibers. The peak at 1210 cm^{-1} corresponds to ring stretching vibrations and C–H deformation, while the peak at 1270 cm^{-1} is specific to aryl alkyl ether (C–O–C) asymmetric stretching vibrations. These results confirm the existence and the chemical integrity of both the PS and the EHO-OPPE components in the e-spun fibers.

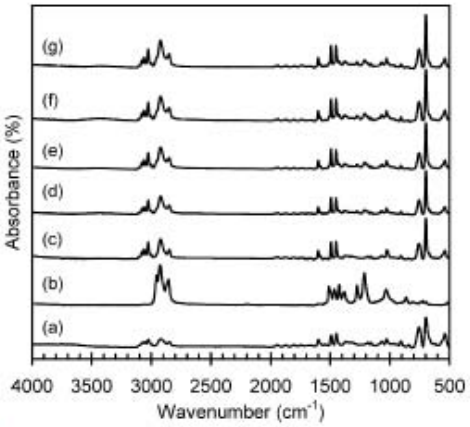

Figure 5. FT-IR spectra of a) as-received neat PS, b) EHO-OPPE powder, and the electrospun fibers from, c) 8.5% (w/v) solution of PS in DCE, 8.5% (w/v) solutions of PS/EHO-OPPE (PS:EHO-OPPE = 7.5:1) in DCE without (d) and with (e) the addition of 8 vol.-% PF, and 8.5% (w/v) solutions of PS/EHO-OPPE (PS:EHO-OPPE = 7.5:1) in CF without (f) and with (g) the addition of 8 vol.-% PF.

The optical properties of the spinning solutions, pristine and annealed e-spun fibers, and spin-coated and solution-cast reference films were investigated by UV-Vis absorption and PL spectroscopy and the results are summarized in Table 3. Figure 6a and b summarize the optical properties of the 8.5% (w/v) spinning solutions of PS/EHO-OPPE (7.5:1 w/w) in DCE and CF with and without 8 vol.-% PF. All spectra were normalized to allow for easy comparison. The emission spectra of 8.5% (w/v) solutions of PS/EHO-OPPE in DCE exhibit sharp peaks at 487 and 508 nm (see Figure 6b). The emission spectra of 8.5% (w/v) solutions of PS/EHO-OPPE in CF are almost identical, displaying maxima at 485 and 507 nm, respectively (see Figure 6b). While the solvent has a slight solvatochromic effect on the absorption and the emission maxima of EHO-OPPE in DCE and CF, the addition of PS and PF does not exert any appreciable influence on the optical characteristics of the conjugated polymer. The features – splitting of the emission spectra into two well-resolved bands and the lack of mirror image similarity between absorption and emission – are related to vibronic coupling and are characteristic of alkyloxy-PPE emission.[12a]

Figure 7a and b show the emission spectra of fibers spun from 8.5% (w/v) solutions of PS/EHO-OPPE with 8 vol.-% PF in DCE and CF, respectively, as a function of the applied electrical potential. All emission spectra exhibit a broad peak centered around 508–519 nm and weak shoulders around 457–461 and 590–599 nm. Compared to the emission spectra of the spinning solutions, the emission spectra of the e-spun fibers show less-well-resolved features and appear somewhat broadened, indicative of aggregation of the conjugated polymer guest in the PS matrix. While the PL spectra of the fibers that had been e-spun at different electrical potential exhibit minor differences (see Table 4), there is no specific correlation between the emission peak positions and the applied electrical potential. It is postulated that the slight variation in the emission peak positions occurs from the fluctuation in the forces acting on jet segments, and hence the EHO-OPPE molecules, during the e-spinning.

Table 2. Analysis of FT-IR spectra of as-received PS, EHO-OPPE and the electrospun products from 8.5% (w/v) solutions of PS in DCE and 8.5% (w/v) solutions of PS/EHO-OPPE (PS:EHO-OPPE = 7.5:1) in DCE and CF without and with the addition of 8 vol.-% PF.

Absorption band / cm^{-1}							Assignment
As-received materials		Electrospun products					
PS	EHO-OPPE	PS/DCE	PS/EHO-OPPE/DCE	PS/EHO-OPPE/DCE + PF	PS/EHO-OPPE/CF	PS/EHO-OPPE/CF + PF	
698	–	698	697	697	697	697	CH bending vibrations in CH deformation
754	–	756	755	756	755	756	CH out-of-plane bending vibrations in –CH=CH–(*cis*) group
–	863	–	–	–	–	–	CH out-of-plane bending vibrations in $C=CH_2$ group
906	–	906	906	906	905	905	CH out-of-plane bending vibrations in $–CH=CH_2$ group
–	1030	1030	1030	1030	1030	1030	Aryl alkyl ether (C–O–C) symmetric stretching vibrations
–	1210	–	1210	1210	1210	1210	Ring-stretching vibrations and CH deformation
–	1270	–	1270	1270	1270	1270	Aryl alkyl ether (C–O–C) asymmetric stretching vibrations
–	1380	–	–	–	–	–	CH bending vibrations in $–CH_3$ deformation
–	1420	–	–	–	–	–	CH bending vibrations in $–CH_2$ and $–CH_3$ deformation
1450	1470	1450	1450	1450	1450	1450	Asymmetric CH bending vibrations in $–CH_3$ group
1490	–	1490	1490	1490	1490	1490	CH bending vibrations in $–CH_2$ scissoring group
1600	1510	1600	1600	1600	1600	1600	C=C stretching vibrations in conjugated bonds
2850	2860	2850	2850	2850	2850	2850	Symmetric CH stretching vibrations in $–CH_2$ group
2920	–	2920	2920	2920	2920	2920	Asymmetric CH stretching vibrations in $–CH_2$ group
–	2930	–	–	–	–	–	Asymmetric CH stretching vibrations in $–CH_3$ group
–	2960	–	–	–	–	–	Asymmetric CH stretching vibrations in $–CH_3$ group
3030	–	3020	3020	3020	3020	3020	CH stretching vibrations in =C–H, $=CH_2$ and CH groups
3060	–	3060	3060	3060	3060	3060	CH stretching vibrations in =C–H, $=CH_2$ and CH groups

For the purpose of comparison, the emission characteristics of films prepared by spin-coating and solution-casting of 8.5% (w/v) solutions of PS/EHO-OPPE in DCE and CF with and without 8 vol.-% PF were also investigated. All spin-coated films [Figure 8a–d, Series (1)] show virtually identical spectra with well-resolved features and maxima at ≈470 and ≈508 nm. The spectral shape is indicative of emission from well dispersed – as opposed to aggregated – PPE molecules, [12a] suggesting that rapid solvent evaporation during spin-coating produces kinetically-trapped, molecularly-mixed PS/EHO-OPPE blends. Presumably due to the less polar nature of PS as the solid solvent, the emission spectra are slightly blue-shifted compared to those recorded in DCE and CF solution (Figure 7). The emission spectra of the solution-cast films [Figure 8a–d, Series (2)] paint a slightly different picture. Here, two major bands centered at ≈465–473 and 529 nm are observed. While the former coincides with the high-energy band observed in the spin-coated films and appears to be associated with emission from well-dispersed PPE molecules, the latter suggests emission from a neat (but disordered) PPE

Macromol. Mater. Eng. **2008**, *293*, 952–963

Macromolecular Journals

DOI: 10.1002/mame.200800268

Table 3. Summary of the positions of peaks and shoulders of the PL emission spectra of 8.5% (w/v) solutions of PS/EHO-OPPE (PS:EHO-OPPE = 7.5:1) in DCE and CF without and with the addition of 8 vol.-% PF, the corresponding spin-coated and solution-cast films, and the as-annealed (i.e., at 110 °C) PS/EHO-OPPE fibers.

Sample	System	Annealing time	Peaks		Shoulders	
		min	nm		nm	
			High intensity	Low intensity	High energy	Low energy
Solutions	DCE	–	487	509	–	–
	DCE + PF	–	487	508	–	–
	CF	–	485	506	–	–
	CF + PF	–	485	508	–	–
Spin-coated films	DCE	–	470	–	490	–
	DCE + PF	–	470	–	490	–
	CF	–	470	–	489	–
	CF + PF	–	470	–	489	–
Solution-cast films	DCE	–	463	529	–	–
	DCE + PF	–	462	529	–	–
	CF	–	463	528	–	–
	CF + PF	–	462	528	–	–
E-spun fibers	DCE	0	503	–	468	594
		5	503	–	473	595
		30	505	–	473	594
		60	505	–	473	595
	DCE + PF	0	516	–	465	594
		5	515	–	469	595
		30	513	–	465	594
		60	507	–	465	596
	CF	0	516	–	464	595
		5	514	–	464	594
		30	509	–	469	594
		60	507	–	470	593
	CF + PF	0	519	–	466	595
		5	517	–	470	594
		30	511	–	469	595
		60	510	–	470	594

phase.[12a,13c] This finding reflects that slow solvent evaporation results in phase-separated PS/EHO-OPPE blends, indicative of thermodynamic immiscibility of the two polymers.

A comparison of the PL emission spectra of pristine e-spun fibers [Figure 8a–d, Series (3)] with those of the spin-coated and the solution-cast films shows that the fiber emission is virtually exclusively due to emission from a phase-separated PPE phase. Assuming that annealing above the T_gs of the polymers (95 °C for PS; 90 °C for EHO-OPPE[12b]) could change the morphology (and therewith the optical properties) of the blends, the e-spun nanofibers were annealed for up to 1 h at 110 °C. The effect of thermal annealing on the emission spectra is reflected by the spectra shown in Figure 8a–d, Series 4–6. Interestingly, annealing leads to the appearance of an emission band around ≈465–470 nm, the intensity of which increases with the annealing time. This finding is consistent with an increased miscibility of the two polymers at higher temperature, causing at least a minor

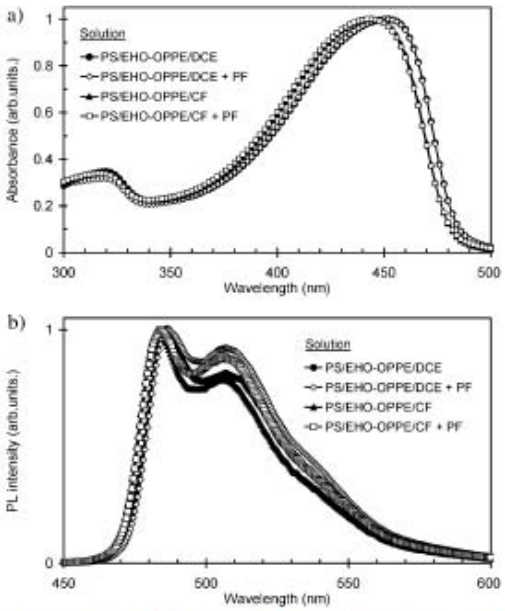

Figure 6. a) Absorption and b) PL emission spectra of 8.5% (w/v) solutions of PS/EHO-OPPE (PS:EHO-OPPE = 7.5:1) in DCE and 8.5% (w/v) solutions of PS/EHO-OPPE (PS:EHO-OPPE = 7.5:1) in CF without and with the addition of 8 vol.-% PF.

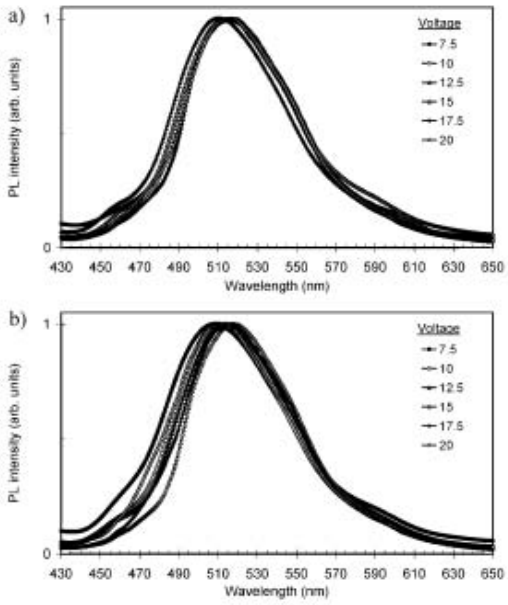

Figure 7. PL emission spectra of the electrospun fibers from 8.5% (w/v) solutions of PS/EHO-OPPE (PS:EHO-OPPE = 7.5:1) with the addition of 8 vol.-% PF in a) DCE, and b) CF at various applied electrical potentials.

Table 4. Summary of the positions of peaks and shoulders of the PL emission spectra of the electrospun fibers from 8.5% (w/v) solutions of PS/EHO-OPPE (PS:EHO-OPPE = 7.5:1) in DCE and CF with 8 vol.-% PF at various applied electrical potentials (HV) (see Figure 7).

Solution	HV	Peak	Shoulders	
	kV	nm	nm	
			High energy	Low energy
PS/EHO-OPPE/DCE + PF	7.5	517	460	595
	10.0	515	461	599
	12.5	510	457	591
	15.0	516	458	594
	17.5	515	459	595
	20.0	516	460	596
PS/EHO-OPPE/CF + PF	7.5	508	460	590
	10.0	511	460	593
	12.5	514	457	591
	15.0	519	459	595
	17.5	515	458	594
	20.0	511	459	596

Macromol. Mater. Eng. **2008**, *293*, 952–963

Macromolecular Journals

DOI: 10.1002/mame.200800268

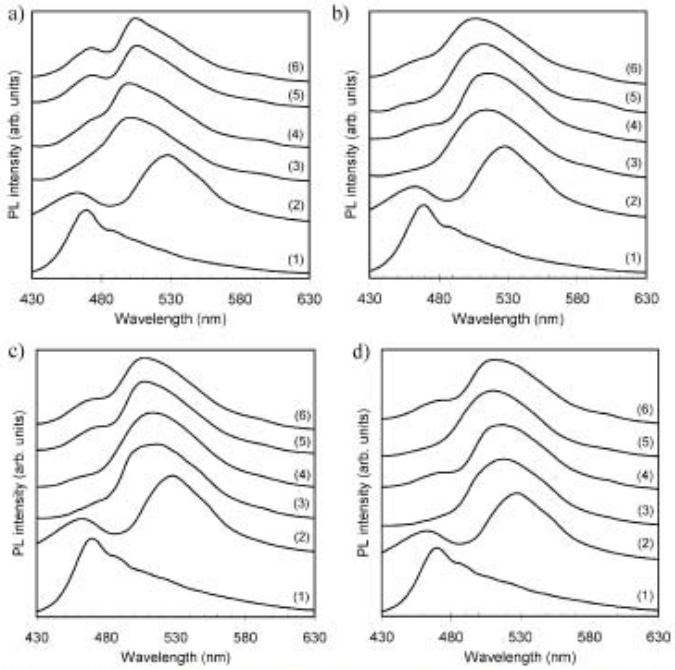

Figure 8. Emission spectra of samples produced from solutions of 8.5% (w/v) PS/EHO-OPPE (PS:EHO-OPPE = 7.5:1) in a) DCE, b) DCE with the addition of 8 vol.-% PF, c) CF and d) CF with the addition of 8 vol.-% PF. Samples were (1) spin-coated films, (2) solution-cast films, (3) pristine e-spun fibers, and e-spun fibers annealed at 110 °C for (4) 5 min, (5) 30 min, and (6) 1 h.

portion of the conjugated polymer molecules to disperse in the PS host upon annealing. Obviously, that morphology is maintained when the samples are cooled to room temperature.

Figure 9 shows representative SEM images of the e-spun PS/EHO-OPPE fibers that had been annealed for 1 h. Minor morphological changes are evident. Many fused sections can be observed and some parts of the annealed fibers flattened into ribbons. Moreover, the size of the annealed fibers is slightly larger when compared with that of the pristine fibers (see Table 5), a result that is consistent with the expansion of the fused sections.

Conclusion

In this work, ultra-fine PS/EHO-OPPE fibers with average diameters ranging from 430 to 1 200 nm were successfully prepared by electrospinning the solutions of 8.5 wt.-% PS/EHO-OPPE (PS/EHO-OPPE = 7.5:1 w/w) in 1,2-dichloroethane (DCE) and chloroform (CF) with and without the addition of pyridinium formate (PF). While the increase in the electrical potential resulted in the observed increase in the diameters of the e-spun fibers, the addition of PF significantly improved the electro-spinnability of the resulting PS/EHO-OPPE solutions, as shown by the decrease in the bead density of the obtained fibers. FT-IR spectroscopy showed that the chemical structure of PS and EHO-OPPE did not change and still existed in the e-spun fibers. The optical properties (e.g., absorption and emission) of the as-prepared solution, the e-spun fibers, the annealed fibers, and both the spin-coated and the solution-cast reference films were studied by UV-vis and PL spectroscopy. A red-shift was observed in emission spectra of the e-spun fibers and the solution-cast films when compared with those of the corresponding solutions. This shift could be attributed to the phase separation of the EHO-OPPE molecules, which resulted in a higher degree of molecular interaction. The shift in the e-spun fibers was less pronounced when they were annealed. Presumably, this was due to increased PPE mobility to disperse much more evenly in the PS matrix, resulting in even lesser aggregation or the destruction of the precedent aggregation.

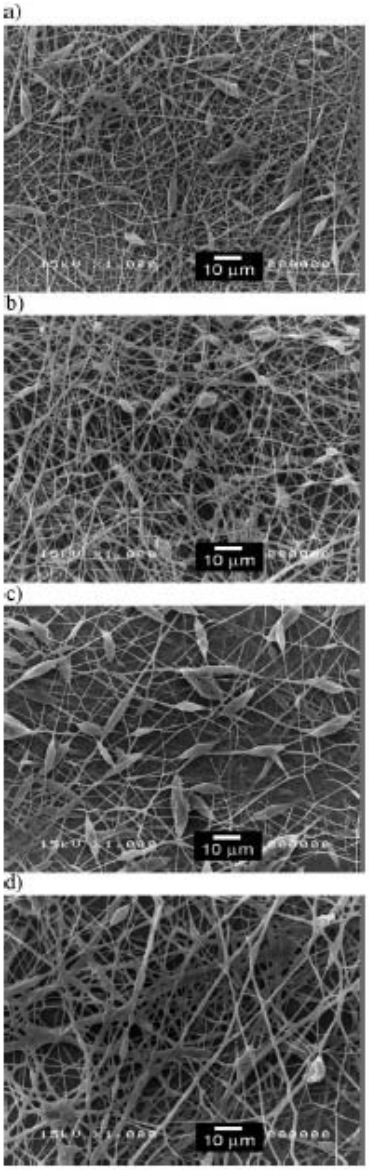

Figure 9. SEM images of the as-annealed fibers (1 h at 110 °C) electrospun from 8.5% (w/v) solutions of PS/EHO-OPPE (PS:EHO-OPPE = 7.5:1) in a) DCE, b) DCE with the addition of 8 vol.-% PF, c) CF and d) CF with the addition of 8 vol.-% PF (×1 000, scale bar = 10 μm).

Table 5. Average fiber diameter, bead size and bead density of the electrospun fibers from 8.5% (w/v) solutions of PS/EHO-OPPE (PS:EHO-OPPE = 7.5:1) in a) DCE, b) DCE with 8 vol.-% PF, c) CF, and d) CF with 8 vol.-% PF. The fibers were electrospun at an applied electrical potential of 15 kV and then annealed for 1 h at 110 °C.

Annealed Fiber	Fiber diameter	Bead size	Bead density
	μm	μm	beads · cm^{-2}
PS/EHO-OPPE/ DCE	0.82 ± 0.25	2.79 ± 1.22	3.26×10^5
PS/EHO-OPPE/ DCE + PF	0.76 ± 0.31	3.53 ± 1.52	1.76×10^5
PS/EHO-OPPE/ CF	0.68 ± 0.28	6.45 ± 1.11	3.74×10^5
PS/EHO-OPPE/ CF + PF	1.15 ± 0.45	3.71 ± 1.34	1.21×10^5

Acknowledgements: PS acknowledges partial support received from the *Thailand Research Fund* (*TRF*) (through a research career development grant: RMU4980045), the *National Center of Excellence for Petroleum, Petrochemicals, and Advanced Materials* (*NCE-PPAM*), and the *Petroleum and Petrochemical College* (*PPC*), *Chulalongkorn University*. SC acknowledges a doctoral scholarship received from the *Royal Golden Jubilee PhD Program*, through the *Thailand Research Fund* (*TRF*). CW acknowledges support received from the *National Science Foundation* (under grant no. DMR-0215342). We thank *Michael Schroeter* for the synthesis of EHO-OPPE.

Received: August 27, 2008; Accepted: September 10, 2008; DOI: 10.1002/mame.200800268

Keywords: electrospinning; photophysics; polymer blend; poly(*p*-phenylene ethynylene); polystyrene

[1] E. Shirakawa, E. J. Louis, A. G. MacDiarmid, C. K. Chiang, A. J. Heeger, *J. Chem. Soc. Chem. Comm.* **1977**, 579.
[2] [2a] A. J. Heeger, *Rev. Mod. Phys.* **2001**, *73*, 681; [2b] A. G. MacDiarmid, *Rev. Mod. Phys.* **2001**, *73*, 701; [2c] H. Shirakawa, *Rev. Mod. Phys.* **2001**, *73*, 713.
[3] [3a] "*Handbook of Organic Conductive Molecules and Polymers*", H. S. Nalva, Ed., Wiley, New York 1997; [3b] T. A. Skoetheim, R. L. Elsenbaumer, J. R. Reynolds, Eds., "*Handbook of Conducting Polymers*", Dekker, New York 1998.
[4] [4a] J. H. Burroughes, D. D. C. Bradley, A. R. Brown, R. N. Marks, K. Mackay, R. H. Friend, P. L. Burns, A. B. Holmes, *Nature* **1990**, *347*, 539; [4b] A. Kraft, A. C. Grimsdale, A. B. Holmes, *Angew. Chem. Int. Ed.* **1998**, *37*, 402; [4c] U. Mitschke, P. Bäuerle, *J. Mater. Chem.* **2000**, *10*, 1471; [4d] A. Greiner, C. Weder, in: "*Encyclopedia of Polymer Science and Technology*", J. I. Kroschwitz, Ed., Wiley-Interscience, New York 2003, p. 87.
[5] G. Horowitz, *Adv. Mater.* **1998**, *10*, 365.
[6] C. J. Brabec, N. S. Sariciftci, J. C. Hummelen, *Adv. Funct. Mater.* **2001**, *11*, 15.

DOI: 10.1002/mame.200800268

[7] D. T. McQuade, A. E. Pullen, T. M. Swager, *Chem. Rev.* **2000**, *100*, 2537.
[8] F. R. Denton, III, P. M. Lahti, "*Photonic Polymer Systems - Fundamentals, Methods, and Applications*", D. L. Wise, G. E. Wnek, D. J. Trantolo, T. M. Cooper, J. D. Gresser, Eds., CRC Press, New York 1998.
[9] U. Scherf, E. J. W. List, *Adv. Mater.* **2002**, *14*, 477.
[10] "*Poly(Arylene Ethynylene)s – From Synthesis to Applications*", C. Weder, Ed., Adv. Polym. Sci. Series, Vol. 177, 2005.
[11] [11a] C. Weder, M. S. Wrighton, R. Spreiter, C. Bosshard, P. Gunter, *J. Phys. Chem.* **1996**, *100*, 18931; [11b] G. S. He, C. Weder, P. Smith, P. N. Prasad, *IEEE J. Quantum Electron.* **1998**, *34*, 2279.
[12] [12a] C. Weder, M. S. Wrighton, *Macromolecules* **1996**, *29*, 5157; [12b] D. Steiger, P. Smith, C. Weder, *Macromol. Rapid Commun.* **1997**, *18*, 643; [12c] S. Dellsperger, F. Dotz, P. Smith, C. Weder, *Macromol. Chem. Phys.* **2000**, *201*, 192; [12d] D. Knapton, P. K. Iyer, S. J. Rowan, C. Weder, *Macromolecules* **2006**, *39*, 4069.
[13] [13a] A. Montali, P. Smith, C. Weder, *Synth. Met.* **1998**, *97*, 123; [13b] C. Schmitz, P. Pösch, M. Thelakkat, H. W. Schmidt, A. Montali, K. Feldman, P. Smith, C. Weder, *Adv. Func. Mater.* **2001**, *11*, 41; [13c] M. Burnworth, J. D. Mendez, M. Schroeter, S. J. Rowan, C. Weder, *Macromolecules* **2008**, *41*, 2157.
[14] [14a] A. Kokil, I. Shiyanovskaya, K. D. Singer, C. Weder, *J. Am. Chem. Soc.* **2002**, *124*, 9978; [14b] A. Kokil, I. Shiyanovskaya, K. D. Singer, C. Weder, *Synth. Met.* **2003**, *138*, 513.
[15] [15a] A. Kokil, P. Yao, C. Weder, *Macromolecules* **2005**, *38*, 3800; [15b] P. K. Iyer, J. B. B. Beck, C. Weder, S. J. Rowan, *Chem. Comm.* **2005**, 319.
[16] G. Voskerician, C. Weder, *Adv. Polym. Sci.* **2005**, *177*, 209.
[17] [17a] C. Weder, C. Sarwa, C. Bastiaansen, P. Smith, *Adv. Mater.* **1997**, *9*, 1035; [17b] A. Montali, G. Bastiaansen, P. Smith, C. Weder, *Nature* **1998**, *392*, 261; [17c] A. R. A. Palmans, M. Eglin, A. Montali, C. Weder, P. Smith, *Chem. Mater.* **2000**, *12*, 472.
[18] C. Weder, C. Sarwa, A. Montali, C. Bastiaansen, P. Smith, *Science* **1998**, *279*, 835.
[19] Y. Xu, P. R. Berger, J. N. Wilson, U. H. F. Bunz, *Appl. Phys. Lett.* **2004**, *85*, 4219.
[20] H. Hoppe, N. S. Sariciftci, D. A. M. Egbe, D. Mühlbacher, M. Koppe, *Mol. Cryst. Liq. Cryst.* **2005**, *426*, 255.
[21] D. Knapton, M. Burnworth, S. J. Rowan, C. Weder, *Angew. Chem. Int. Ed.* **2006**, *45*, 5825.
[22] [22a] E. Hittinger, A. Kokil, C. Weder, *Angew. Chem. Int. Ed.* **2004**, *43*, 1808; [22b] E. Hittinger, A. Kokil, C. Weder, *Macromol. Rapid Commun.* **2004**, *25*, 710.
[23] [23a] J. X. Jiang, F. Su, A. Trewin, C. D. Wood, N. L. Campbell, H. Niu, C. Dickinson, A. Y. Ganin, M. J. Rosseinsky, Y. Z. Khimyak, A. I. Cooper, *Angew. Chem. Int. Ed.* **2007**, *46*, 8574; [23b] C. Weder, *Angew. Chem. Int. Ed.* **2008**, *47*, 448.
[24] Y. Wang, J. S. Park, J. P. Leech, S. Miao, U. H. F. Bunz, *Macromolecules* **2007**, *40*, 1843.
[25] P. Wutticharoenmongkol, P. Supaphol, T. Srikhirin, T. Kerdcharoen, T. Osotchan, *J. Polym. Sci., Part A: Polym. Phys.* **2005**, *43*, 1881.
[26] H. Wang, X. Lu, Y. Zhao, C. Wang, *Mater. Lett.* **2006**, *60*, 2480.
[27] N. Dharmaraj, C. H. Kim, K. W. Kim, H. Y. Kim, E. K. Suh, *Spectrochim. Acta A* **2006**, *64*, 136.
[28] R. Luoh, H. T. Hahn, *Compos. Sci. Technol.* **2006**, *66*, 2436.
[29] S. Tungprapa, I. Jangchud, P. Ngamdee, M. Rutnakornpituk, P. Supaphol, *Mater. Lett.* **2006**, *60*, 2920.
[30] X. Li, X. Hao, D. Xu, G. Zhang, S. Zhong, H. Na, D. Wang, *J. Membrane Sci.* **2006**, *281*, 1.
[31] Y. C. Ahn, S. K. Park, G. T. Kim, Y. J. Hwang, C. J. Lee, H. S. Shin, J. K. Lee, *Curr. Appl. Phys.* **2006**, *6*, 1030.
[32] J. S. Jeong, J. S. Moon, S. Y. Jeon, J. H. Park, P. S. Alegaonkar, J. B. Yoo, *Thin Solid Films* **2007**, *515*, 5136.
[33] D. Kawaguchi, K. Tanaka, A. Takahara, T. Kajiyama, *Macromolecules* **2001**, *34*, 6164.
[34] T. Jarusuwannapoom, W. Hongrojjanawiwat, S. Jitjaicham, L. Wannatong, M. Nithitanakul, C. Pattamaprom, P. Koombhongse, R. Rangkupan, P. Supaphol, *Eur. Polym. J.* **2005**, *41*, 409.
[35] C. Mit-Uppatham, M. Nithitanakul, P. Supaphol, *Macromol. Chem. Phys.* **2004**, *205*, 2327.
[36] S. Chuangchote, T. Srikhirin, P. Supaphol, *Macromol. Rapid Commun.* **2007**, *28*, 651.
[37] H. Fong, I. Chun, D. H. Reneker, *Polymer* **1999**, *40*, 4585.
[38] Z. M. Huang, Y. Z. Zhang, M. Kotaki, S. Ramakrishna, *Compos. Sci. Technol.* **2003**, *63*, 2223.